Response to Editor

Comments to the Author:

Dear authors,

three reviewers have given feedback on your manuscript. The reviewers give generally very positive feedbacks and state they were intrigued by the analysis and results. All find that it is a timely and valuable contribution to the field of global hydrology. The paper is well structured and written. The reviewers have also given constructive feedback and criticism and you have addressed several of those comments in your response.

I agree with the assessment of the reviewers on the merit and novelty of the presented analysis. I would however like to emphasize one point: All of the reviewers comment, in one way or the other, on the fact that the results hinge upon the correctness of the CDR dataset. In your response you emphasize how carefully the CDR dataset was developed and validated, and also your own efforts to validate e.g. the standard deviation of E. I appreciate this. However, some of the standard variations in the dataset are not yet validated. I agree with reviewer #2 (René Orth) that a cross-validation would be desirable to learn whether the observed variance patterns are a property of the CDR dataset or hold with other datasets. At the very least, and since the main message of the manuscript is a call for investigation into the causes of the observed hydroclimatic variability, the discussion should more than now acknowledge to that fact that any efforts towards validation of those patterns are equally warranted.

Please submit the revised manuscript, with changes highlighted, together with a point by point response to all of the reviewers comments.

I thank both the authors and reviewers for the constructive discussion and look forward to the revised manuscript,

Anke Hildebrandt.

Response: We thank the editor for the evaluation and comment on the manuscript. As suggested by the editor and reviewers, we have carefully read and revised the manuscript accordingly as well as conducted a point-by-point response to all the comments.

The main comment here is a further cross-validation of the CDR data results based on atmospheric reanalysis (e.g., the state-of-the-art ERA5 dataset). As suggested by both editor and R2, in this response we report a comparison of the CDR (P, E, Q and ΔS) with the same from the recently released ERA5. We found P to be similar in both CDR and ERA5, but we found E and Q to be generally **much** higher in ERA5 compared to CDR (please see details in response to R2C3). As a consequence, in ERA5 we found that the sum of E and Q regularly exceeded P by large amounts. For example, in the Amazon, E and Q exceeded P by up to 1000 mm each and every year. So over a 27 year period, the predicted decline in storage in the Amazon region embedded in ERA5 approached 27000 mm (27 m)! This represents a major problem in the mass balance (or a lack of mass balance) in the ERA5 reanalysis and is physically not plausible. In contrast, over ice covered regions (e.g., Greenland), the hydrologic balance implied a continuing gain in storage of roughly similar magnitudes (i.e., 27 m in 27 years). Again, this is also physically not plausible.

Though the ERA5 is the state-of-the-art atmospheric reanalysis, we concluded that there was a major problem with the hydrologic (mass) balance and that the "atmospheric-centric" ERA5 database was not yet suitable for use in hydrologic studies.

As suggested by the editor, we also added the statement about the importance towards further improvement and validation of the patterns obtained in this manuscript in the revised manuscript.

Another important point raised by the reviewers (R2, R3) were (divergent) criticisms of the summary sections of the original manuscript. After carefully looking at comments from R2 and R3 and the structure and content of the original manuscript, we concluded that the underlying problem was that the original Discussion and Conclusions were repetitive and generally not well formulated. In response, we decided to combine the original sections (sections 5 and 6) into a new single section 5 (Discussion and Conclusions), and have streamlined the text accordingly by integrating the comments by reviewers. We believe that this has made the summary section more concise and that this change has substantially improved the manuscript.

We sincerely appreciate both the editor and reviewers for constructive suggestions and comments on the manuscript.

Response to Referee #1 (Anonymous)

In the following we use R1C1 (etc) to refer to comment 1 (C1) by referee 1 (R1).

R1C1: This is an excellent paper with major implications to our understanding of long term water balance and their climatic and landscape controls.

Response: We thank the anonymous reviewer for the evaluation and positive comment on the manuscript.

R1C2: This kind of work could not have been even just a few years ago, but as more and more reanalysis data become available the ability to do this kind of work and learn from it improves (given the caveat that this is ultimately model generated data, but the best we have).

I have no problems with the analyses that have been done, and the presentation. The authors use monthly data but the analysis is about inter-annual variability, although they do use the monthly data to estimate the storage capacity. I would like to see a categorical statement about this, I found it confusing. This means they only have 28 years of data (28 numbers) - they need to make an assessment/statement about the implications of this for their estimates of the various statistics, given potential non-stationarities etc.

Response: In this initial investigation, we use the CDR (monthly database) and as the reviewer has noted this is an entirely new field of research since global hydrologic reanalysis data has not previously been available. We chose to focus on the inter-annual variability to establish links directly with important earlier work on this topic (e.g., Koster & Suarez, 1999). We plan to extend this work to a seasonal time scale in future research. To eliminate the potential confusion, we made a statement as the reviewer suggested in the revised version of manuscript:

(Lines 100-101): "*In this study we focus on the inter-annual variability and the monthly water cycle variables (P, E, Q and ΔS) are aggregated to annual totals.*". Also, another statement about the limitations of 27-year study period has be added in the revision (Lines 457-460): "*The CDR is one of the first dedicated hydrologic reanalysis databases and includes data for a 27-year period. Accordingly, we could only examine hydrologic variability over this relatively short period. Further, we expect future improvements and modifications as the hydrologic community seeks to further develop and refine these new reanalysis databases*". Thanks.

R1C3: The main issue that I have with the paper is that (as the authors themselves admit) is the preliminary nature of the discussion and conclusions. The results, to say the least, are quite interesting and intriguing. Without further analysis, one can only speculate. The dependence on storage capacity and temperature are potential clues. This is a concern for me - one solution is to delay the paper until further analysis is done to elucidate these results. It seems the main route to explanations is to use the monthly data that they already have, to see if there is an extension of the variances and especially cross-covariances into the seasonal regime. In other words, I am speculating if the causes of the inter-annual variability lie in the intra-annual variability of the fluxes and the storage, and in the role of vegetation (and soils) buffering the variability in the climate.

Response: We agree with R1 about the likely importance of the seasonal (i.e. intra-annual) cycle to further explain these results. However, given the new approach developed in this manuscript we deliberately chose to publish the somewhat simpler inter-annual results first.

Please also see R1C2.

R1C4: For now there is a decision to be made - I am comfortable with going ahead with publication of the current paper (in spite of its preliminary nature) in view of the fact publication of the paper may trigger follow-on research by other research groups as well.

Response: We appreciate the comments of the reviewer.

Response to Referee #2 (Dr René Orth)

R2C1: Review of Dongqin and Roderick "Inter-annual variability of the global terrestrial cycle" This study investigates the propagation of precipitation variability into the water cycle, i.e. into variations of runoff, evapotranspiration, and of storage changes. The authors show that this is mostly controlled by temperature (in wet regions), long-term aridity (in transitional regions), and by soil water storage capacity (in dry regions). Further, the results illustrate that the corresponding partitioning is different from the partitioning of mean precipitation into the means of these water cycle variables.

——————-

Recommendation: I think the paper requires major revisions.

The analysis is very interesting and provides new and fundamental insights into large- scale land surface hydrology. Related variability analyses are still not commonly done due to a lack of reliable data and underlying theory. This study can foster theory development in this area, and it underlines the importance of continuous improvement of the just-emerging global hydrological re-analysis datasets. Therefore I would be happy to see it published in HESS, but after some general revisions.

Response: We thank R2 for the evaluation and helpful comments on the manuscript.

R2C2: (1) Next to the consideration of the soil water storage capacity and the mean temperature to explain variations in the partitioning of precipitation variability, I am missing the inclusion of vegetation type as an explanatory variable. It might have strong implications on evapotranspiration variability, and therefore also on runoff and storage variabilities.

Response: We agree with Dr René Orth that the inter-annual variability might be related to the other factors, e.g., vegetation type. However, given the fact that this is a new approach and the research is exploratory, we focused on relating the inter-annual variability with the most general hydrologic factors (i.e., the air temperature as a surrogate for snow/ice and water storage capacity). We expect to extend the current work to a more complete analysis (e.g., relation to vegetation) in future research and we hope others will follow by examining factors like vegetation since this will require the effort of many scientists.

R2C3: (2) I agree with the authors that comprehensive hydrological reanalysis datasets are lacking, and the CDR dataset is an important contribution in that respect. Further, I appreciate the effort they make to validate the applicability of the dataset in the context of this study. However, also the CDR dataset is (necessarily) based on a model and hence it is not clear that the reported relationships are operating in nature, and not only in this model. To address this issue, I would like to see the key analyses from this study repeated with the state-of-the-art ERA5 reanalysis, which should be superior to ERA-Interim also in terms of land surface representation.

Response: As suggested by both R2 and the editor, we have compared the CDR (P, E, Q and ΔS) with the same from the recently released ERA5. For this comparison, we use the same 1984-2010 period. We downloaded monthly P, E and Q (denoted as total runoff and calculated by ERA5 as surface plus sub-surface runoff) from the ERA5 website. The water storage change (ΔS) is not included in the ERA5 database, and we calculated it using mass balance for each individual month during 1984-2010. We then conducted further analysis and found P to be similar in both CDR and ERA5 (Fig. R1). However, we found E and (especially) Q to be generally **much** higher in ERA5 compared to CDR (Figs. R2-R3). This has important consequences for the change in storage as described below.

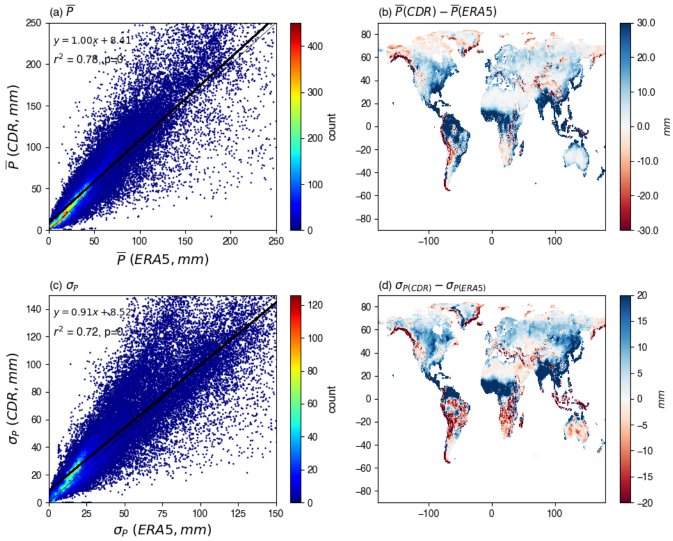

Figure R1. Comparison of monthly precipitation P between ERA5 and CDR databases. Top panels (a) (b) show comparison of the mean monthly ($\bar{P}$) while bottom panels (c) (d) show comparison of the standard deviation (σ_P) of monthly P.

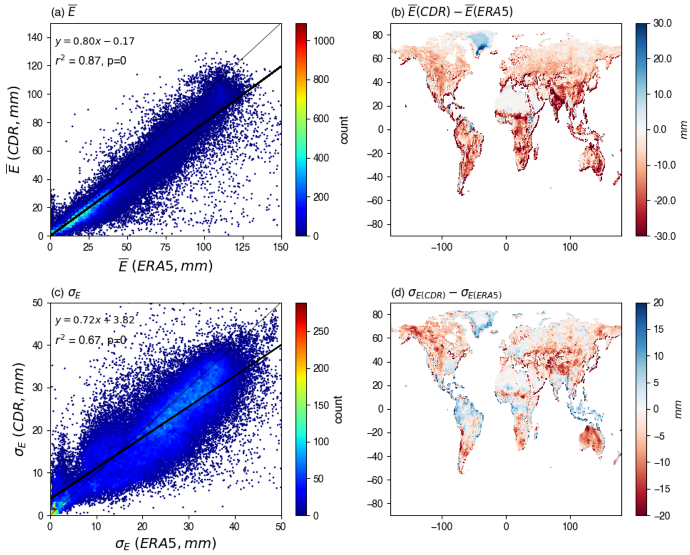

Figure R2. The same as Fig. R1 but using monthly evapotranspiration E from ERA5 and CDR databases.

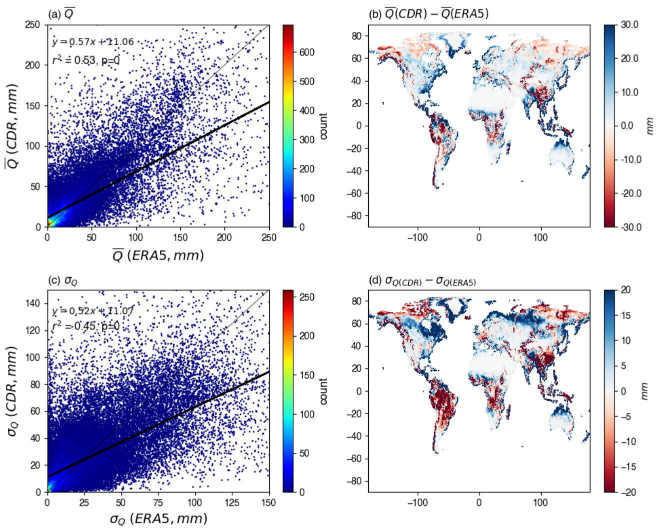

Figure R3. The same as Fig. R1 but using monthly runoff Q from ERA5 and CDR databases.

While the comparison with *P* (CDR vs ERA5 is reasonable, i.e., slope of the regression in Fig. R1a = 1.0), we find that *E* from ERA5 is on average 25% larger (i.e. slope is 0.8, see Fig. R2a) than *E* in CDR. Further, *Q* from ERA5 is on average 75% larger (i.e., slope is 0.57, see Fig. R3a) than *Q* in CDR. Now we know that in CDR, the mass balance was enforced. The obvious implication from these regressions is that in ERA5 the sum of *E* and *Q* must substantially exceed *P*.

To further evaluate ERA5, we then integrated the monthly data to annual totals. Visually, the results visually show similar global spatial patterns of long-term mean *P*, *E* and *Q* in the ERA5 database (see the Fig. R4a-c) to those in the CDR database (see Fig. 1 in the revised manuscript). However, as noted above, the long-term mean annual water storage change (ΔS, Fig. R4d) implied by ERA5 showed evidence of a major problem with the local hydrology. In particular, most regions of the earth surface show very large negative values for ΔS, e.g., in the Amazon long term mean annual ΔS is around -1000 mm. The implication is that over the 27-year period (1984-2010), the annual storage change in ERA5 over the Amazon region is -1000 mm every year and this equal 27 meters of storage change over the full period. This occurs in ERA5 because the sum of long-term mean annual *E* and *Q* is substantially greater than *P* in the Amazon. This is physically not plausible. The same problem holds for many other warm regions. In contrast, over the ice covered regions (e.g., Greenland), the hydrologic balance implied a continuing gain in storage. Again, this is physically not plausible.

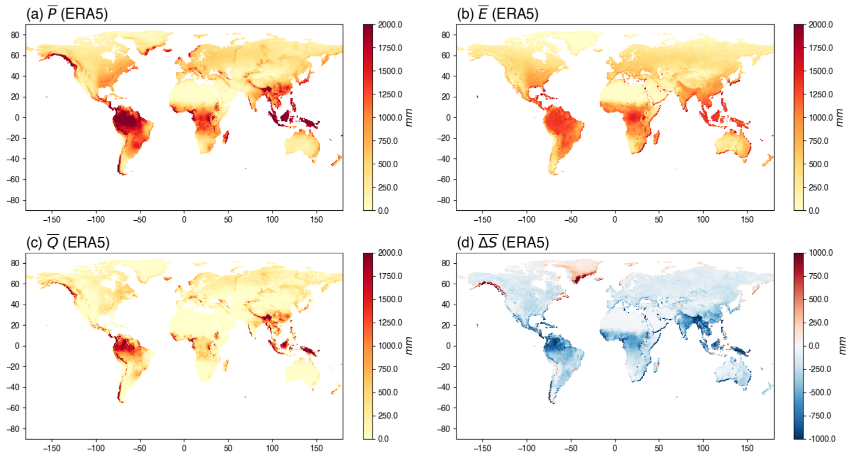

Figure R4. Mean annual (1984-2010) (a) *P*, (b) *E*, (c) *Q* and (d) ΔS in the ERA5 database.

Though the ERA5 is the state-of-the-art atmospheric reanalysis, we concluded that there was a major problem with the hydrologic (mass) balance and that the “atmospheric-centric” ERA5 database was not yet suitable for use in hydrologic studies.

Returning to the suitability of the CDR database and its relation to the real world, there is ample evidence that it is suitable for the analysis conducted here including:

(i) The enforcement of basic hydrologic concepts (mass balance).

(ii) The numerous tests of CDR reported in the original Zhang et al 2018 HESS publication (that are summarized on lines 134-139 of the HESSD manuscript). Those tests include a (successful) comparison of CDR runoff to observations of monthly runoff at 165 medium size basins and 862 small basins. In fact, the assessment of CDR in the original paper was quite comprehensive as you would expect.

(iii) We have augmented those extensive original tests by independently comparing monthly *E* with FLUXNET tower data at 32 sites which confirmed that the CDR captured the general seasonal cycle in both *P* and *E* at those 32 sites (Fig. S3, S4, S5, Table S1 in the revised manuscript). We also used the same FLUXNET data to compare the variability in *P* with variability in *E* (Fig. S6 in the revised manuscript).

(iv) We further compared CDR *E* with two gridded *E* databases that are not included in the source databases of CDR (LandFluxEval, MPI, see lines 159-166 in the revised manuscript and Fig. S7, S8) and the comparison was satisfactory.

(v) We compared how the standard deviation for *E* and the mean for *E* are related in the CDR (Fig. 4 in the revised manuscript) and compared that with the same relations in LandFluxEval and MPI (Fig. S10 in the revised manuscript). Those two comparisons were satisfactory.

(vi) The mean water cycle (*P*, *E*, *Q*) in CDR was shown to be consistent with the long-standing Budyko framework (Fig. 2 in the revised manuscript).

(vii) The CDR data were consistent with the Koster & Suarez (1999) theory in the limit of sites that have limited water storage (Fig. 5 in the revised manuscript).

That is a very comprehensive assessment.

Further, we readily acknowledge that the CDR database is the first hydrologic reanalysis and we expect more ‘hydrologic-centered’ databases to compare it to in the near future. For that reason we chose to only investigate the most general factors that we believe will stand the test of time and we have also described the study as an initial exploratory survey at several places in the manuscript.

R2C4: (3) I appreciate the idea of investigating the influence of the soil water storage capacity and the mean temperature on the variability partitioning. However, I think parts of the conclusions drawn by the authors from Figures 8-10 are not supported by the data. For example, I cannot see in Figure 10 that the temperature influence is particularly strong in very wet regions. Rather, to me it seems to be strong in moderately wet and dry regions (Fig 10b,d,f,h,j,l,n,p). Further, also the aridity limit of 6 which the authors suggest in their interpretation of the results in Figure 9, is arbitrary and not supported by the actual results. Storage capacity is obviously having an influence already for aridity values above 2-3 (Fig. 9b,c,f,j,k). Overall, in these Figures there are many interesting patterns but the authors focus only on few sub-plots and limit their interpretation to these. Therefore, I suggest to either show less information/sub-plots there, or to develop explanations also for patterns emerging within other sub-plots.

Response: We accept that Fig. 10 (Fig. 8 in the revised manuscript) is hard to interpret. On reading the reviewers comments and going over the manuscript we realize the problem was that we did not explicitly indicate the relevant panels (i.e., a, b, c, ….) and the text was not well-formulated. This was an oversight correctly identified by the reviewer. In general, the data in Fig. 10 was not particularly revealing (i.e., a negative result) but we actually focused the discussion to the first and third columns but we did not identify them properly. In response, we replaced the original text with the following (lines 307-314):

"*To understand the potential role of snow/ice in modifying the variance partitioning, we repeat the previous analysis (Fig. 7) but here we use the mean annual air temperature ($\overline{T_a}$) to colour the grid-cells to (crudely) indicate the presence of snow/ice (Fig. 8). The results are complex and not easy to simply understand. The most important difference revealed by this analysis is in the hydrologic partitioning between cold (first column) and hot (third column) conditions in wet environments ($\overline{E_o}/\overline{P} \leq 0.5$). In particular, when $\overline{T_a}$ is high, σ_P^2 is almost completely partitioned into σ_Q^2 in wet environments (e.g., $\overline{E_o}/\overline{P} \leq 0.5$, Fig. 8g). In contrast, when $\overline{T_a}$ is low in a wet environment ($\overline{E_o}/\overline{P} \leq 0.5$ in first column of Fig. 8), there are substantial variations in the hydrologic partitioning. That result reinforces the complexity of variance partitioning in the presence of snow/ice.*"

R2C5: (4) The paper contains (too) many figures, which is diluting the main message(s), I feel. For example, Figures 1 and 2 could be merged, Figure 5 could be moved to the supplementary material, Figure 13 could be merged into Figure 8. The authors might have further ideas to reduce the amount of figures. Moreover, I do not really understand the difference between Figures 7 and 8, and why both are needed.

I do not wish to remain anonymous - René Orth.

Response: We respect the reviewer's opinion that we have too many figures – this is always a hard balance to get right to everyone's satisfaction. We have moved the original Fig. 1 and Fig. 5 to the supporting material as suggested. There are now 12 figures in the revised manuscript with another 12 in the supporting material. However, we do not think the original Fig. 13 (Fig. 11 in the revision) should be merged into original Fig. 8 (Fig. 6 in the revision) since the two figures belong to different sections (original Fig. 8 for the relation between variance partitioning and aridity section, original Fig. 13 for the case study section). Original Fig. 7 (Fig.5 in the revision) is a direct link to previous work while original Fig. 8 is the variance partitioning in the CDR database. Hence while these two figures are similar, they make separate independent contributions to the manuscript.

———————

Specific comments:

R2C6: line 8: Equation 2 not introduced yet line 13: It should be 'variabilities'.

Response: We have deleted the text 'Eq. 2' and changed 'the variability…' to 'that variability…' to make the text clear to understand in the revised version of manuscript. Thanks.

R2C7: line 15: Some word is missing towards the end of the line

Response: We have checked line 15 in the original manuscript and did not find missing words?

R2C8: lines 35-39: Orth & Destouni (2018) might be relevant in this context and could be cited.

Response: The reference has now been cited in the revised manuscript.

R2C9: line 37: Not sure I get the point here.

Response: We mean that droughts and floods are typical extremes but that hydrologic variability encompasses more than just droughts and floods, i.e., hydrologic variability occurs across all time-space scales.

R2C10: lines 106-118: Please clarify that what you are determining here is actually not the soil water storage capacity, but rather the active range within which the soil moisture varies.

Response: Yes, exactly. We have modified the text and state the calculation to make this explicit in Lines 108-110 in the revised manuscript: "*For the storage, the active range of the monthly water storage variation was used to approximate the water storage capacity (S_{max}).*".

R2C11: lines 157-163: I would recommend to replace the LandFluxEVAL and the Jung et al. datasets with more recent gridded ET datasets such as the Jung et al. 2019 dataset and the GLEAM dataset (Martens et al. 2017).

Response: The reason we chose the LandFluxEVAL and MPI databases is that they are among the most widely used and validated *E* data that were also **not used** to develop the CDR database. We do not think adding a comparison to the latest GLEAM database would be as useful since an earlier version of GLEAM (v2a) was actually an input to the data assimilation scheme used to construct the CDR (see Table 1 in Zhang et al., 2018, HESS). Instead, the more appropriate approach would be to revise the CDR data assimilation but incorporating the latest GLEAM database but that is well beyond the scope of this work. (Also see R2C3 for similar comments about ERA.) We could replace the MPI we used with the updated database (Jung et al., 2019) but we do not see how that would alter the results.

R2C12: line 180: Gudmundsson et al. (2016) might be relevant in this context and could be cited.

Response: The reference has been cited in the revised manuscript. Thanks.

R2C13: line 181: What is meant by seasonality here? I thought you are considering annual data? In general, I think the considered temporal and spatial scales and resolution need to be more clearly stated and motivated at the beginning of the manuscript. Also, the role of these decisions on the results could be discussed.

Response: Yes, we are using annual data. But we know that differences of the intra-year seasonal timing (phase) of precipitation and E_o do have an effect on the annual water balance (as per the seminal work by Chris Milly in the early 1990s.). To make this more clear, we have added a statement in in the revised manuscript (Lines 100-101): "*In this study we focus on the inter-annual variability and the monthly water cycle variables (P, E, Q and ΔS) to annual totals.*"

Given the initial stage for this type of research and our plan to include the seasonal variations in future work (also see R1C2 and R1C3), a statement has been added in the revised manuscript (Lines 505-508): "*That result demonstrates that deeper understanding of the process-level interactions that are embedded within each of the three covariance terms (e.g., the role of seasonal vegetation variation) will be needed to develop process-based understanding of variability in the water cycle in these biologically productive regions (0.5<$\overline{E_o}/\overline{P}$ <1.5).*".

R2C14: line 252/253: I could not find this discussion in section 5!? Would be important to explain these discrepancies, though.

Response: Thanks for pointing this oversight out. The underlying scientific issue here is that the original Koster and Suarez (1999) work assumed negligible water storage change. In that sense the original results of Koster and Suarez (1999) can be seen as an upper limit and any variance in storage can only reduce the partitioning of variability in *P* to variability in *E* under dry conditions (Fig. 7). We have added a short discussion on this in the revised manuscript (Lines 488-492): "*This result explains the overestimation of σ_E/σ_P by the empirical theory of Koster and Suarez (1999) which implicitly assumed no inter-annual change in storage. The Koster and Suarez empirical theory is perhaps better described as an upper limit that is based on minimal storage capacity, and that any increase in storage capacity would promote the partitioning of σ_P^2 to $\sigma_{\Delta S}^2$ particularly under dry conditions (Figs. 10-12).*".

R2C15: line 327 & 333: 'leaving very limited variance' - not really true given your statement in lines 385-387

Response:

We show the *P*, *E*, *Q* and ΔS time series along with the relevant variances and covariances in Fig. 12. Starting with the two dry sites, at the site with low storage capacity (Site 1), the time series shows that *E* closely follows *P* leaving annual *Q* and ΔS close to zero (Fig. 12a). The variance of *P* (σ_P^2 = 206.9 mm^2) is small and almost completely partitioned into the variance of *E* (σ_E^2 = 196.9 mm^2), leaving very limited variance for *Q*, ΔS and all three covariance components (Fig. 12b). At the site with high storage capacity (Site 2), *E*, *Q* and ΔS do not simply follow *P* (Fig. 12c). As a consequence, the variance of *P* (σ_P^2 = 2798.0 mm^2) is shared between *E* (σ_E^2 = 1150.2 mm^2), ΔS ($\sigma_{\Delta S}^2$ = 800.5 mm^2) and their covariance component ($2cov(E, \Delta S)$ = 538.4 mm^2, Fig. 12d). Switching now to the remaining wet and hot site (Site 3), *Q* closely follows *P*, with ΔS close to zero and *E* showing little inter-annual variation (Fig. 12e). The variance of *P* (σ_P^2 = 57374.4 mm^2) is relatively large and almost completely partitioned into the variance of *Q* (σ_Q^2 = 57296.4 mm^2), leaving very limited variance for *E* and ΔS and the three covariance components (Fig. 12f). We also examined numerous other sites with similar extreme conditions as the three case study sites and found the same basic patterns as reported above.

The text here refers to the site-based case studies (line 327 – Fig. 12a (Fig. 10 in the revised manuscript) – Site 1; line 333 – Fig. 12 f – Site 3) while the later text (lines 385-387) refers to the general pattern across all grid-boxes, i.e., Fig. 4 (Fig. 3 in the revised manuscript). We have corrected this misunderstanding by rewriting lines 385-387 (lines 470-478 in revised manuscript) to indicate the relevant figures as follows:

"With that in mind, we were surprised that the inter-annual variability of water storage change ($\sigma^2_{\Delta S}$) is typically larger than the inter-annual variability of evapotranspiration (σ^2_E) (cf. Fig. 3b and 3d). The consequence is that $\sigma^2_{\Delta S}$ is more important than σ^2_E for understanding inter-annual variability of global water cycle. A second important generalisation is that unlike the variance components which are all positive, the three covariance components in the theory (Eq. 2) can be both positive and negative. We report results here showing both large positive and negative values for the three covariance terms (Fig. 3efg). This was especially prevalent in biologically productive regions ($0.5<\overline{E_o}/\overline{P}<1.5$, Fig. 3eg)."

R2C16: lines 403-405: I cannot see this from Figure 8.

Response: Agreed. That was our mistake. The reference to Fig. 8 (Fig. 6 in the revised manuscript) should be to Fig. 4 (Fig. 3 in the revised manuscript, global pattern of water cycle variability) and we have revised that in the revision.

R2C17: Section 5: Overall a bit lengthy with too much summarizing, I think. Could be shorter, and more concise.

Response: Both R2 & R3 (see R3C4) had divergent views about the summary sections of our original manuscript.

After looking at both comments (R2, R3) and the structure of the original manuscript, we concluded that the original Discussion and Conclusions sections were repetitive and not well formulated.

In response, we have combined the original sections into a single section 5 (Discussion and Conclusions) and have streamlined the text accordingly. We believe that this has substantially improved the manuscript.

R2C18: Figure 3: Why are there data points outside the physically plausible range?

Response: We assume you mean points with E exceeding P? This is possible in for example, regions with run-on, or irrigation. We have further investigated those points and also find that some of them come from the parts of Greenland that had not been masked out (Fig. 1).

R2C19: Figure 4: Many values seem to be cut at 10 as this is the end of the color bar. You could use log scale here for the color bar.

Response: Yes, the scale for P in Fig. 4a (new Fig. 3a in the revised manuscript) is saturated with the maximum value of the color bar 10,000. The reason we chose 10,000 as the limit was to show the patterns for both the relatively high (e.g., σ^2_P, σ^2_Q and $\sigma^2_{\Delta S}$) and low variabilities (e.g., σ^2_E, 2cov(E, ΔS)) while keeping the same scale for all panels. We have tried to modify this figure by using a log scale (see Fig. R5) to mitigate saturation, but it made the spatial patterns very difficult to distinguish compared with Fig. 3 in the revised manuscript (original Fig. 4) especially for the covariance panels (Fig. R5e-g). Therefore, we thought it better to keep the original legend in Fig. 3.

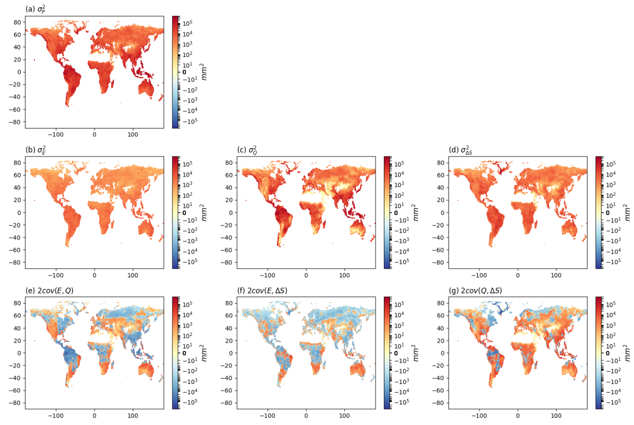

Figure R5. Water cycle variances (σ_P^2, σ_E^2, σ_Q^2, $\sigma_{\Delta S}^2$) and covariances ($cov(E,Q)$, $cov(E,\Delta S)$, $cov(Q,\Delta S)$). Note that we have multiplied the covariances by two (see Eq. 2).

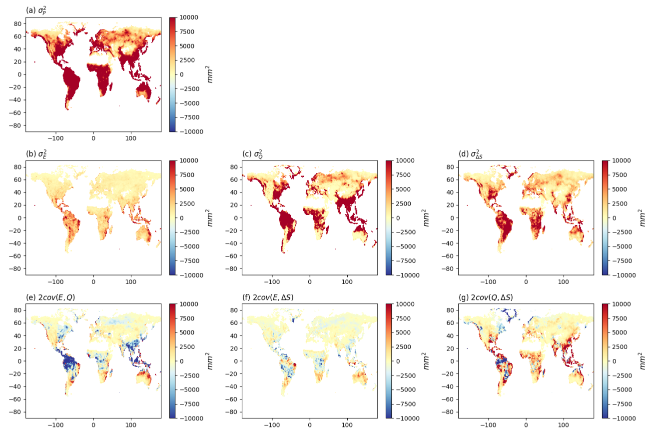

Figure 3 (original Figure 4). Water cycle variances (σ_P^2, σ_E^2, σ_Q^2, $\sigma_{\Delta S}^2$) and covariances ($cov(E,Q)$, $cov(E,\Delta S)$, $cov(Q,\Delta S)$). Note that we have multiplied the covariances by two (see Eq. 2).

R2C20: References:

Gudmundsson, L., P. Greve, and S. I. Seneviratne, 2016: The sensitivity of water avail- ability to changes in the aridity index and other factorsâA˘T˘A probabilistic analysis in the Budyko space, Geophys. Res. Lett. 43 (13), 6985-6994.

Jung, M., S. Koirala, U. Weber, K. Ichii, F. Gans, G. Camps-Valls, D. Papale, C. Schwalm, G. Tramontana, and M. Reichstein, 2019: The FLUXCOM ensemble of global land-atmosphere energy fluxes. Scientific Data, 6 (74).

Martens, B., D. G. Miralles, H. Lievens, R. van der Schalie, R. A. M. de Jeu, D. Fernández-Prieto, H. E. Beck, W. A. Dorigo, and N. E. C. Verhoest, 2017: GLEAM v3: satellite-based land evaporation and root-zone soil moisture, Geosci. Model Dev. 10, 1903–1925.

Orth, R., and G. Destouni, 2018: Drought reduces blue-water fluxes more strongly than green-water fluxes in Europe. Nature Communications, 9, 3602, doi: 10.1038/s41467- 018-06013-7

Response: We appreciate Dr René Orth for listing all the reference mentioned above in the comments, and we have read and cite these reference accordingly in the revised manuscript. Thanks.

Response to Referee #3 (Anonymous)

R3C1: This study tries to partition the inter-annual variability in precipitation (P), i.e., the source term in terrestrial water cycle, into variabilities in three sink terms in terrestrial water cycle (ET, Q, ΔS), and then to relate the partitioning of variabilities to various factors like temperature, aridity, and storage capacity. I think this type of study at global scale is rather new, if not first of its kind at global scale, and thus very interesting to the hydrology community. This is the case mostly because there has been a lack of "hydrologic reanalysis" (CDR) for such kind of analysis in the first place. At the same time, this effort couldn't fully answer many of the questions set forth at the beginning, leaving perhaps "more questions than answers" (as phrased by another referee). The authors have done a solid amount of thorough analysis and experiments toward the questions of interest and these analyses are also well designed too.

Overall I consider this manuscript of good quality, both scientifically and technically, and thus publishable in HESS with several concerns addressed.

Response: We agree that this is a first-of-its-kind study and thank the referee for the encouraging positive comments on the manuscript.

R3C2: My primary concern is there is a lack of general "signal-to-noise" discussions to better inform readers to what extent the findings are significant signals from the underlying data (CDR, Zhang et al., 2018) and how much of it could be due to data uncertainties (or possible artifacts due to how the data is produced). For example, the ET products that went into the CDR (satellite products, reanalysis, etc.) share some similarity in their production methods (e.g., Penman-Monteith or Priestley-Taylor type of schemes). Such similarity may limit the variability of ET in CDR. Of course, the plants do apply a strong filter on the inter-annual variability based on their survival need. Such uncertainty analysis may be difficult but I think some qualitative and general assessment would be very beneficial.

Response: The CDR uses a formal data assimilation scheme based on mass balance that weights the various inputs, and thereby produces uncertainty estimates for each variable (P, E, Q, ΔS). The original paper (Zhang et al., 2018 HESS) includes a formal assessment of the sensitivity of P, E, Q over large regions (continents, basins) using the coefficient of variation (see original Figures 2, 3, 4, 5, 6, 7 in Zheng et al., 2018 HESS). We actually followed from that work and used those uncertainty estimates (lines 124-132 in the revised manuscript) to identify and mask out regions where the uncertainty was large relative to the magnitude of the fluxes. This screening procedure removed most grid-boxes from the Himalayas, Sahara Desert and Greenland (see Fig. S2 in the revised manuscript).

Secondly, while it is true that some of the products might share similarity in producing, for example, E (Penman-Monteith, Priestley-Taylor as the examples noted by the reviewer) the data assimilation is a comprehensive approach that includes all available estimates of P, E, Q and ΔS at each grid box. With mass balance enforced, the CDR estimates represent a composite product that is designed to avoid bias of the type described by the reviewer as much as possible by using all available estimates of the hydrologic fluxes. As we have described in a response to Reviewer 2 (see R2C3), the CDR has been extensively validated in the original publication.

In that context, our goal was not to assess the CDR, but rather to use it for this "first-of-a-kind" study on the sources and sinks of inter-annual hydrologic variability. We have added words at the end of the manuscript that we expect further improvement and validation of obtained patterns (Lines 459-460): "*Further, we expect future improvements and modifications as the hydrologic community seeks to further develop and refine these new reanalysis databases.".*

R3C3: Also, at the scale of the CDR (0.5 degree), I would say the partitioning is more complicated than just a result of several factors. The horizontal transport of water, seasonality, local water use, etc., can add a lot of noise. I wouldn't say it is not possible to do it at 0.5 degree, but it would probably be less noisy at a slightly coarser scale. Also, there could be much more controlling factors for the partitioning than being investigated, e.g., land cover/land use, LAI, topography.

Response: We agree with the reviewer that the partitioning is complex and could be related to the other factors, e.g., land cover/land use, LAI and horizontal transport of water due to topography, etc. In this first-of-a-kind analysis we chose to focus on the zero'th order physical factors (storage capacity, snow/ice) at the CDR data resolution (0.5 degree), but we fully expect more detailed analysis to follow, e.g., vegetation plant-based variables as discussed by the reviewer. We have added new text in the last paragraph of section 4.5 that speculates on the important role of vegetation processes that addresses this comment by R3. We have also emphasized that again in the final concluding paragraph of the manuscript.

R3C4: Finally, given that this study does tend to raise more questions than answers, I feel the authors should provide some more insights on what we can do from the analysis and findings in this study. What can we do with the numbers concluded here? Validating models? Improving single models like Budyko? Hydrologic/water risk analysis? Climate system behavior/sensitivity and hydrologic impacts of climate changes? And how can we improve our understanding in the future? What kind of new data at what scales would be critical to answering such questions? I feel this paper is incomplete without offering some of such insights.

Response: Please also see R2C17.

In further response, we have modified the final paragraph to set out a rough guideline for future research (lines 511-515): "*The hydrologic data needed to understand hydrologic variability are only now becoming available. With those data we can begin to develop a process-based understanding of hydrologic variability that can be used for a variety of purposes, e.g., deeper understanding of hydro-climatic behaviour, hydrologic risk analysis, climate change assessments and hydrologic sensitivity studies are just a few applications that spring to mind.*".

Inter-annual variability of the global terrestrial water cycle

Dongqin Yin[1,2], Michael L. Roderick[1,3]

[1]Research School of Earth Sciences, Australian National University, Canberra, ACT, 2601, Australia

[2]Australian Research Council Centre of Excellence for Climate System Science, Canberra, ACT, 2601, Australia

[3]Australian Research Council Centre of Excellence for Climate Extremes, Canberra, ACT, 2601, Australia

Correspondence to: (dongqin.yin@anu.edu.au)

Abstract:

Variability of the terrestrial water cycle, i.e., precipitation (*P*), evapotranspiration (*E*), runoff (*Q*) and water storage change (Δ*S*) is the key to understanding hydro-climate extremes. However, a comprehensive global assessment for the partitioning of variability in *P* between *E*, *Q* and Δ*S* is still not available. In this study, we use the recently released global monthly hydrologic reanalysis product known as the Climate Data Record (CDR) to conduct an initial investigation of the inter-annual variability of the global terrestrial water cycle. We first examine global patterns in partitioning the long-term mean $\bar{P}$ between the various sinks $\bar{E}$, $\bar{Q}$ and $\overline{\Delta S}$ and confirm the well-known patterns with $\bar{P}$ partitioned between $\bar{E}$ and $\bar{Q}$ according to the aridity index. In a new analysis based on the concept of variability source and sinks we then examine how variability in the precipitation σ_P^2 (the source) is partitioned between the three variability sinks σ_E^2, σ_Q^2 and $\sigma_{\Delta S}^2$ along with the three relevant covariance terms, and how that partitioning varies with the aridity index. We find that the partitioning of inter-annual variability does not simply follow the mean state partitioning. Instead we find that σ_P^2 is mostly partitioned between σ_Q^2, $\sigma_{\Delta S}^2$ and the associated covariances. We also find that the magnitude of the covariance components can be large and often negative, indicating that variability in the sinks (e.g., σ_Q^2, $\sigma_{\Delta S}^2$) can, and regularly does, exceed variability in the source (σ_P^2). Further investigations under extreme conditions revealed that in extremely dry environments the variance partitioning is closely related to the water storage capacity. With limited storage capacity the partitioning of σ_P^2 is mostly to σ_E^2, but as the storage capacity increases the partitioning of σ_P^2 is increasingly shared between σ_E^2, $\sigma_{\Delta S}^2$ and the covariance between those variables. In other environments (i.e., extremely wet and semi-arid/semi-humid) the variance partitioning proved to be extremely complex and a synthesis has not been developed. We anticipate that a major scientific effort will be needed to develop a synthesis of hydrologic variability.

Deleted:

Deleted: 2,

Deleted: (Eq. 2)

Deleted: , with

Deleted:

Deleted: e

Deleted:

Deleted: was

Deleted: .

1. Introduction

In describing the terrestrial branch of the water cycle, the precipitation (P) is partitioned into evapotranspiration (E), runoff (Q) and change in water storage (ΔS). With averages taken over many years, $\overline{\Delta S}$ is usually assumed to be zero and it has long been recognized that the partitioning of the long-term mean annual precipitation ($\bar{P}$) between $\bar{E}$ and $\bar{Q}$ was jointly determined by the availability of both water ($\bar{P}$) and energy (represented by the net radiation expressed as an equivalent depth of water and denoted $\overline{E_o}$). Using data from a large number of watersheds, Budyko (1974) developed an empirical relation relating the evapotranspiration ratio ($\bar{E}/\bar{P}$) to the aridity index ($\overline{E_o}/\bar{P}$). The resultant empirical relation and other Budyko-type forms (e.g., Fu, 1981; Choudhury, 1999; Yang et al., 2008, Roderick and Farquhar, 2011; Sposito, 2017) that partition P between E and Q have proven to be extremely useful in both understanding and characterising the long-term mean annual hydrological conditions in a given region.

However, the long-term mean annual hydrologic fluxes rarely occur in any given year. Instead, society must (routinely) deal with variability around the long-term mean. The classic hydro-climate extremes are droughts and floods but the key point here is that hydrologic variability is expressed on a full spectrum of time and space scales. To accommodate that perspective, we need to extend our thinking beyond the long-term mean to ask how the variability of P is partitioned into the variability of E, Q and ΔS (e.g., Orth and Destouni, 2018).

Early research on hydrologic variability focussed on extending the Budyko curve. In particular, Koster and Suarez (1999) used the Budyko curve to investigate inter-annual variability in the water cycle. In their framework, the evapotranspiration standard deviation ratio (defined as the ratio of standard deviation for E to P, σ_E/σ_P) was (also) estimated using the aridity index ($\overline{E_o}/\bar{P}$). The classic Koster and Suarez framework has been widely applied and extended in subsequent investigations of the variability in both E and Q, using catchment observations, reanalysis data and model outputs (e.g., McMahon et al., 2011; Wang and Alimohammadi 2012; Sankarasubramanian and Vogel, 2002; Zeng and Cai, 2015). However, typical applications of the Koster and Suarez framework have previously been at regional scales and there is still no comprehensive global assessment for partitioning the variability of P into the variability of E, Q and ΔS. One reason for the lack of a global comprehensive assessment is the absence of gridded global hydrologic data. Interestingly, the atmospheric science community have long

Deleted: fluxes

Deleted: ?

Deleted: analyse

Deleted: the

Deleted: of

used a combination of observations and model outputs to construct gridded global-scale atmospheric re-analyses and such products have become central to atmospheric research. Those atmospheric products also contain estimates of some of the key water cycle variables (e.g., *P*, *E*), such as in the widely used interim ECMWF Re-Analysis (ERA-Interim; Dee et al. 2011). However, the central aim of atmospheric re-analysis is to estimate atmospheric variables, which, understandably, ignores many of the nuances of soil water infiltration, vegetation water uptake, runoff generation and many other processes of central importance in hydrology.

Hydrologists have only recently accepted the challenge of developing their own re-analysis type products with perhaps the first serious hydrologic re-analysis being published as recently as a few years ago (Rodell et al., 2015). More recently, the Princeton University group has extended this early work by making available a gridded global terrestrial hydrologic re-analysis product known as the Climate Data Record (CDR) (Zhang et al., 2018). Briefly, the CDR was constructed by synthesizing multiple in-situ observations, satellite remote sensing products, and land surface model outputs to provide *gridded* estimates of global land precipitation *P*, evapotranspiration *E*, runoff *Q* and total water storage change ΔS (0.5° × 0.5°, monthly, 1984-2010). In developing the CDR, the authors adopted local water budget closure as the fundamental hydrologic principle. That approach presented one important difficulty. Global observations of ΔS start with the GRACE satellite mission from 2002. Hence before 2002 there is no direct observational constraint on ΔS and the authors made the further assumption that the mean annual ΔS over the full 1984-2010 period was zero at every grid-box. That is incorrect in some regions (e.g. Scanlon et al., 2018) and represents an observational problem that cannot be overcome. However, our interest is in the year-to-year variability and for that application, the assumption of no change in the mean annual ΔS over the full 1984-2010 period is unlikely to lead to major problems since we are not looking for subtle changes over time. With that caveat in mind, the aim of this study is to use this new 27-year gridded hydrologic re-analysis product to conduct an initial investigation of the inter-annual variability of the terrestrial branch of the global water cycle.

The paper is structured as follows. We begin in Section 2 by describing the various climate and hydrologic databases including a further assessment of the suitability of the CDR database for this initial variability study. In Section 3, we examine relationships between the mean and variability in the four water cycle variables (*P*, *E*, *Q* and ΔS). In Section 4, we first relate the variability to the classical aridity index and then use those results to

Deleted:

Deleted: the full time series

evaluate the theory of Koster and Suarez (1999). Subsequently we examine how the variance of P is partitioned into the variances (and relevant covariances) of E, Q and ΔS and undertake an initial survey that investigates some of the factors controlling the variance partitioning. We conclude the paper with a discussion summarising what we have learnt about water cycle variability over land by using the CDR database.

2. Methods and Data

2.1 Methods

The water balance is defined by,

$$P(t) = E(t) + Q(t) + \Delta S(t) \qquad (1)$$

with P the precipitation, E the evapotranspiration, Q the runoff and ΔS the total water storage change in time step t. By the usual variance law, we have,

$$\sigma_P^2 = \sigma_E^2 + \sigma_Q^2 + \sigma_{\Delta S}^2 + 2cov(E, Q) + 2cov(E, \Delta S) + 2cov(Q, \Delta S) \qquad (2)$$

that includes all relevant variances (denoted σ^2) and covariances (denoted cov). Eq. (1) is the familiar hydrologic mass balance equation. In that context, Eq. (2) can be thought of as the hydrologic variance balance equation.

2.2 Hydrologic and Climatic Data

We use the recently released global land hydrologic re-analysis known here as the Climate Data Record (CDR) (Zhang et al., 2018). This product includes global precipitation P, evapotranspiration E, runoff Q and water storage change ΔS (0.5° × 0.5°, monthly, 1984-2010). In this study we focus on the inter-annual variability and the monthly water cycle variables (P, E, Q and ΔS) are aggregated to annual totals. The CDR does not report additional radiation variables and we use the NASA/GEWEX Surface Radiation Budget (SRB) Release-3.0 (monthly, 1984-2007, 1° × 1°) database (Stackhouse et al., 2011) to calculate E_o (defined as the net radiation expressed as an equivalent depth of liquid water, Budyko, 1974). We then calculate the aridity index ($\overline{E_o}/\overline{P}$) using P from the CDR and E_o from the SRB databases (see Fig. S1a in the Supplementary Material).

On general grounds, we anticipate that two important factors likely to influence the partitioning of hydrologic variability were the water storage capacity and the presence of ice/snow at the surface. For the storage, the active range of the monthly water storage variation was used to approximate the water storage capacity (S_{max}). In more

Deleted: finalise

Formatted: Justified, Right: 0.03 cm

Deleted: ve

Deleted: control

Deleted: ly we estimaterepresent

Deleted: in this study

Deleted: using the monthly ΔS data in CDR database detail, the water storage $S(t)$ at each time step t (monthly here) was first calculated from the accumulation of $\Delta S(t)$, i.e., $S(t) = S(t\text{-}1) + \Delta S(t)$ where we assumed zero storage at the beginning of the study period (i.e., $S(0) = 0$). With the resulting time series available, S_{max} was estimated as the difference between the maximum and minimum $S(t)$ during the study period at each grid-box (see Fig. S1b in the Supplementary Material). The estimated S_{max} shows a large range from 0 to 1000 mm with the majority of values from 50 to 600 mm (Fig. S1b), which generally agrees with global rooting depth estimates assuming that water occupies from 10 to 30% of the soil volume at field capacity (Jackson et al., 1996; Wang-Erlandsson et al., 2016; Yang et al., 2016). To characterise snow/ice cover, and to distinguish extremely hot and cold regions, we also make use of a gridded global land air temperature dataset from the Climatic Research Unit (CRU TS4.01 database, monthly, 1901-2016, 0.5° × 0.5°) (Harris et al., 2014). (see Fig. S1c in the Supplementary Material).

Deleted: T

2.3 Spatial Mask to Define Study Extent

The CDR database provides an estimate of the uncertainty (± 1σ) for each of the hydrologic variables (P, E, Q, ΔS) in each month. We use those uncertainty estimates to identify and remove regions with high relative uncertainty in the CDR data. The relative uncertainty is calculated as the ratio of root mean square of the uncertainty (± 1σ) to the mean annual P, E and Q at each grid-box following the procedure used by Milly and Dunne (2002a). Note that the long term mean ΔS is zero by construction in the CDR database, and for that reason we did not use ΔS to calculate the relative uncertainty. Grid-boxes with a relative uncertainty (in P, E and Q) of more than 10% are deemed to have high relative uncertainty (Milly and Dunne, 2002a) and were excluded from the study extent. The excluded grid-boxes were mostly in the Himalayan region, the Sahara Desert and in Greenland. The final spatial mask is shown in Fig. S2 and this has been applied throughout this study.

Deleted: 0.1

Deleted: Fig. 1

2.4 Further Evaluation of CDR Data for Variability Analysis

In the original work, the CDR database was validated by comparison with independent observations including (i) mean seasonal cycle of Q from 26 large basins (see Fig. 8 in Zhang et al., 2018), (ii) mean seasonal cycle of ΔS from 12 large basins (Fig. 10 in Zhang et al., 2018), (iii) monthly runoff from 165 medium size basins and a further 862 small basins (Fig. 14 in Zhang et al., 2018), (iv) summer E from 47 flux towers (Fig. 16 in Zhang et al., 2018). Those evaluations did not directly address variability in various water cycle elements. With our focus on the variability we decided to conduct further validations of the CDR database beyond those described in the original work. In particular, we focussed on further independent assessments of E and we use monthly (as opposed to summer) observations of E from FLUXNET to evaluate the variability in E. We also compare the CDR with two other gridded global E products that were not used to develop the CDR including the LandFluxEval database (1° × 1°, monthly, 1989-2005) (Mueller et al., 2013) and the Max Planck Institute database (MPI, 0.5° × 0.5°, monthly, 1982-2011) (Jung et al., 2010).

For the comparison to FLUXNET observations (Baldocchi et al., 2001; Agarwal et al., 2010) we identified 32 flux tower sites (site locations are shown in Fig. S3 and details are shown in Table S1) having at least three years of continuous (monthly) measurements using the FluxnetLSM R package (v1.0) (Ukkola et al. 2017). The monthly totals and annual climatology of P and E from CDR generally follow FLUXNET observations, with high correlations and reasonable Root Mean Square Error (Figs. S4-S5, Table S1). Comparison of the point-based FLUXNET (~ 100 m – 1 km scale) with the grid-based CDR (~ 50 km scale) is problematic since the CDR represents an area that is at least 2500 times larger than the area represented by the individual FLUXNET towers and we anticipate that the CDR record would be "smoothed" relative to the FLUXNET record. With that in mind, we chose to compare the ratio of the standard deviation of E to P between the CDR and FLUXNET databases and this normalised comparison of the hydrologic variability proved encouraging (Fig. S6).

The comparison of E between the CDR and the LandFluxEval and MPI databases also proved encouraging. We found that the monthly mean E from the CDR database is slightly underestimated compared with LandFluxEVAL database (Fig. S7a), but agrees closely with the MPI database (Fig. S8a). In terms of variability, the standard deviations of monthly E from the CDR are in very close agreement with the LandFluxEVAL database (Fig. S7c) but there was a bias and scaling offset for the comparison with the MPI database (Fig. S8c).

We concluded that while the CDR database was unlikely to be perfect, it was nevertheless suitable for an initial exploratory survey of inter-annual variability in the terrestrial branch of the global water cycle.

3. Mean and Variability of Water Cycle Components

3.1 Mean Annual P, E, Q and the Budyko Curve

Deleted: product

Deleted: Fig. S2

Deleted:

Deleted: S3-S4

Deleted: Fig. S5

Formatted: Font:Italic

Deleted: As a further evaluation, we compare gridded E data in the CDR database against two other global E databases (including i.e., LandFluxEVAL (1° × 1°, monthly, 1989-2005) (Mueller et al., 2013) and Max Planck Institute (MPI), 0.5° × 0.5°, monthly, 1982-2011) (Jung et al., 2010) that were not used to construct the CDR database.

Deleted: Fig. S6

Deleted: Fig. S7

Deleted: slightly different than those in the MPI database (Fig. S7Fig. S8c) but were in very close agreement with the LandFluxEVAL database (Fig. S6Fig. S7c).

Deleted: In summary, w

Deleted: the

Deleted: suitable

Deleted: investigation

Deleted: the

The global pattern of mean annual P, E, Q using the CDR data (1984-2007) is shown in Fig. 1. The mean annual P ($\bar{P}$) is prominent in tropical regions, southern China, eastern and western North America (Fig. 1a). The magnitude of mean annual E ($\bar{E}$) more or less follows the pattern of $\bar{P}$ in the tropics (Fig. 1b) while the mean annual Q ($\bar{Q}$) is particularly prominent in the Amazon, South and Southeast Asia, tropical parts of west Africa and in some other coastal regions at higher latitudes (Fig. 1c).

We relate the grid-box level ratio of $\bar{E}$ to $\bar{P}$ in the CDR database to the classical Budyko (1974) curve using the aridity index ($\overline{E_o}/\bar{P}$) (Fig. 2a). As noted previously, in the CDR database, $\overline{\Delta S}$ is forced to be zero and this enforced steady state (i.e., $\bar{P} = \bar{E} + \bar{Q}$) allowed us to also predict the ratio of $\bar{Q}$ to $\bar{P}$ using the same Budyko curve (Fig. 2b). The Budyko curves follow the overall trend in the CDR data, which agrees with previous studies showing that the aridity index can be used to predict water availability (e.g., Gudmundsson et al., 2016). However, there is substantial scatter due to, for example, regional variations related to seasonality, water storage change and the physics of runoff generation (Milly, 1994a, b). With that caveat in mind, the overall patterns are as expected with $\bar{E}$ following $\bar{P}$ in dry environments ($\overline{E_o}/\bar{P} > 1.0$) while $\bar{E}$ follows $\overline{E_o}$ in wet environments ($\overline{E_o}/\bar{P} \leq 1.0$) (Fig. 2).

3.2 Inter-annual Variability in P, E, Q and ΔS

We use the variance balance equation (Eq. 2) to partition the inter-annual σ_P^2 into separate components due to σ_E^2, σ_Q^2, $\sigma_{\Delta S}^2$ along with the three covariance components ($2cov(E,Q)$, $2cov(E,\Delta S)$, $2cov(Q,\Delta S)$) (Fig. 3). The spatial pattern of σ_P^2 (Fig. 3a) is very similar to that of $\bar{P}$ (Fig. 1a), which implies that the σ_P^2 is positively correlated with $\bar{P}$. In contrast the partitioning of σ_P^2 to the various components is very different from the partitioning of $\bar{P}$ (cf. Fig. 1 and 3). First we note that while the overall spatial pattern of σ_E^2 more or less follows σ_P^2, the overall magnitude of σ_E^2 is much smaller than σ_P^2 and σ_Q^2 in most regions, and in fact σ_E^2 is also generally smaller than $\sigma_{\Delta S}^2$. The prominence of $\sigma_{\Delta S}^2$ (compared to σ_E^2) surprised us. The three covariance components ($cov(E,Q)$, $cov(E,\Delta S)$, $cov(Q,\Delta S)$) are also important in some regions. In more detail, the $cov(E,Q)$ term is prominent in regions where σ_Q^2 is large and is mostly negative in those regions (Fig. 3e), indicating that years with lower E are associated with higher Q and vice-versa. There are also a few regions with prominent positive values for $cov(E,Q)$ (e.g., the seasonal hydroclimates of northern Australia) indicating that in those regions, years with a higher E are associated with higher Q. The $cov(E,\Delta S)$ term (Fig. 3f) has a similar spatial pattern to the $cov(E,Q)$ term (Fig. 3e) but with a smaller overall magnitude. Finally, the $cov(Q,\Delta S)$ term shows a more

Deleted: Fig. 2
Deleted: Fig. 2
Deleted: Fig. 2
Deleted: Fig. 2
Deleted: Fig. 3
Deleted: Fig. 3
Deleted: dominant effect of
Deleted: on
Deleted: T
Deleted: Fig. 3
Deleted: Fig. 4
Deleted: Fig. 4
Deleted: Fig. 2
Deleted: Fig. 2
Deleted: 4
Deleted: Fig. 4
Deleted: Fig. 4
Deleted: Fig. 4

complex spatial pattern, with both prominent positive and negative values (Fig. 3g) in regions where σ_Q^2 (Fig. 3c) and $\sigma_{\Delta S}^2$ (Fig. 3d) are both large.

These results show that the spatial patterns in variability are not simply a reflection of patterns in the long-term mean state. On the contrary, we find that of the three primary variance terms, the overall magnitude of (inter-annual) σ_E^2 is the smallest implying the least (inter-annual) variability in *E*. This is very different from the conclusions based on spatial patterns in the mean *P*, *E* and *Q* (see section 3.1). Further, while σ_Q^2 more or less follows σ_P^2 as expected, we were surprised by the magnitude of $\sigma_{\Delta S}^2$ which, in general, substantially exceeds the magnitude of σ_E^2. Further, the magnitude of the covariance terms can be important, especially in regions with high σ_Q^2. However, unlike the variances, the covariance can be both positive and negative and this introduces additional complexity. For example, with a negative covariance it is possible for the variance in *Q* (σ_Q^2) to exceed the variance in *P* (σ_P^2). To examine that in more detail we calculated the equivalent frequency distribution for each of the plots in Fig. 3. The results (Fig. S9) further emphasise that in general, σ_E^2 is the smallest of the variances (Fig. S9b). We also note that the frequency distributions for the covariances (Fig. S9efg) are not symmetrical. In summary, it is clear that spatial patterns in the inter-annual variability of the water cycle (Fig. 3) do not simply follow the spatial patterns for the inter-annual mean (Fig. 1).

3.3 Relation Between Variability and the Mean State for *P*, *E*, *Q*

Differences in the spatial patterns of the mean (Fig. 1) and inter-annual variability (Fig. 3) in the global water cycle led us to further investigate the relation between the mean and the variability for each separate component. Here we relate the standard deviation (σ_P, σ_E, σ_Q) instead of the variance to the mean of each water balance flux (Fig. 4) since the standard deviation has the same physical units as the mean making the results more comparable. As inferred previously, we find σ_P to be positively correlated with $\bar{P}$ but with substantial scatter (Fig. 4a). The same result more or less holds for the relation between σ_Q and $\bar{Q}$ (Fig. 4c). In contrast the relation between σ_E and $\bar{E}$ is very different (Fig. 4b). In particular, σ_E is a small fraction of $\bar{E}$ and this complements the earlier finding (Fig. 4b) that the inter-annual variability for *E* is generally smaller than for the other physical variables (*P*, *Q* and Δ*S*). (The same result was also found using both LandFluxEVAL and MPI databases, see Fig. S10 in the Supplementary Material.) Importantly, unlike *P* and *Q*, *E* is constrained by both water and energy availability

Deleted: Fig. 4
Deleted: Fig. 4
Deleted: Fig. 4
Deleted: previous
Deleted: Fig. 4
Deleted: Fig. 5
Deleted: Fig. 5
Deleted: Fig. 5
Deleted: Fig. 4
Deleted: Fig. 2
Deleted: Fig. 2
Deleted: Fig. 4
Deleted: Fig. 6
Deleted: Fig. 6
Deleted: Fig. 6
Deleted: Fig. 6
Deleted: Fig. 6
Deleted: ,
Deleted: or
Formatted: Font:Not Italic
Deleted: Fig. S8

(Budyko, 1974) and the limited inter-annual variability in E presumably reflects limited inter-annual variability in the available (radiant) energy (E_o). This is something that could be investigated in a future study.

4. Relating the Variability of Water Cycle Components to Aridity

In the previous section, we investigated spatial patterns of the mean and the variability in the global water cycle. In this section, we extend that by investigating the partitioning of σ_P^2 to the three primary physical terms (σ_E^2, σ_Q^2, $\sigma_{\Delta S}^2$) along with the three relevant covariances. For that, we begin by comparing the Koster and Suarez (1999) theory against the CDR data and then investigate how the partitioning of the variance is related to the aridity index $\overline{E_o}/\overline{P}$ (see Fig. S1a in the Supplementary Material). Following that, we investigate variance partitioning in relation to both our estimate of the storage capacity S_{max} (see Fig. S1b in the Supplementary Material) as well as the mean annual air temperature $\overline{T_a}$ (see Fig. S1c in the Supplementary Material) that we use as a surrogate for snow/ice cover. We finalise this section by examining the partitioning of variance at three selected study sites that represent extremely dry/wet, high/low water storage capacity and the hot/cold spectrums.

4.1 Comparison with the Koster and Suarez (1999) Theory

We first evaluate the classical empirical curve of Koster and Suarez (1999) by relating ratios σ_E/σ_P and σ_E/σ_P to the aridity index (Fig. 5). The ratio σ_E/σ_P in the CDR database is generally overestimated by the empirical Koster and Suarez curve, especially in dry environments (e.g., $\overline{E_o}/\overline{P}$ > 3) (Fig. 5a). The inference here is that the Koster and Suarez theory predicts σ_E/σ_P to approach unity in dry environments while the equivalent value in the CDR data is occasionally unity but is generally smaller. With σ_E/σ_P generally overestimated by the Koster and Suarez theory we expect, and find, that σ_Q/σ_P is generally underestimated by the same theory (Fig. 5b). The same overestimation was found based on the other two independent databases for E (LandFluxEVAL and MPI) (Fig. S11). This overestimation is discussed further in section 5.

4.2 Relating Inter-annual Variability to Aridity

Here we examine how the fraction of the total variance in precipitation accounted for by the three primary variance terms along with the three covariance terms varies with the aridity index ($\overline{E_o}/\overline{P}$) (Fig. 6). (Also see Fig. S12 for the spatial maps.) The ratio σ_E^2/σ_P^2 is close to zero in extremely wet regions and has an upper limit noted

Deleted: ***P E*, *Q* and Δ*S***

Deleted:

Deleted: Fig. 7

Deleted: Fig. 7

Deleted: Fig. S9

Deleted: Fig. 8

Deleted: Fig. S10

previously (Fig. 5a) that approaches unity in extremely dry regions (Fig. 6a). The ratio σ_Q^2/σ_P^2 is close to zero in extremely dry regions but approaches unity in extremely wet regions but with substantial scatter (Fig. 6b). The ratio $\sigma_{\Delta S}^2/\sigma_P^2$ is close to zero in both extremely dry/wet regions (Fig. 6c) and shows the largest range at an intermediate aridity index ($\overline{E_o}/\overline{P}$ ~ 1.0).

Deleted: Fig. 7
Deleted: Fig. 8
Deleted: Fig. 8
Deleted: Fig. 8
Deleted: but

The covariance ratios are all small in extremely dry (e.g., $\overline{E_o}/\overline{P}$ ≥6.0) environments and generally show the largest range in semi-arid and semi-humid environments. The peak magnitudes for the three covariance components consistently occur when $\overline{E_o}/\overline{P}$ is close to 1.0 which is the threshold often used to separate wet and dry environments.

4.3 Further Investigations on the Factors Controlling Partitioning of the Variance

Results in the previous section demonstrated that spatial variation in the partitioning of σ_P^2 into σ_E^2, σ_Q^2, $\sigma_{\Delta S}^2$ and the three covariance components is complex (Fig. 6). To help further understand inter-annual variability of the terrestrial water cycle, we conduct further investigations in this section using two factors likely to have a major influence on the variance partitioning of σ_P^2. The first is the storage capacity $S_{\max}$ (see Fig. S1b in the Supplementary Material). The second is the mean annual air temperature $\overline{T_a}$ (see Fig. S1c in the Supplementary Material) which is used here as a surrogate for snow/ice presence.

Deleted: T
Deleted: results (Sections 4.1 and 4.2) have

4.3.1 Relating Inter-annual Variability to Storage Capacity

We first relate the partitioning of σ_P^2 to water storage capacity ($S_{\max}$) by repeating Fig. 6 but instead we use a logarithmic scale for the x-axis and we distinguish $S_{\max}$ via the background colour (Fig. 7). To eliminate the possible overlap of grid-cells in the colouring process, all the grid-cells over land are further separated using different latitude ranges (as shown in the four columns of Fig. 7), i.e., 90N-60N, 60N-30N, 30N-0 and 0-90S. We find that $S_{\max}$ is relatively high in wet environments ($\overline{E_o}/\overline{P}$ ≤1.0, Fig. 7a) but shows no obvious relation to the partitioning of σ_P^2. However, in dry environments ($\overline{E_o}/\overline{P}$ >1.0) the ratio σ_E^2/σ_P^2 apparently decreases with the increase of $S_{\max}$ (Fig. 7a-d). That relation is particularly obvious in extremely dry environments ($\overline{E_o}/\overline{P}$ ≥ 6.0) at equatorial latitudes where there is an upper limit of σ_E^2/σ_P^2 close to 1.0 when $S_{\max}$ is small (blue grid-cells in Fig. 7c). The interpretation for those extremely dry environments is that when $S_{\max}$ is small, σ_P^2 is almost completely

Deleted: Fig. 8
Deleted: Fig. 9
Deleted: Fig. 9
Deleted: with
Deleted: Fig. 9
Deleted: Fig. 9

partitioned into σ_E^2 (Fig. 7bc) with the other variance and covariance components close to zero. While for those same extremely dry environments, as S_{max} increases, the partitioning of σ_P^2 is shared between σ_E^2 and $\sigma_{\Delta S}^2$ and their covariance (Fig. 7cks) while σ_Q^2 and its covariance components remain close to zero (Fig. 7gow). However, at polar latitudes in the northern hemisphere (panels in the first and second columns of Fig. 7) there are variations that could not be easily associated with variations in S_{max} which led us to further investigate the role of snow/ice on the variance partitioning in the following section.

4.3.2 Relating Inter-annual Variability to Mean Air Temperature

To understand the potential role of snow/ice in modifying the variance partitioning, we repeat the previous analysis (Fig. 7) but here we use the mean annual air temperature ($\overline{T_a}$) to colour the grid-cells to (crudely) indicate the presence of snow/ice (Fig. 8). The results are complex and not easy to simply understand. The most important difference revealed by this analysis is in the hydrologic partitioning between cold (first column) and hot (third column) conditions in wet environments ($\overline{E_o}/\overline{P} \leq 0.5$). In particular, when $\overline{T_a}$ is high, σ_P^2 is almost completely partitioned into σ_Q^2 in wet environments (e.g., $\overline{E_o}/\overline{P} \leq 0.5$, Fig. 8g). In contrast, when $\overline{T_a}$ is low in a wet environment ($\overline{E_o}/\overline{P} \leq 0.5$ in first column of Fig. 8), there are substantial variations in the hydrologic partitioning. That result reinforces the complexity of variance partitioning in the presence of snow/ice.

4.4 Case Studies

The previous results (Section 4.3) have demonstrated that the partitioning of σ_P^2 is influenced by the water storage capacity (S_{max}) in extremely dry environments ($\overline{E_o}/\overline{P} \geq 6.0$) and that the presence of snow/ice is important (as indicated by mean air temperature ($\overline{T_a}$)) in extremely wet environments ($\overline{E_o}/\overline{P} \leq 0.5$). In this section, we examine, in greater detail, several sites to gain deeper understanding of the partitioning of σ_P^2. For that purpose, we selected three sites based on extreme values for the three explanatory parameters, i.e., $\overline{E_o}/\overline{P}$ (Fig. S1a), S_{max} (Fig. S1b) and $\overline{T_a}$ (Fig. S1c). The criteria to select three climate sites are as follows, Site 1: dry ($\overline{E_o}/\overline{P} \geq 6.0$) and small S_{max} ($S_{max} \approx 0$), Site 2: dry ($\overline{E_o}/\overline{P} \geq 6.0$) and relatively large S_{max} ($S_{max} \gg 0$) and Site 3: wet ($\overline{E_o}/\overline{P} \leq 0.5$) and hot ($\overline{T_a}$ > 25 ˚C). For each of the three classes, we use a representative grid-cell (Fig. 9) to show the original time series (Fig. 10) and the partitioning of the variability (Fig. 11).

Deleted: Fig. 9

Deleted: Fig. 9

Deleted: ith

Deleted: Fig. 9

Deleted: Fig. 9

Deleted: Fig. 9

Deleted: identify

Deleted: Fig. 10

Deleted: Most of the variations at polar latitudes in the northern hemisphere (panels in the first and second columns of Fig. 10Fig. 8) is associated with low air temperature (e.g., $\overline{T_a}$ < 0 ˚C in blue colour), making the results associated with high air temperature (e.g., $\overline{T_a}$ > 10 ˚C in the third and fourth columns of Fig. 8green-yellow-red colours) relatively more compactshow less scatters. That pattern is particularly obvious in extremely wet environment ($\overline{E_o}/\overline{P} \leq 0.5$), where the ratio σ_Q^2/σ_P^2 is close to 1.0 when $\overline{T_a}$ is high (e.g., $\overline{E_o}/\overline{P} \leq$ 0.5 and $\overline{T_a}$ > 10 ˚C, with green-yellow-red grid-cells on the panels in the second row of Fig. 10Fig. 8gh) but shows lots of scatters when $\overline{T_a}$ is low (e.g., $\overline{T_a}$ < 0 ˚C, Fig. 8ef)with the other variance-covariance components close to zero. This indicates that in extremely wet environment, when $\overline{T_a}$ is high, σ_P^2 is almost completely partitioned into σ_Q^2 (e.g., $\overline{E_o}/\overline{P} \leq 0.5$ and T_a > 10 ˚C in the third and fourth columns of Fig. 8). However, when $\overline{T_a}$ is low in extremely wet environment, there are substantial variations in all variance-covariance components (e.g., $\overline{E_o}/\overline{P} \leq 0.5$ and $\overline{T_a}$ < 0 ˚C, see the blue grid-cells on the panels in the first and second columns column of Fig. 10Fig. 8). That result indicates the complexity of variance partitioning associated with the presence of snow/ice.

Formatted: Font:10 pt, Not Italic

Formatted: Font:10 pt

Formatted: Font:10 pt

Formatted: Font:10 pt

Formatted: Font:10 pt

Formatted: Font:10 pt

Formatted: Font:10 pt, Not Italic

Formatted: Font:10 pt, Not Italic

Formatted: Font:10 pt, Not Italic

Formatted: Font:10 pt, Not Italic

Deleted: predominantly

Deleted:

Deleted: sites,

Deleted: Fig. 11

Deleted: Fig. 12

Deleted: Fig. 13

We show the P, E, Q and ΔS time series along with the relevant variances and covariances in Fig. 10. Starting with the two dry sites, at the site with low storage capacity (Site 1), the time series shows that E closely follows P leaving annual Q and ΔS close to zero (Fig. 10a). The variance of P (σ_P^2 = 206.9 mm^2) is small and almost completely partitioned into the variance of E (σ_E^2 = 196.9 mm^2), leaving very limited variance for Q, ΔS and all three covariance components (Fig. 10b). At the dry site with larger storage capacity (Site 2), E, Q and ΔS do not simply follow P (Fig. 10c). As a consequence, the variance of P (σ_P^2 = 2798.0 mm^2) is shared between E (σ_E^2 = 1150.2 mm^2), ΔS ($\sigma_{\Delta S}^2$ = 800.5 mm^2) and their covariance component ($2cov(E, \Delta S)$ = 538.4 mm^2, Fig. 10d). Switching now to the remaining wet and hot site (Site 3), we note that Q closely follows P, with ΔS close to zero and E showing little inter-annual variation (Fig. 10e). The variance of P (σ_P^2 = 57374.4 mm^2) is relatively large and almost completely partitioned into the variance of Q (σ_Q^2 = 57296.4 mm^2), leaving very limited variance for E and ΔS and the three covariance components (Fig. 10f). We also examined numerous other sites with similar extreme conditions as the three case study sites and found the same basic patterns as reported above.

To put the data from the three case study sites into a broader variability context we position the site data onto a backdrop of original Fig. 6. As noted previously, at Site 1, the ratio σ_E^2/σ_P^2 is very close to unity (Fig. 11a), and under this extreme condition, we have the following approximation,

$$\sigma_P^2 \approx \sigma_E^2 \quad \text{(Site 1, dry and } S_{max} \approx 0) \tag{3}$$

In contrast, for Site 2 with the same aridity index but higher S_{max}, we have,

$$\sigma_P^2 \approx \sigma_E^2 + \sigma_{\Delta S}^2 + 2cov(E, \Delta S) \quad \text{(Site 2, dry and } S_{max} \gg 0) \tag{4}$$

Finally, at Site 3, we have,

$$\sigma_P^2 \approx \sigma_Q^2 \quad \text{(Site 3, wet and hot)} \tag{5}$$

4.5 Synthesis

The above simple examples demonstrate that aridity $\overline{E_o}/\overline{P}$, storage capacity S_{max} and to a lesser extent, air temperature $\overline{T_a}$, all play some role in the partitioning of σ_P^2 to the various components. Our synthesis of the results for the partitioning of σ_P^2 is summarised in Fig. 12. In dry environments with low storage capacity ($S_{max} \approx 0$) we have minimal runoff and expect that σ_P^2 is more or less completely partitioned into σ_E^2 (Fig. 12a). In those environments, (inter-annual) variations in storage $\sigma_{\Delta S}^2$ play a limited role in setting the overall variability. However, in dry environments with larger storage capacity ($S_{max} \gg 0$), σ_E^2 is only a small fraction of σ_P^2 (Fig. 12a)

Deleted: Fig. 12
Deleted: Fig. 12
Deleted: Fig. 12
Deleted: high
Deleted: Fig. 12
Deleted: Fig. 12
Deleted: Fig. 12
Deleted: Fig. 12
Deleted: Fig. 8
Deleted: Fig. 13
Deleted:
Deleted: roles
Deleted: Fig. 14
Deleted: and
Deleted:
Deleted: environments
Deleted: Fig. 14
Deleted: and
Deleted: environments

leaving most of the overall variance in σ_P^2 to be partitioned to $\sigma_{\Delta S}^2$ and the covariance between E and ΔS (Fig. 12c and Fig. 12e). This emphasises the hydrological importance of water storage capacity in buffering variations of the water cycle under dry conditions.

Under extremely wet conditions, the largest difference in variance partitioning is not due to differences in storage capacity but is instead related to differences in mean air temperature. In wet and hot environments, we have maximum runoff and find that σ_P^2 is more or less completely partitioned into σ_Q^2 (Fig. 12b) while the partitioning to σ_E^2 and $\sigma_{\Delta S}^2$ is small. However, in wet and cold environments, the variance partitioning shows great complexity with σ_P^2 being partitioned into all possible components. We suggest that this emphasises the hydrological importance of thermal processes (melting/freezing) under extremely cold conditions.

However, the most complex patterns to interpret are those for semi-arid to semi-humid environments (i.e., $\overline{E_o}/\overline{P}$ ~1.0). Despite a multitude of attempts over an extended period we were unable to develop a simple useful synthesis to summarise the partitioning of variability in those environments. We found that the three covariance terms all play important roles and we also found that simple environmental gradients (e.g., dry/wet, high/low storage capacity, hot/cold) could not easily explain the observed patterns. We anticipate that vegetation related processes (e.g., phenology, rooting depth, gas exchange characteristics, disturbance, etc.) may prove to be important in explaining hydrologic variability in these biologically productive regions that support most of human population. This result implies that a major scientific effort will be needed to develop a synthesis of the controlling factors for variability of the water cycle in these environments.

5. Discussion and Conclusions

Importantly, hydrologists have long been interested in hydrologic variability, but without readily available databases it has been difficult to quantify water cycle variability. For example, we are not aware of maps showing global spatial patterns in variance for any terms of the water balance (except for P). In this study, we describe an initial investigation of the inter-annual variability of the terrestrial branch in the global water cycle that uses the recently released global monthly Climate Data Record (CDR) database for P, E, Q and ΔS. The CDR is one of the first dedicated hydrologic reanalysis databases and includes data for a 27-year period. Accordingly, we could only examine hydrologic variability over this relatively short period. Further, we expect future improvements and

Deleted: attributed

Deleted: Fig. 14

Deleted: Fig. 14

Deleted: implies

Deleted: huge

Deleted: occurs between the hot and cold conditions instead of water storage capacity conditions in dry conditionsenvironments.

Deleted: expect

Deleted: Fig. 14

Deleted: , and the variations in evapotranspiration

Deleted: storage

Deleted: play a limited role in setting the overall variability.

Deleted: , with σ_Q^2/σ_P^2 and $\sigma_{\Delta S}^2/\sigma_P^2$ vary a lot caused by snow/ice melting.

Deleted: This signifies

Deleted: T

Deleted: In those environments,

Deleted: A

Deleted: iscover

Deleted: ... [1]

Deleted: aware that the water storage effects were going to be important for understanding water cycle variability (e.g., Milly and Dunne, 2002b; Zhang et al., 2008; Donohue et al., 2010; Wang and Alimohammadi, 2012)

Deleted: in a consistent way.

Moved (insertion) [1]

Deleted: We start by investigating the partitioning of P in the water cycle in terms of long-term mean and then extend that to the inter-annual variability.

modifications as the hydrologic community seeks to further develop and refine these new reanalysis databases. With those caveats in mind, we started this analysis by first investigating the partitioning of P in the water cycle in terms of long-term mean and then extended that to the inter-annual variability using a theoretical variance balance equation (Eq. 2). Despite the initial nature of this investigation we have been able to establish some useful general principles.

The mean annual P is mostly partitioned into mean annual E and Q, as is well known, and the results using the CDR were generally consistent with the earlier Budyko framework (Fig. 2). Having established that, the first general finding is that the spatial pattern in the partitioning of inter-annual variability in the water cycle is not simply a reflection of the spatial pattern in the partitioning of the long-term mean. In particular, with the variance calculations, the annual anomalies are squared and hence the storage anomalies do not cancel out like they do when calculating the mean. With that in mind, we were surprised that the inter-annual variability of water storage change ($\sigma^2_{\Delta S}$) is typically larger than the inter-annual variability of evapotranspiration (σ^2_E) (cf. Fig. 3b and 3d). The consequence is that $\sigma^2_{\Delta S}$ is more important than σ^2_E for understanding inter-annual variability of global water cycle. A second important generalisation is that unlike the variance components which are all positive, the three covariance components in the theory (Eq. 2) can be both positive and negative. We report results here showing both large positive and negative values for the three covariance terms (Fig. 3efg). This was especially prevalent in biologically productive regions ($0.5<\overline{E_o}/\overline{P}<1.5$, Fig. 3eg). When examining the mean state, we are accustomed to think that P sets a limit to E, Q and ΔS, as per the mass balance (Eq. 1). But the same thinking does not extend to the variance balance since the covariance terms on the right hand side of Eq. 2 can be both large and negative leading to circumstances where the variability in the sinks (σ^2_E, σ^2_Q, $\sigma^2_{\Delta S}$) could actually exceed variability in the source (σ^2_P).

Our initial attempt to develop deeper understanding of variance partitioning was based on a series of case studies located in extreme environments (wet/dry vs hot/cold vs high/low water storage capacity). The results offered some further insights about hydrologic variability. For example, under extremely dry (water-limited) environments, with limited storage capacity (S_{max}) we found that E follows P and σ^2_E follows σ^2_P, with σ^2_Q and $\sigma^2_{\Delta S}$ both approaching zero. However, as S_{max} increases, the partitioning of σ^2_P progressively shifts to a balance between σ^2_E, $\sigma^2_{\Delta S}$ and cov(E, ΔS) (Figs. 10-12). This result explains the overestimation of σ_E/σ_P by the empirical theory of

Deleted:

Deleted:

Deleted: From this

Deleted: previous

Deleted: work

Deleted: W

Deleted: initially

Deleted: can be relatively large and are negative in some regions

Deleted: The consequence is that variability in the sinks (e.g., σ^2_Q, $\sigma^2_{\Delta S}$) can, and do, exceed the variability in the source (σ^2_P)

Deleted: , especially

Moved (insertion) [2]

Koster and Suarez (1999) which implicitly assumed no inter-annual change in storage. The Koster and Suarez empirical theory is perhaps better described as an upper limit that is based on minimal storage capacity, and that any increase in storage capacity would promote the partitioning of σ_P^2 to $\sigma_{\Delta S}^2$ particularly under dry conditions (Figs. 10-12).

In extremely wet/hot environments (i.e., no snow/ice presence) we found σ_P^2 to be mostly partitioned to σ_Q^2 (with both σ_E^2 and $\sigma_{\Delta S}^2$ approaching zero, Fig. 10). In contrast, in extremely wet/cold environments, the partitioning of σ_P^2 was highly (spatially) variable presumably because of spatial variability in the all-important thermal processes (freeze/melt).

The most complex results were found in mesic biologically productive environments ($0.5<\overline{E_o}/\overline{P}<1.5$), where all three covariance terms (Eq. 2) were found to be relatively large and therefore they all played critical roles in the overall partitioning of variability (Fig. 6). As noted above, in many of these regions, the (absolute) magnitudes of the covariances were actually larger than the variances of the water balance components E, Q and ΔS (e.g., Fig. 3). That result demonstrates that deeper understanding of the process-level interactions that are embedded within each of the three covariance terms (e.g., the role of seasonal vegetation variation) will be needed to develop process-based understanding of variability in the water cycle in these biologically productive regions ($0.5<\overline{E_o}/\overline{P}<1.5$).

The syntheses of the long-term mean water cycle originated in 1970s (Budyko, 1974), and it took several decades for those general principles to become widely adopted in the hydrologic community. The hydrologic data needed to understand hydrologic variability are only now becoming available. With those data we can begin to develop a process-based understanding of hydrologic variability that can be used for a variety of purposes, e.g., deeper understanding of hydro-climatic behaviour, hydrologic risk analysis, climate change assessments and hydrologic sensitivity studies are just a few applications that spring to mind. The initial results presented here show that a major intellectual effort will be needed to develop a general understanding of hydrologic variability.

Deleted: negligible storage variation.

Deleted: at

Deleted: Under

Deleted: impact

Deleted: under

Deleted: conditions,

Deleted: the

Deleted: These results highlight a key point that while the long-term mean state is not especially sensitive to variations in either water storage or physical phase (liquid/solid), the overall hydrologic variability is expected to be sensitive to those same variations.

Deleted: In

Deleted: for instance,

Deleted: such as hydrologic water risk analysis,

Deleted: . Major

Deleted: s

Deleted: are still needed

Moved up [1]: We start by investigating the partitioning of P in the water cycle in terms of long-term mean and then extend that to the inter-annual variability.

Moved up [2]: $0.5<\overline{E_o}/\overline{P}<1.5$

Deleted: . We start by investigating the partitioning of P in the water cycle in terms of long-term mean and then extend that to the inter-annual variability. While the mean annual P is mostly partitioned into mean annual E and Q, as is well known. However, we find that the variance of P (σ_P^2) is mostly partitioned into the variance of Q (σ_Q^2) and variance of ΔS ($\sigma_{\Delta S}^2$). This result indicates that the global patterns of inter-annual variability in the water cycle do not simply follow the long-term mean. A second general finding is that the covariance components are important and can be negative in some regions, indicating the variability in the sinks (e.g., σ_Q^2, $\sigma_{\Delta S}^2$) can, and do, exceed the variability in the source (σ_P^2). Our attempts to develop deeper understanding of variance partitioning led to some syntheses in extreme environments (wet/dry vs hot/cold). In particular, we find that in extremely dry environments (either hot/cold) the partitioning of σ_P^2 is closely related to the water storage capacity. With limited storage capacity, the partitioning of σ_P^2 is mostly to σ_E^2 but as the storage capacity increases, the partitioning of σ_P^2 is increasingly shared between σ_E^2 and $\sigma_{\Delta S}^2$ and the covariance between those variables (Fig. 14Fig. 12). In contrast, in extremely wet environments, there are large divergences in the variance partitioning between hot and cold conditions. In hot conditions, σ_P^2 is mostly partitioned to σ_Q^2 but under cold conditions, σ_P^2 is partitioned to all available variability sinks (Fig. 14Fig. 12). However, in biologically productive semi-arid/semi-humid ($0.5<\overline{E_o}/\overline{P}<1.5$) environments, we found the variance partitioning to be very complex and that partitioning was not obviously associated with simple environmental factors. A general understanding of hydro-climatic variability remains a major intellectual challenge and we anticipate major efforts will be needed to synthesise general principles that cover the full spectrum of hydrologic variability.

Acknowledgements

This research was supported by the Australian Research Council (CE11E0098, CE170100023), and D.Y. also acknowledges support by the National Natural Science Foundation of China (51609122). We thank Dr Anna Ukkola for help in accessing the FLUXNET database. We thank the reviewers (including Dr René Orth and two anonymous reviewers) for helpful comments that improved the manuscript. The authors declare that there is no conflict of interests regarding the publication of this paper. All data used in this paper are available online as referenced in the 'Methods and Data' section.

References

Agarwal, D. A., Humphrey, M., Beekwilder, N. F., Jackson, K. R., Goode, M. M., and van Ingen, C.: A data-centered collaboration portal to support global carbon-flux analysis, Concurr. Comp-Pract. E., 22, 2323-2334, https://doi.org/10.1002/cpe.1600, 2010.

Baldocchi, D., Falge, E., Gu, L., Olson, R., Hollinger, D., Running, S., Anthoni, P., Bernhofer, C., Davis, K., Evans, R., Fuentes, J., Goldstein, A., Katul, G., Law, B., Lee, X., Malhi, Y., Meyers, T., Munger, W., Oechel, W., Paw U, K. T., Pilegaard, K., Schmid, H. P., Valentini, R., Verma, S., Vesala, T., Wilson, K., and Wofsy, S.: FLUXNET: A New Tool to Study the Temporal and Spatial Variability of Ecosystem-Scale Carbon Dioxide, Water Vapor, and Energy Flux Densities, B. Am. Meteorol. Soc., 82, 2415-2434, https://doi.org/10.1175/1520-0477(2001)082<2415:FANTTS>2.3.CO;2, 2001.

Budyko, M. I.: Climate and Life. Academic Press, London, 1974.

Choudhury, B. J.: Evaluation of an empirical equation for annual evaporation using field observations and results from a biophysical model, J. Hydrol., 216, 99-110, https://doi.org/10.1016/S0022-1694(98)00293-5, 1999.

Dee, D. P., Uppala, S. M., Simmons, A. J., Berrisford, P., Poli, P., Kobayashi, S., Andrae, U., Balmaseda, M. A., Balsamo, G., Bauer, P., Bechtold, P., Beljaars, A. C. M., van de Berg, L., Bidlot, J., Bormann, N., Delsol, C., Dragani, R., Fuentes, M., Geer, A. J., Haimberger, L., Healy, S. B., Hersbach, H., Hólm, E. V., Isaksen, L., Kållberg, P., Köhler, M., Matricardi, M., McNally, A. P., Monge-Sanz, B. M., Morcrette, J. J., Park, B. K., Peubey, C., de Rosnay, P., Tavolato, C., Thépaut, J. N., and Vitart, F.: The ERA-Interim reanalysis: configuration and performance of the data assimilation system, Q. J. R. Meteorol. Soc., 137, 553-597, https://doi.org/10.1002/qj.828, 2011.

Donohue, R. J., Roderick, M. L., and McVicar, T. R.: Can dynamic vegetation information improve the accuracy of Budyko's hydrological model?, J. Hydrol., 390, 23-34, https://doi.org/10.1016/j.jhydrol.2010.06.025, 2010.

Fu, B. P.: On the Calculation of the Evaporation from Land Surface, Sci. Atmos. Sin., 5, 23-31, 1981.

Gudmundsson, L., Greve, P., and Seneviratne, S. I.: The sensitivity of water availability to changes in the aridity index and other factors—A probabilistic analysis in the Budyko space, Geophys. Res. Lett., 43, 6985-6994, https://doi.org/10.1002/2016GL069763, 2016.

Harris, I., Jones, P. D., Osborn, T. J., and Lister, D. H.: Updated high‐resolution grids of monthly climatic observations–the CRU TS3. 10 Dataset, Int. J. Climatol., 34, 623-642, https://doi.org/10.1002/joc.3711, 2014.

Huning, L. S., and AghaKouchak, A.: Mountain snowpack response to different levels of warming, Proc. Natl. Acad. Sci. U. S. A., 115, 10932, https://doi.org/10.1073/pnas.1805953115, 2018.

Jackson, R. B., Canadell, J., Ehleringer, J. R., Mooney, H. A., Sala, O. E., and Schulze, E. D.: A Global Analysis of Root Distributions for Terrestrial Biomes, Oecologia, 108, 389-411, https://doi.org/10.1007/BF00333714, 1996.

Jung, M., Reichstein, M., Ciais, P., Seneviratne, S. I., Sheffield, J., Goulden, M. L., Bonan, G., Cescatti, A., Chen, J., de Jeu, R., Dolman, A. J., Eugster, W., Gerten, D., Gianelle, D., Gobron, N., Heinke, J., Kimball, J., Law, B. E., Montagnani, L., Mu, Q., Mueller, B., Oleson, K., Papale, D., Richardson, A. D., Roupsard, O., Running, S., Tomelleri, E., Viovy, N., Weber, U., Williams, C., Wood, E., Zaehle, S., and Zhang, K.: Recent decline in the global land evapotranspiration trend due to limited moisture supply, Nature, 467, 951, https://doi.org/10.1038/nature09396, 2010.

Koster, R. D., and Suarez, M. J.: A Simple Framework for Examining the Interannual Variability of Land Surface Moisture Fluxes, J. Clim., 12, 1911-1917, https://doi.org/10.1175/1520-0442(1999)012<1911:ASFFET>2.0.CO;2, 1999.

McMahon, T. A., Peel, M. C., Pegram, G. G. S., and Smith, I. N.: A Simple Methodology for Estimating Mean and Variability of Annual Runoff and Reservoir Yield under Present and Future Climates, J. Hydrometeorol., 12, 135-146, https://doi.org/10.1175/2010jhm1288.1, 2011.

Milly, P. C. D.: Climate, soil water storage, and the average annual water balance, Water Resour. Res., 30, 2143-2156, https://doi.org/10.1029/94WR00586, 1994a.

Milly, P. C. D.: Climate, interseasonal storage of soil water, and the annual water balance, Adv. Water Resour., 17, 19-24, https://doi.org/10.1016/0309-1708(94)90020-5, 1994b.

Milly, P. C. D., and Dunne, K. A.: Macroscale water fluxes 1. Quantifying errors in the estimation of basin mean precipitation, Water Resour. Res., 38, 23-21-23-14, https://doi.org/10.1029/2001WR000759, 2002a.

Milly, P. C. D., and Dunne, K. A.: Macroscale water fluxes 2. Water and energy supply control of their interannual variability, Water Resour. Res., 38, 24-21-24-29, https://doi.org/10.1029/2001WR000760, 2002b.

Mueller, B., Hirschi, M., Jimenez, C., Ciais, P., Dirmeyer, P. A., Dolman, A. J., Fisher, J. B., Jung, M., Ludwig, F., Maignan, F., Miralles, D. G., McCabe, M. F., Reichstein, M., Sheffield, J., Wang, K., Wood, E. F., Zhang, Y., and Seneviratne, S. I.: Benchmark products for land evapotranspiration: LandFlux-EVAL multi-data set synthesis, Hydrol. Earth. Syst. Sci., 17, 3707-3720, https://doi.org/10.5194/hess-17-3707-2013, 2013.

Norby, R. J., Ledford, J., Reilly, C. D., Miller, N. E., and O'Neill, E. G.: Fine-root production dominates response of a deciduous forest to atmospheric CO2 enrichment, Proc. Natl. Acad. Sci. U. S. A., 101, 9689-9693, https://doi.org/10.1073/pnas.0403491101, 2004.

Orth, R., and Destouni, G.: Drought reduces blue-water fluxes more strongly than green-water fluxes in Europe, Nat. Commun., 9, 3602, https://doi.org/10.1038/s41467-018-06013-7, 2018.

Rodell, M., Beaudoing, H. K., L'Ecuyer, T. S., Olson, W. S., Famiglietti, J. S., Houser, P. R., Adler, R., Bosilovich, M. G., Clayson, C. A., Chambers, D., Clark, E., Fetzer, E. J., Gao, X., Gu, G., Hilburn, K., Huffman, G. J., Lettenmaier, D. P., Liu, W. T., Robertson, F. R., Schlosser, C. A., Sheffield, J., and Wood, E. F.: The Observed State of the Water Cycle in the Early Twenty-First Century, J. Clim., 28, 8289-8318, https://doi.org/10.1175/JCLI-D-14-00555.1, 2015.

Roderick, M. L., and Farquhar, G. D.: A simple framework for relating variations in runoff to variations in climatic conditions and catchment properties, Water Resour. Res., 47, https://doi.org/10.1029/2010WR009826, 2011.

Sankarasubramanian, A., and Vogel, R. M.: Annual hydroclimatology of the United States, Water Resour. Res., 38, 19-11-19-12, https://doi.org/10.1029/2001WR000619, 2002.

Scanlon, B. R., Zhang, Z., Save, H., Sun, A. Y., Müller Schmied, H., van Beek, L. P. H., Wiese, D. N., Wada, Y., Long, D., Reedy, R. C., Longuevergne, L., Döll, P., and Bierkens, M. F. P.: Global models underestimate large decadal declining and rising water storage trends relative to GRACE satellite data, Proc. Natl. Acad. Sci. U. S. A., https://doi.org/10.1073/pnas.1704665115, 2018.

Sposito, G.: Understanding the Budyko Equation, Water, 9, https://doi.org/10.3390/w9040236, 2017.

Stackhouse, P. W., Gupta, S. K., Cox, S. J., Mikovitz, J. C., Zhang, T., and Hinkelman, L. M.: The NASA/GEWEX Surface Radiation Budget Release 3.0: 24.5-Year Dataset. In: GEWEX News, No. 1, 2011.

Ukkola, A. M., Haughton, N., De Kauwe, M. G., Abramowitz, G., and Pitman, A. J.: FluxnetLSM R package (v1.0): a community tool for processing FLUXNET data for use in land surface modelling, Geosci. Model. Dev., 10, 3379-3390, https://doi.org/10.5194/gmd-10-3379-2017, 2017.

Wang, D., and Alimohammadi, N.: Responses of annual runoff, evaporation, and storage change to climate variability at the watershed scale, Water Resour. Res., 48, https://doi.org/10.1029/2011WR011444, 2012.

Wang-Erlandsson, L., Bastiaanssen, W. G. M., Gao, H., Jägermeyr, J., Senay, G. B., van Dijk, A. I. J. M., Guerschman, J. P., Keys, P. W., Gordon, L. J., and Savenije, H. H. G.: Global root zone storage capacity from satellite-based evaporation, Hydrol. Earth Syst. Sci., 20, 1459-1481, https://doi.org/10.5194/hess-2015-533, 2016.

Yang, H., Yang, D., Lei, Z., and Sun, F.: New analytical derivation of the mean annual water-energy balance equation, Water Resour. Res., 44, https://doi.org/10.1029/2007WR006135, 2008.

Yang, Y., Donohue, R. J., and McVicar, T. R.: Global estimation of effective plant rooting depth: Implications for hydrological modeling, Water Resour. Res., 52, 8260-8276, https://doi.org/10.1002/2016WR019392, 2016.

Zeng, R., and Cai, X.: Assessing the temporal variance of evapotranspiration considering climate and catchment storage factors, Adv. Water Resour., 79, 51-60, https://doi.org/10.1016/j.advwatres.2015.02.008, 2015.

Zhang, L., Potter, N., Hickel, K., Zhang, Y., and Shao, Q.: Water balance modeling over variable time scales based on the Budyko framework – Model development and testing, J. Hydrol., 360, 117-131, https://doi.org/10.1016/j.jhydrol.2008.07.021, 2008.

Zhang, Y., Pan, M., Sheffield, J., Siemann, A. L., Fisher, C. K., Liang, M. L., Beck, H. E., Wanders, N., MacCracken, R. F., Houser, P. R., Zhou, T., Lettenmaier, D. P., Ma, Y., Pinker, R. T., Bytheway, J., Kummerow, C. D., and Wood, E. F.: A Climate Data Record (CDR) for the global terrestrial water budget: 1984-2010, Hydrol. Earth Syst. Sci., 22, 241-263, https://doi.org/10.5194/hess-22-241-2018, 2018.

List of Figures:

Deleted: Figure 1. Spatial mask used in this study.

Deleted: 2

Deleted: 3

Deleted: 4

Deleted: Figure 5. Distribution of water cycle variances (σ_P^2, σ_E^2, σ_Q^2, $\sigma_{\Delta S}^2$) and covariances ($cov(E, Q)$, $cov(E, \Delta S)$, $cov(Q, \Delta S)$).

Deleted: 6

Deleted: 7

Deleted: 8

Deleted: Fig. 4

Deleted: 9

Deleted: Fig. 4

Deleted: 10

Deleted: Fig. 4

Deleted: 11

Deleted: 2

Deleted: 3

Deleted: 4

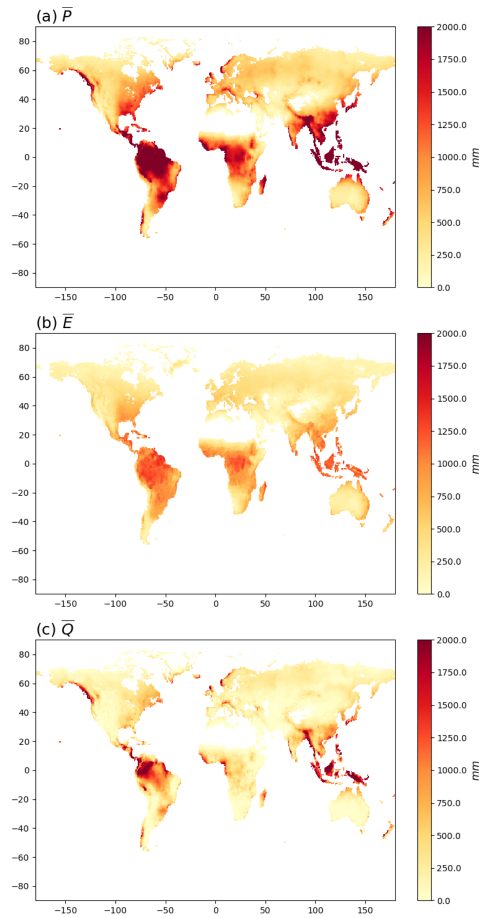

Figure 1. Mean annual (1984-2010) (a) P, (b) E and (c) Q. Note that the mean annual ΔS in the CDR database is zero by construction and is not shown.

Deleted:

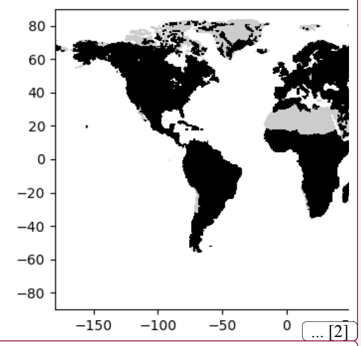

... [2]

Formatted: Font:(Default) Times New Roman, (Asian) MS Mincho, 10 pt, Font color: Text 1

Deleted: Page Break

Deleted: 2

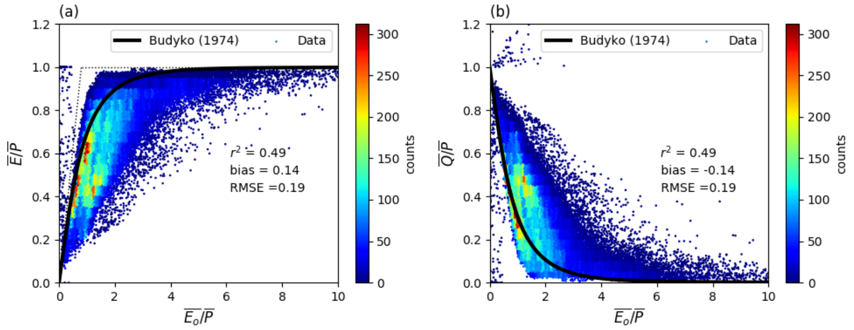

Figure 2. Relationship of mean annual (a) evapotranspiration ($\overline{E}/\overline{P}$) and (b) runoff ($\overline{Q}/\overline{P}$) ratios to the aridity index ($\overline{E_o}/\overline{P}$) from the CDR and SRB databases. For comparison, the Budyko (1974) curve is shown on the left panel (Fig. 2a). The curve on the right panel (Fig. 2b) is calculated assuming a steady state ($\overline{Q}/\overline{P} = 1 - \overline{E}/\overline{P}$).

Deleted: 3

Deleted: Fig. 3

Deleted: Fig. 3

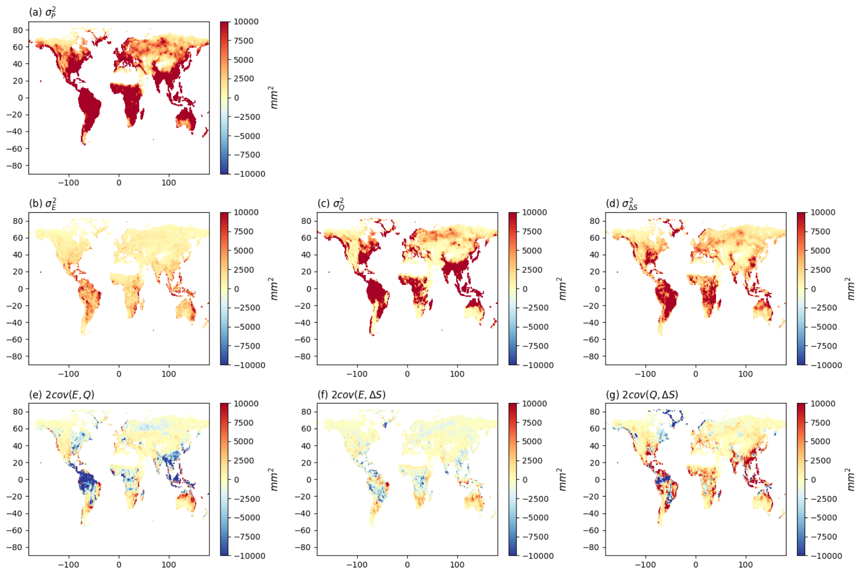

Figure 3. Water cycle variances (σ_P^2, σ_E^2, σ_Q^2, $\sigma_{\Delta S}^2$) and covariances ($cov(E,Q)$, $cov(E,\Delta S)$, $cov(Q,\Delta S)$). Note that we have multiplied the covariances by two (see Eq. 2).

Deleted: 4

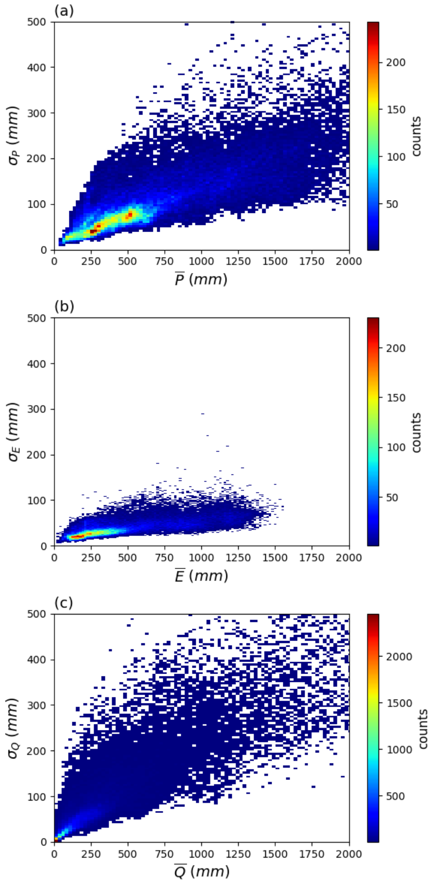

Figure 4. Relation between inter-annual mean and standard deviation for (a) *P*, (b) *E* and (c) *Q* from the CDR database. Note that the mean annual ∆*S* is zero by construction and is not shown.

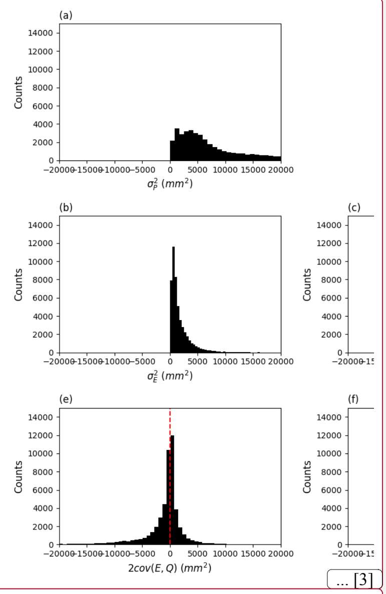

Deleted: ... [3]

Formatted: Font:(Default) Times New Roman, 10 pt

Deleted: Page Break

Deleted: 6

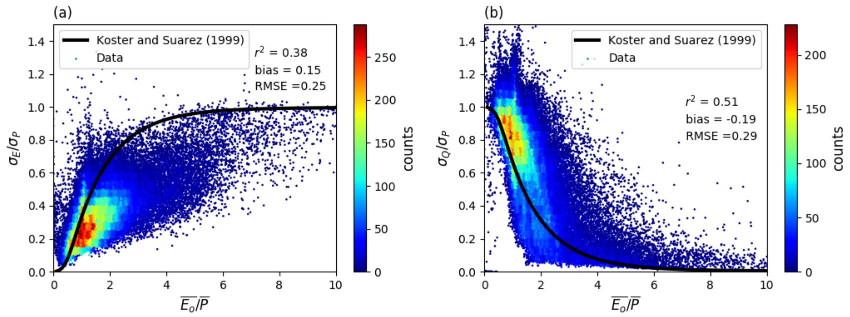

Figure 5. Relationship of inter-annual standard deviation of (a) evapotranspiration (σ_E/σ_P) and (b) runoff (σ_Q/σ_P) ratios to aridity ($\overline{E_o}/\overline{P}$). The curves represent the semi-empirical relations from Koster and Suarez (1999).

Deleted: 7

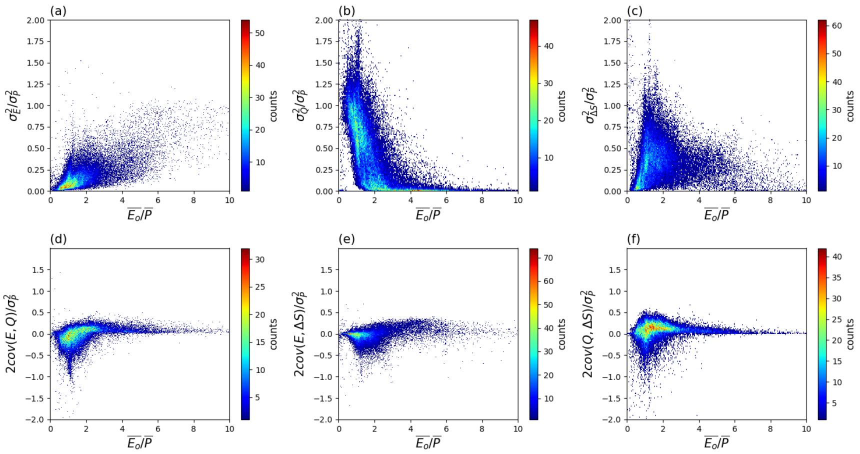

Figure 6. Relation between water cycle variances-covariances (see Fig. 3b-g) as a fraction of the variance of P (σ_P^2) and the aridity index ($\overline{E_o}/\overline{P}$) coloured by density. Note that we have multiplied the covariance components by two (see Eq. 2).

Deleted: 8

Deleted: Fig. 4

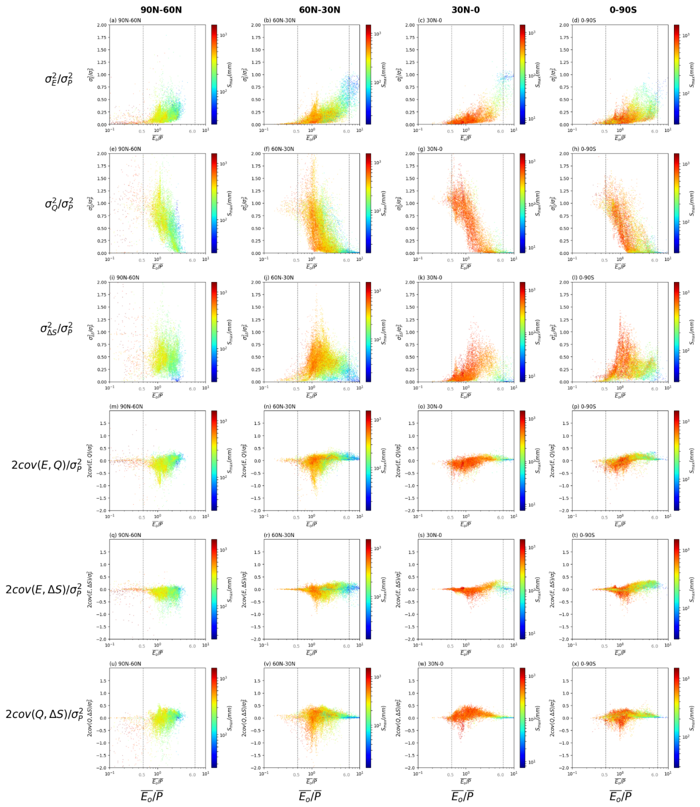

Figure 7. Relation between water cycle variances-covariances (see Fig. 3b-g) as a fraction of the variance for P (σ_P^2) and the aridity index ($\overline{E_o}/\overline{P}$) for grid-cells over different latitude ranges (i.e., 90N-60N, 60N-30N, 30N-0 and 0-90S). The colours relate to the water storage capacity $S_{\max}$. Note that we have multiplied the covariances by two (see Eq. 2). The vertical grey dashed lines represent thresholds used to separate extremely dry ($\overline{E_o}/\overline{P} \geq 6.0$) and wet ($\overline{E_o}/\overline{P} \leq 0.5$) environments. Note the use of a logarithmic x-axis and scale bar for $S_{\max}$.

Deleted: 9

Deleted: Fig. 4

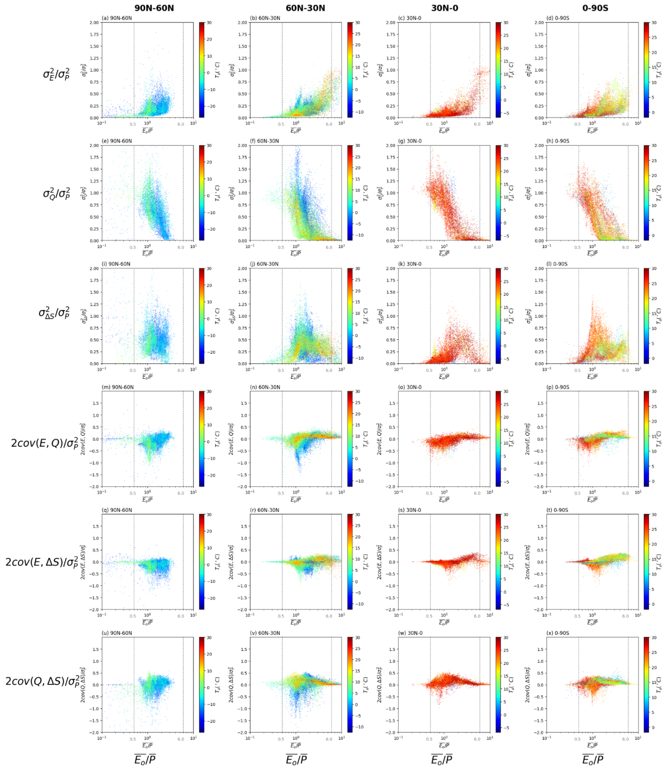

Figure 8. Relation between water cycle variances-covariances (see Fig. 3b-g) as a fraction of the variance for P (σ_P^2) and the aridity index ($\overline{E_o}/\overline{P}$) for grid-cells over different latitude ranges (i.e., 90N-60N, 60N-30N, 30N-0 and 0-90S). The colours relate to the mean air temperature ($\overline{T_a}$). Note that we have multiplied the covariances by two (see Eq. 2). The vertical grey dashed lines represent thresholds used to separate extremely dry ($\overline{E_o}/\overline{P} \geq 6.0$) and wet ($\overline{E_o}/\overline{P} \leq 0.5$) environments.

Deleted: 10

Deleted: Fig. 4

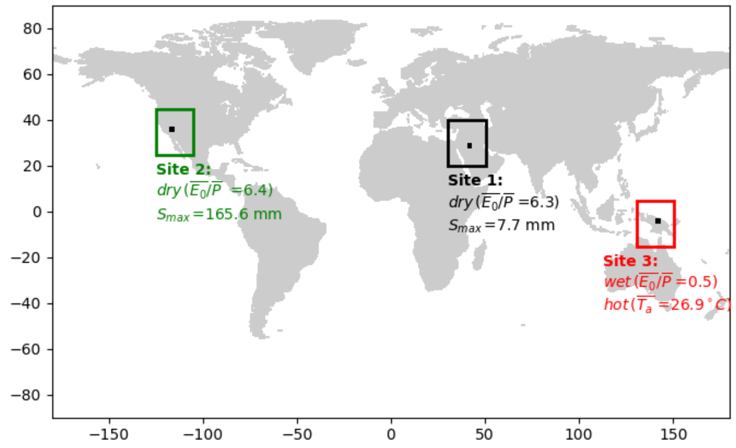

Figure 9. Locations of three representative grid-cells used as case study sites.

Deleted: 11

(a) Site 1

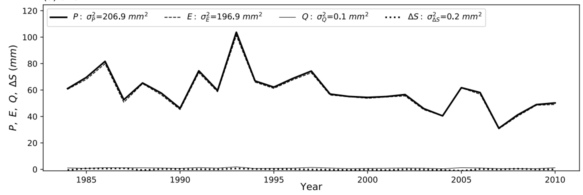

(b) Variance-covariance matrix (Site 1, unit: mm^2)

	E	Q	ΔS
E	196.9	3.4	1.5
Q	3.4	0.1	0.0
ΔS	1.5	0.0	0.2
Inter-annual variance of P : 206.9			

*Note: The values along the diagonal of each line are variance values for E, Q, and ΔS, and other values are covariance values between the two crossed components.

(c) Site 2

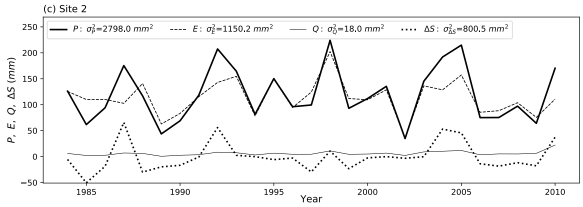

(d) Variance-covariance matrix (Site 2, unit: mm^2)

	E	Q	ΔS
E	1150.2	71.2	269.2
Q	71.2	18.0	74.3
ΔS	269.2	74.3	800.5
Inter-annual variance of P : 2798.0			

(e) Site 3

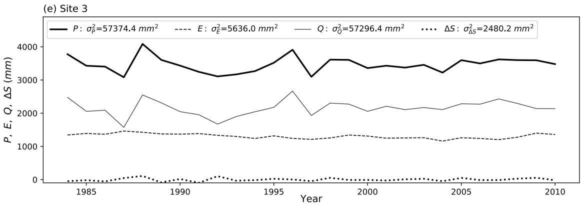

(f) Variance-covariance matrix (Site 3, unit: mm^2)

	E	Q	ΔS
E	5636.0	-4548.6	651.7
Q	-4548.6	57296.4	-122.2
ΔS	651.7	-122.2	2480.2
Inter-annual variance of P : 57374.4			

Figure 10. Inter-annual time series (*P*, *E*, *Q* and ΔS) and the associated variance-covariance matrix (*E*, *Q* and ΔS) for case study Sites 1-3. Left column shows time series for (a) Site 1, (c) Site 2 and (e) Site 3, with right column i.e., (b), (d) and (f), the associated variance-covariance matrix for three sites. Note that the covariance values in the tables should be multiplied by two to agree with the variance-covariance balance in Eq. (2).

Deleted: 2

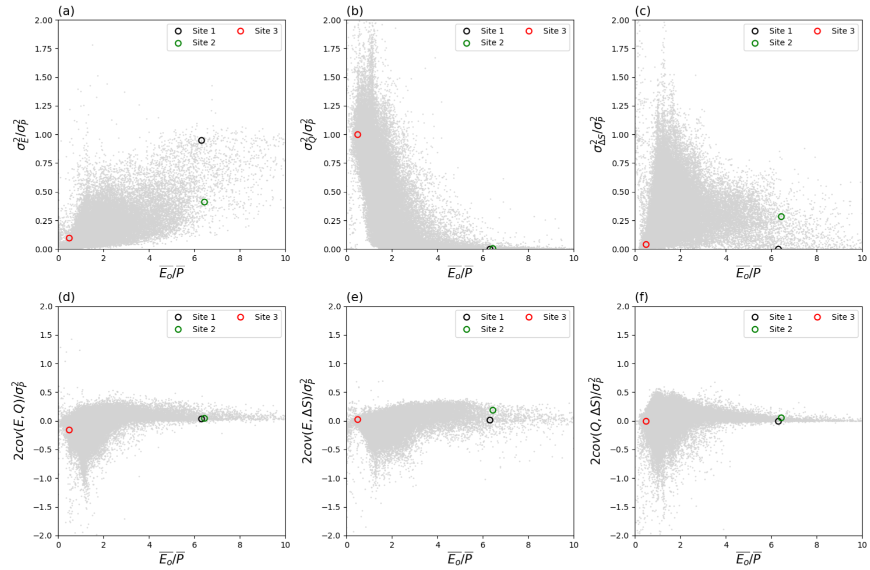

Figure 11. Location of three case study sites in the water cycle variability space. The grey background dots are from Fig. 6.

Deleted: 3

Deleted: Fig. 8

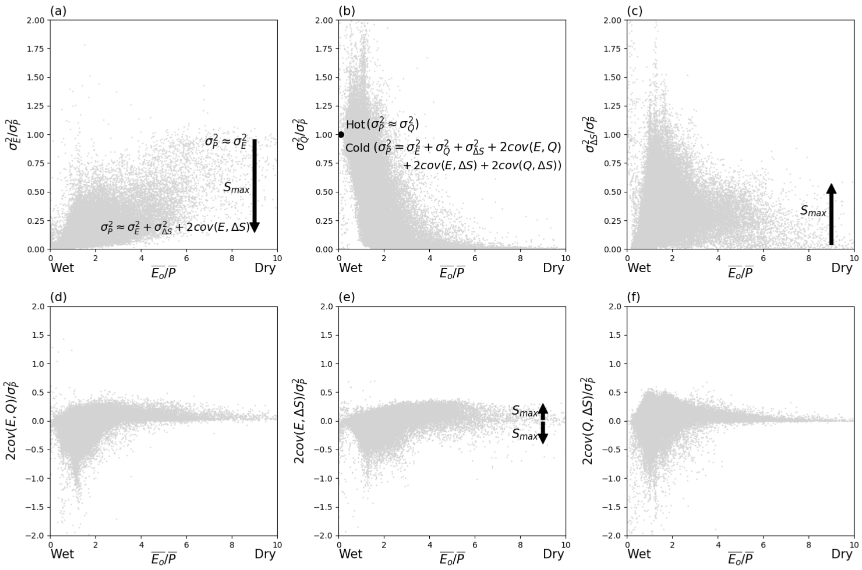

Figure 12. Synthesis of factors controlling variance partitioning. The arrows denote trends with increasing S_{max}. The grey background dots are from Fig. 6.

Deleted: 4

Deleted: Fig. 8

Response to Editor

Dear authors,

thank you very much for the revised version of your manuscript. Since all other reviewers suggested minor revisions, I only requested one of the reviewers (René Orth) to comment on the new version.

He appreciates the additional analyses performed, but still feels that some of the variables have not been validated, such as run-off. The reviewer suggests additional analyses, regarding (1) use updated version of the Jung et al. dataset (Jung et al., 2019) and (2) use the E-RUN dataset (Gudmundsson and Seneviratne, 2016) to validate the runoff.

I find that the manuscript has much improved and you have made good effort addressing the reviewers comments. I think the manuscript is almost ready for publication, given some amendments. In view of the fact that the Jung et al. (2019) paper was published only after the submission of the manuscript (although the data were available earlier), I will not insist on this additional analysis. However, please consider the Gudmundson and Seneviratne (2016) dataset. Please also attend to the detailed comments of the reviewer.

I am looking forward to your resubmitted manuscript,

Anke Hildebrandt.

Response: We thank the editor for the evaluation and comment on the revised manuscript. As suggested by the editor and reviewer, we have conducted additional analyses using the E-RUN database (Gudmundson and Seneviratne, 2016) and the FLUXCOM database (updated version of MPI database, Jung et al., 2019). We also revised the manuscript accordingly as well as conducted a point-by-point response to all the comments by the reviewer.

The main comment here is a further cross-validation of the CDR runoff based on the E-RUN database. The comparison results show that both the long-term mean ($\bar{Q}$) and standard deviation (σ_Q) of the monthly runoff in the E-RUN database are very similar with those in the CDR database. We further added the comparison results of runoff in the revised Supplementary Material, and also changed the text accordingly in the revised manuscript. Please also see R2C3 for a detailed response to this point.

Another comment is about using the FLUXCOM database instead of MPI in the validation of the CDR evapotranspiration *E*. As has been noted by the editor, the FLUXCOM database paper was published after the submission of this manuscript. In addition, the monthly FLUXCOM data is currently only available (open to public) for a much shorter period (2001-2010) compared with both the monthly CDR (1984-1010) and the original MPI (1982-1011) databases. As strongly suggested by R2, we conducted further comparison between the CDR and FLUXCOM databases, and the results are similar with those comparison between the CDR and MPI databases. Given the limited time period in the FLUXCOM database and the similarity of comparison results using the MPI and FLUXCOM databases, we choose to keep the results of the MPI database in the Supplementary Material. Please also see R2C2 for detailed response.

Again, we sincerely appreciate both the editor and reviewer for constructive suggestions and comments on the revised manuscript.

Response to Referee #2 (Dr René Orth)

R2C1: Second review of Yin and Roderick "Inter-annual variability of the global terrestrial cycle"

The paper has overall improved as the authors have addressed many of the concerns raised by me and the other reviewers. However, one important issue, and several minor points remain unresolved.

Response: We thank Dr René Orth for the evaluation and helpful comments on the revised manuscript. Please see detailed response to all the comments as follows.

R2C2: Main comment: As mentioned in my previous review, I think it is critical for this study to show that the discovered patterns are not just implemented in the model used to derive the CDR dataset. It has to be shown that similar patterns are present across independent datasets, as only this can indicate that nature is indeed operating this way. I appreciate efforts in this direction made by the authors, namely the consideration of the LandFlux-EVAL dataset, the Jung et al. dataset, and the ERA5 reanalysis. But I believe that these analyses need to be expanded before the paper can be published:

(1) I understand that the authors do not want to use GLEAM as a reference dataset as this was used in the derivation of the CDR reanalysis. But instead the Jung et al. dataset should be updated to the 2019 version (Jung et al. 2019). The authors stated in their response: 'We could replace the MPI we used with the updated database (Jung et al., 2019) but we do not see how that would alter the results.' This is not about altering the results, but about using state-of-the-art alternative datasets to illustrate the robustness of the CDR-based results. I do not see the point in using an almost 10-year old dataset while updated and much evolved datasets exist.

Response: As suggested by R2, we conducted further comparison between the CDR and FLUXCOM (0.5° × 0.5°, monthly, 2001-2010) (updated version of MPI database, Jung et al., 2019) databases, and the results are shown in Fig. R1. The results are similar with the previous comparison between the CDR and MPI databases, showing underestimation of the monthly mean *E* and bias and scaling offset in the standard deviations of monthly *E* in the CDR database compared with the FLUXCOM database.

However, currently the monthly FLUXCOM database is only available (open to public) for the restricted period 2001-2010, which is much shorter than both the CDR (available during 1984-2010) and the MPI (available during 1982-2011) databases. Given the limited time period for the FLUXCOM database and the similar comparison results of the MPI and FLUXCOM to the CDR databases, we propose to keep the results based on the original MPI database in the Supplementary material.

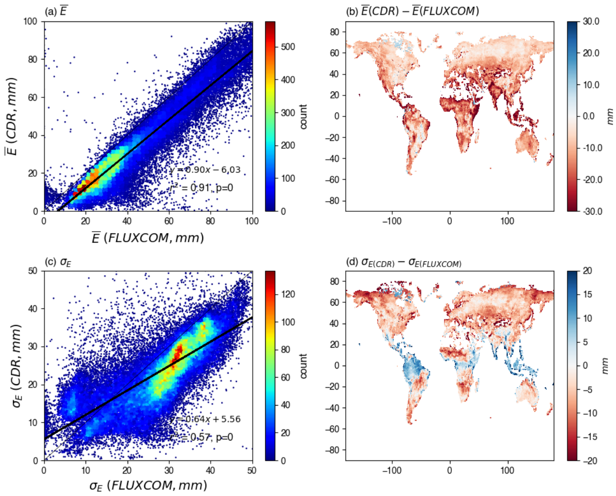

Figure R1. Comparison of monthly evapotranspiration *E* between FLUXCOM and Climate Data Record (CDR) databases. Top panels (a) (b) show comparison of the mean monthly ($\overline{E}$) while bottom panels (c) (d) show comparison of the standard deviation (σ_E) of monthly *E*.

R2C3: (2) I also appreciate the ERA5-based analyses which the authors have done in response to my previous comments. I share their conclusion that this dataset is not suitable to be used in the context of this study. However, this way the runoff results remain not confirmed with independent data. Therefore I suggest to use the E-RUN gridded runoff dataset (Gudmundsson and Seneviratne 2016) for this purpose.

I do not wish to remain anonymous - Rene Orth.

Response: As suggested, we conduct further comparison of the monthly runoff between the E-RUN (0.5° × 0.5°, monthly, 1951-2015) (Gudmundsson and Seneviratne, 2016) and CDR databases. The comparison is conducted based on the overlap of time (1984-2010) and space (Europe) in both databases, and the results are shown in Figs. R2-R3. We can see that both the long-term mean ($\overline{Q}$) and standard deviation (σ_Q) of the monthly runoff show very similar spatial patterns in the E-RUN and CDR databases (Fig. R2). The grid-by-grid comparison also shows close agreement (Fig. R3). We have added these results to the revised Supplementary Material (Figs. S10-S11), and also added the text in the revised manuscript as follows (lines 165-169): "*The comparison of runoff Q between the E-RUN and CDR databases show that the two databases have very similar spatial patterns of both the long-term mean ($\overline{Q}$) and standard deviation (σ_Q) of the monthly Q (Fig. S10). The grid-by-grid comparison results are also encouraging, showing slight bias of both the long-term mean and standard deviation of monthly Q in the CDR database compared with the E-RUN database (Fig. S11).*".

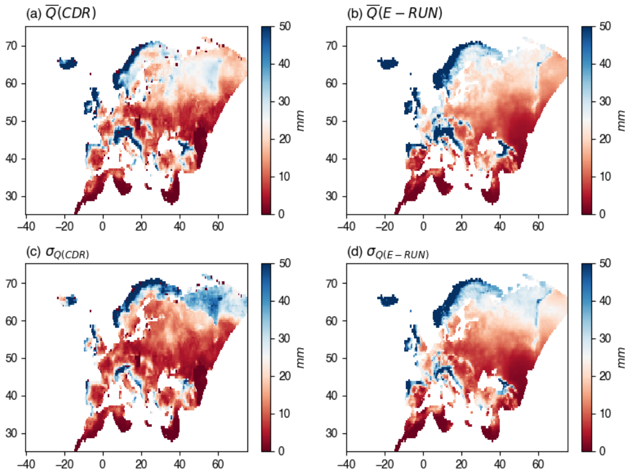

Figure R2. Mean ($\overline{Q}$) and standard deviation (σ_Q) of monthly runoff Q in the E-RUN and Climate Data Record (CDR) databases in the area of spatial overlap (Europe). Top panels (a) (b) show the mean monthly ($\overline{Q}$) while bottom panels (c) (d) show the standard deviation (σ_Q) of monthly Q.

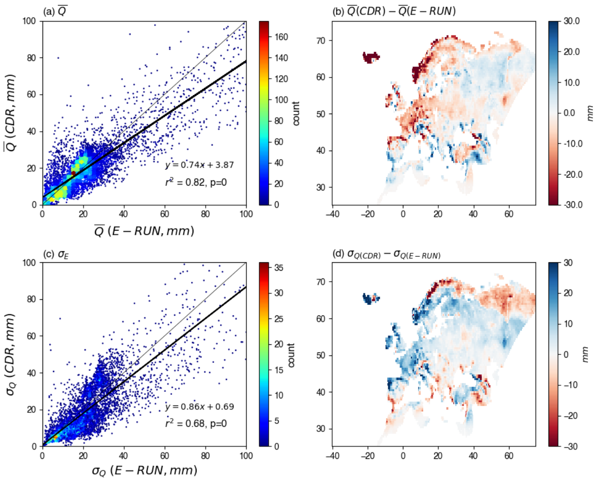

Figure R3. Comparison of monthly runoff Q between the E-RUN and Climate Data Record (CDR) databases in the area of spatial overlap (Europe). Top panels (a) (b) show comparison of the mean monthly ($\overline{Q}$) while bottom panels (c) (d) show comparison of the standard deviation (σ_Q) of monthly Q.

Specific comments:

R2C4: lines 53-55: This statement somewhat ignores the efforts leading to the ERA-Land (Balsamo et al. 2013) and MERRA-Land (Reichle et al. 2011) datasets.

Response: We have acknowledged the efforts in developing land-based products in the revised manuscript by modifying the sentence to (lines 53-57): "*Though efforts have been taken to develop land-based products from atmospheric reanalyses, e.g., ERA-Land (Balsamo et al. 2013) and MERRA-Land (Reichle et al. 2011) databases, however, the central aim of atmospheric re-analysis is to estimate atmospheric variables. That atmospheric-centric aim, understandably, ignores many of the nuances of soil water infiltration, vegetation water uptake, runoff generation and many other processes of central importance in hydrology.*". The relevant reference has also been cited in the revised manuscript.

R2C5: line 75: 'the various ... databases' - after only reading the text up to this point it is not clear what is meant here

Response: It means the databases used in this study will be introduced and described in Section 2. To make this sentence more clear, we have modified it in the revised manuscript as follows (lines 77-79): "*We begin in Section 2 by describing the various climate and hydrologic databases used in this study, and also include a further assessment of the suitability of the CDR database for this initial variability study.*".

R2C6: line 78: it should be 'these variabilities'

Response: Done. Thank you.

R2C7: lines 88/89: 'in time step t' - these are all fluxes which are accumulated during time steps t-1 and t; also, I would mention here that the time step considered in this study is 1 year

Response: We have added the annual time step in this sentence to make it more clear in the revised version (lines 90-91): "*with P the precipitation, E the evapotranspiration, Q the runoff and ΔS the total water storage change in time step t (annual in this study).*". Thank you.

R2C8: lines 91/92: 'Eq (1) is the familiar...' - this sentence is an unnecessary repetition

Response: This sentence has been deleted in the revised manuscript. Thanks.

R2C9: line 96: known here?

Response: To make the meaning of this sentence more clear, we have removed the word 'known' and modified it in the revised manuscript as follows (lines 98-99): "*We use the Climate Data Record (CDR) database (Zhang et al., 2018) which is a recently released global land hydrologic re-analysis.*".

R2C10: line 103: The SRB dataset only extents until 2007 (if I am not mistaken) while the analyses in this study consider a time period until 2010. How can you still use the SRB data then?

Response: The aim of this study is to investigate the inter-annual variability of global water cycle based on the CDR database, which extends from 1984 to 2010. During the construction process, the CDR database made some assumptions considering the 27-year period (1984-2010) as an integrity, e.g., the long-term (27-year) storage change to be zero. To better investigate the inter-annual variability by using the CDR database in this study, we choose to stick to the CDR period, i.e., 1984-2010.

While the SRB database is only available from 1984 to 2007 (not to 2010), we only use it to calculate the long-term E_o ($\overline{E_o}$) and further estimate the aridity index ($\overline{E_o}/\overline{P}$). We believe the three-year period difference would not have a material impact on the aridity index estimation or change the general conclusions in this study. Thanks.

R2C11: lines 105/106: Sentence is hard to understand, please rephrase.

Response: We have rephrased this sentence in the revised manuscript as follows (lines 107-108): "*In general, we anticipate two important factors, i.e., the water storage capacity and the presence of ice/snow at the surface, which are most likely to have influence on the partitioning of hydrologic variability.*". Thanks.

R2C12: line 160: Please comment on the offset.

Response: We have added more details for the offset and modified the sentence in the revised manuscript as follows: "*In terms of variability, the standard deviations of monthly E from the CDR are in very close agreement with the LandFluxEVAL database (Fig. S7c), but there is a bias and scaling offset for the comparison with the MPI database particularly for the grid-cells with low standard deviation of E (Fig. S8c).*".

R2C13: line 177: I would replace 'trend' with 'pattern'

Response: Done. Thank you.

R2C14: line 180: not clear what is meant here with 'physics of runoff generation'

Response: Yes, we agree that the 'physics of runoff generation' is not clear and we have replaced it with more specific term in the revised manuscript as follows (lines 187-189): "*However, there is substantial scatter due to, for example, regional variations related to seasonality, water storage change and the landscape characteristics*".

R2C15: lines 178-181: Padron et al. 2017 is relevant in this context, and could be cited.

Response: The reference has now been cited in the revised manuscript. Thank you.

R2C16: lines 188, 203, 223: 'very different' is not obvious to me from the comparison of Figs 1 and 3. Please clarify.

Response: Here we mean it is very different between the partitioning of $\bar{P}$ and σ_P^2**.** In brief, the $\bar{P}$ is mostly partitioned into $\bar{E}$ or $\bar{Q}$. However, for the partitioning of σ_P^2, σ_E^2 is generally very small with σ_P^2 mostly partitioned into σ_Q^2, $\sigma_{\Delta S}^2$ and even the covariance components. Please see the more comprehensive and detailed analyses in the revised manuscript (lines 199-209).

R2C17: lines 225-226: This is an important finding which should be highlighted in the abstract and/or conclusions.

Response: Yes, the finding here has been added in the abstract (lines 11-12): "*Instead we find that σ_P^2 is mostly partitioned between σ_Q^2, $\sigma_{\Delta S}^2$ and the associated covariances with limited partitioning to σ_E^2.*".

R2C18: lines 294-303: If the main conclusion is that things are complex, and there is no particular lesson learned here, then I would suggest to remove this section. It confuses readers and distracts from the relevant main messages of the study.

Response: While the results here are complex and not easy to understand, we still could have some implications obtained here, for example, the difference between partitioning of σ_P^2 at high and low temperature. That difference does show the important role of temperature in the partitioning of σ_P^2, which might be helpful for the future studies. Therefore, we would like to keep this section in the revised manuscript.

R2C19: lines 307-328: It feels inconsistent that in addition to the wet and hot grid cell no wet and cold grid cell has been selected as a case study (as was done in the case of high and low water storage capacity).

Response: The reason we did not pick any case study site here is because there is substantial scatter in wet and cold conditions ($\overline{E_o}/\bar{P} \leq 0.5$ in first column of Fig. 8). The partitioning of σ_P^2 in wet and cold conditions is so complex that no grid-cell could be chosen as a representative case study site. Instead of a case study site, we further illustrate the importance of snow/ice presence in variance partitioning (lines 425-426) and expect more emphasis on this in the future studies that our manuscript will inspire.

R2C20: - While this study is performed at annual time scales, the authors could add some outlook/clarification that the revealed variability propagation across the water cycle might behave differently at shorter time scales

Response: Yes, we agree that the variability partitioning might be different at various time scales. In response, we have added an expectation for future work at various time scales in the revised manuscript (lines 408-410): "*These general principles of variance partitioning in the water cycle above may vary at different time scales (e.g., monthly, daily), and we expect more details of the variability partitioning across various temporal scales to be investigated in future studies.*".

R2C21: - Figures 2,5, and others display physically implausible values - please comment on this

Response: Yes, there are some grid-cells showing physically implausible values in Figs. 2 and 5. In this study, we have tried to exclude the grid-cells with high uncertainty (please see Section 2.3 and Fig. S2), therefore, it is unlikely that those implausible values are caused by data uncertainty/error. While checking the location of those grid-cells, we found that they almost appear in/close to the Greenland. Therefore, we guess those physically implausible values are caused by the permanent ice/glacier. As also noted in this study, with the presence of snow/ice, it is very complex in the variance partitioning. In this study, we highlighted regions with snow/ice coverage. We except future studies to further uncover the role of snow/ice in the variance partitioning and show details of these physically implausible values.

R2C22: - It is not intuitive that non-consistent (logarithmic/non-lagarithmic) axes are used for E0/P across different figures.

Response: Yes, the axes for the aridity index (E_o/P) are linear in Figs. 2, 5 and 6 and logarithmic in Figs. 7 and 8. The underlying reason for that is because there are different purposes in presenting the results in these figures. In Figs. 2, 5 and 6, we show the relation of long-term mean and variance to E_o/P. It is better to use the regular non-logarithmic axes to compare with results in previous studies (e.g., Budyko-curve and Koster and Suarez analyses) that also use linear axes. While in Figs. 7 and 8, we highlight the role of storage capacity and physical phase (solid/liquid) in variance partitioning in both extremely dry and wet environments. We found the logarithmic axes to better show the necessary details in Figs. 7 and 8.

R2C23: References:

Balsamo, G., C. Albergel, A. Beljaars, S. Boussetta, E. Brun, H. Cloke, D. Dee, E. Dutra, J. Muñoz-Sabater, F. Pappenberger, P. de Rosnay, T. Stockdale, and F. Vitart, 2013: ERA Interim Land: a global land water resources dataset. Hydrol. Earth Syst. Sci., 19, 389–407.

Gudmundsson, L., and S.I. Seneviratne, 2016: Observation-based gridded runoff estimates for Europe (E-RUN version 1.1). Earth Syst. Sci. Data, 8 (2), 279–295.

Jung, M., S. Koirala, U. Weber, K. Ichii, F. Gans, G. Camps-Valls, D. Papale, C. Schwalm, G. Tramontana, and M. Reichstein, 2019: The FLUXCOM ensemble of global land-atmosphere energy fluxes. Scientific Data, 6 (74).

Padron, R.S., L. Gudmundsson, P. Greve, and S.I. Seneviratne, 2017: Large-Scale Controls of the Surface Water Balance Over Land: Insights From a Systematic Review and Meta-Analysis. Water Res. Resour., 53 (11), 9659-9678.

Reichle, R.H., R.D. Koster, G.J.M.D. Lannoy, B.A. Forman, Q. Liu, S.P.P. Mahanama, and A. Toure, 2011: Assessment and enhancement of MERRA land surface hydrology estimates. J. Clim., 24, 6322–6338,

Response: We thank Dr René Orth for listing all the reference in the comments, and we have read and cite these reference accordingly in the revised manuscript.

Inter-annual variability of the global terrestrial water cycle

Dongqin Yin[1,2], Michael L. Roderick[1,3]

[1]Research School of Earth Sciences, Australian National University, Canberra, ACT, 2601, Australia

[2]Australian Research Council Centre of Excellence for Climate System Science, Canberra, ACT, 2601, Australia

[3]Australian Research Council Centre of Excellence for Climate Extremes, Canberra, ACT, 2601, Australia

Correspondence to: (dongqin.yin@anu.edu.au)

Abstract:

Variability of the terrestrial water cycle, i.e., precipitation (*P*), evapotranspiration (*E*), runoff (*Q*) and water storage change (ΔS) is the key to understanding hydro-climate extremes. However, a comprehensive global assessment for the partitioning of variability in *P* between *E*, *Q* and ΔS is still not available. In this study, we use the recently released global monthly hydrologic reanalysis product known as the Climate Data Record (CDR) to conduct an initial investigation of the inter-annual variability of the global terrestrial water cycle. We first examine global patterns in partitioning the long-term mean $\bar{P}$ between the various sinks $\bar{E}$, $\bar{Q}$ and $\overline{\Delta S}$ and confirm the well-known patterns with $\bar{P}$ partitioned between $\bar{E}$ and $\bar{Q}$ according to the aridity index. In a new analysis based on the concept of variability source and sinks we then examine how variability in the precipitation σ_P^2 (the source) is partitioned between the three variability sinks σ_E^2, σ_Q^2 and $\sigma_{\Delta S}^2$ along with the three relevant covariance terms, and how that partitioning varies with the aridity index. We find that the partitioning of inter-annual variability does not simply follow the mean state partitioning. Instead we find that σ_P^2 is mostly partitioned between σ_Q^2, $\sigma_{\Delta S}^2$ and the associated covariances with limited partitioning to σ_E^2. We also find that the magnitude of the covariance components can be large and often negative, indicating that variability in the sinks (e.g., σ_Q^2, $\sigma_{\Delta S}^2$) can, and regularly does, exceed variability in the source (σ_P^2). Further investigations under extreme conditions revealed that in extremely dry environments the variance partitioning is closely related to the water storage capacity. With limited storage capacity the partitioning of σ_P^2 is mostly to σ_E^2, but as the storage capacity increases the partitioning of σ_P^2 is increasingly shared between σ_E^2, $\sigma_{\Delta S}^2$ and the covariance between those variables. In other environments (i.e., extremely wet and semi-arid/semi-humid) the variance partitioning proved to be extremely complex and a synthesis has not been developed. We anticipate that a major scientific effort will be needed to develop a synthesis of hydrologic variability.

Deleted:

1. Introduction

In describing the terrestrial branch of the water cycle, the precipitation (*P*) is partitioned into evapotranspiration (*E*), runoff (*Q*) and change in water storage (ΔS). With averages taken over many years, $\overline{\Delta S}$ is usually assumed to be zero and it has long been recognized that the partitioning of the long-term mean annual precipitation ($\bar{P}$) between $\bar{E}$ and $\bar{Q}$ was jointly determined by the availability of both water ($\bar{P}$) and energy (represented by the net radiation expressed as an equivalent depth of water and denoted $\overline{E_o}$). Using data from a large number of watersheds, Budyko (1974) developed an empirical relation relating the evapotranspiration ratio ($\bar{E}/\bar{P}$) to the aridity index ($\overline{E_o}/\bar{P}$). The resultant empirical relation and other Budyko-type forms (e.g., Fu, 1981; Choudhury, 1999; Yang et al., 2008, Roderick and Farquhar, 2011; Sposito, 2017) that partition *P* between *E* and *Q* have proven to be extremely useful in both understanding and characterising the long-term mean annual hydrological conditions in a given region.

However, the long-term mean annual hydrologic fluxes rarely occur in any given year. Instead, society must (routinely) deal with variability around the long-term mean. The classic hydro-climate extremes are droughts and floods but the key point here is that hydrologic variability is expressed on a full spectrum of time and space scales. To accommodate that perspective, we need to extend our thinking beyond the long-term mean to ask how the variability of *P* is partitioned into the variability of *E*, *Q* and ΔS (e.g., Orth and Destouni, 2018).

Early research on hydrologic variability focussed on extending the Budyko curve. In particular, Koster and Suarez (1999) used the Budyko curve to investigate inter-annual variability in the water cycle. In their framework, the evapotranspiration standard deviation ratio (defined as the ratio of standard deviation for *E* to *P*, σ_E/σ_P) was (also) estimated using the aridity index ($\overline{E_o}/\bar{P}$). The classic Koster and Suarez framework has been widely applied and extended in subsequent investigations of the variability in both *E* and *Q*, using catchment observations, reanalysis data and model outputs (e.g., McMahon et al., 2011; Wang and Alimohammadi 2012; Sankarasubramanian and Vogel, 2002; Zeng and Cai, 2015). However, typical applications of the Koster and Suarez framework have previously been at regional scales and there is still no comprehensive global assessment for partitioning the variability of *P* into the variability of *E*, *Q* and ΔS. One reason for the lack of a global comprehensive assessment is the absence of gridded global hydrologic data. Interestingly, the atmospheric science community have long used a combination of observations and model outputs to construct gridded global–scale atmospheric re-analyses and such products have become central to atmospheric research. Those atmospheric products also contain estimates of some of the key water cycle variables (e.g., P, E), such as in the widely used interim ECMWF Re-Analysis (ERA-Interim; Dee et al. 2011). Though efforts have been taken to develop land-based products from atmospheric reanalyses, e.g., ERA-Land (Balsamo et al., 2013) and MERRA-Land (Reichle et al., 2011) databases, however, the central aim of atmospheric re-analysis is to estimate atmospheric variables. That atmospheric-centric aim, understandably, ignores many of the nuances of soil water infiltration, vegetation water uptake, runoff generation and many other processes of central importance in hydrology.

Deleted: However

Deleted: ,

Deleted: which

Hydrologists have only recently accepted the challenge of developing their own re-analysis type products with perhaps the first serious hydrologic re-analysis being published as recently as a few years ago (Rodell et al., 2015). More recently, the Princeton University group has extended this early work by making available a gridded global terrestrial hydrologic re-analysis product known as the Climate Data Record (CDR) (Zhang et al., 2018). Briefly, the CDR was constructed by synthesizing multiple in-situ observations, satellite remote sensing products, and land surface model outputs to provide *gridded* estimates of global land precipitation P, evapotranspiration E, runoff Q and total water storage change ΔS (0.5° × 0.5°, monthly, 1984-2010). In developing the CDR, the authors adopted local water budget closure as the fundamental hydrologic principle. That approach presented one important difficulty. Global observations of ΔS start with the GRACE satellite mission from 2002. Hence before 2002 there is no direct observational constraint on ΔS and the authors made the further assumption that the mean annual ΔS over the full 1984-2010 period was zero at every grid-box. That is incorrect in some regions (e.g. Scanlon et al., 2018) and represents an observational problem that cannot be overcome. However, our interest is in the year-to-year variability and for that application, the assumption of no change in the mean annual ΔS over the full 1984-2010 period is unlikely to lead to major problems since we are not looking for subtle changes over time. With that caveat in mind, the aim of this study is to use this new 27-year gridded hydrologic re-analysis product to conduct an initial investigation of the inter-annual variability of the terrestrial branch of the global water cycle.

The paper is structured as follows. We begin in Section 2 by describing the various climate and hydrologic databases used in this study, and also include a further assessment of the suitability of the CDR database for this

Deleted: ing

initial variability study. In Section 3, we examine relationships between the mean and variability in the four water cycle variables (P, E, Q and ΔS). In Section 4, we first relate the variabilities to the classical aridity index and then use those results to evaluate the theory of Koster and Suarez (1999). Subsequently we examine how the variance of P is partitioned into the variances (and relevant covariances) of E, Q and ΔS and undertake an initial survey that investigates some of the factors controlling the variance partitioning. We conclude the paper with a discussion summarising what we have learnt about water cycle variability over land by using the CDR database.

Deleted: variability

2. Methods and Data

2.1 Methods

The water balance is defined by,

$$P(t) = E(t) + Q(t) + \Delta S(t) \quad (1)$$

with P the precipitation, E the evapotranspiration, Q the runoff and ΔS the total water storage change in time step t (annual in this study). By the usual variance law, we have,

$$\sigma_P^2 = \sigma_E^2 + \sigma_Q^2 + \sigma_{\Delta S}^2 + 2cov(E,Q) + 2cov(E,\Delta S) + 2cov(Q,\Delta S) \quad (2)$$

that includes all relevant variances (denoted σ^2) and covariances (denoted cov). Eq. (2) can be thought of as the hydrologic variance balance equation.

Deleted: Eq. (1) is the familiar hydrologic mass balance equation. In that context,

2.2 Hydrologic and Climatic Data

We use the Climate Data Record (CDR) database (Zhang et al., 2018) which is a recently released global land hydrologic re-analysis. This product includes global precipitation P, evapotranspiration E, runoff Q and water storage change ΔS (0.5° × 0.5°, monthly, 1984-2010). In this study we focus on the inter-annual variability and the monthly water cycle variables (P, E, Q and ΔS) are aggregated to annual totals. The CDR does not report additional radiation variables and we use the NASA/GEWEX Surface Radiation Budget (SRB) Release-3.0 (monthly, 1984-2007, 1° × 1°) database (Stackhouse et al., 2011) to calculate E_o (defined as the net radiation expressed as an equivalent depth of liquid water, Budyko, 1974). We then calculate the aridity index ($\overline{E_o}/\overline{P}$) using P from the CDR and E_o from the SRB databases (see Fig. S1a in the Supplementary Material).

Deleted: known here as the Climate Data Record (CDR) (Zhang et al., 2018)

In general, we anticipate two important factors, i.e., the water storage capacity and the presence of ice/snow at the surface, which are most likely to have influence on the partitioning of hydrologic variability. For the storage, the active range of the monthly water storage variation was used to approximate the water storage capacity (S_{max}). In more detail, the water storage $S(t)$ at each time step t (monthly here) was first calculated from the accumulation of $\Delta S(t)$, i.e., $S(t) = S(t\text{-}1) + \Delta S(t)$ where we assumed zero storage at the beginning of the study period (i.e., $S(0) = 0$). With the resulting time series available, S_{max} was estimated as the difference between the maximum and minimum $S(t)$ during the study period at each grid-box (see Fig. S1b in the Supplementary Material). The estimated S_{max} shows a large range from 0 to 1000 mm with the majority of values from 50 to 600 mm (Fig. S1b), which generally agrees with global rooting depth estimates assuming that water occupies from 10 to 30% of the soil volume at field capacity (Jackson et al., 1996; Wang-Erlandsson et al., 2016; Yang et al., 2016). To characterise snow/ice cover, and to distinguish extremely hot and cold regions, we also make use of a gridded global land air temperature dataset from the Climatic Research Unit (CRU TS4.01 database, monthly, 1901-2016, 0.5° × 0.5°) (Harris et al., 2014). (see Fig. S1c in the Supplementary Material).

2.3 Spatial Mask to Define Study Extent

The CDR database provides an estimate of the uncertainty (± 1σ) for each of the hydrologic variables (P, E, Q, ΔS) in each month. We use those uncertainty estimates to identify and remove regions with high relative uncertainty in the CDR data. The relative uncertainty is calculated as the ratio of root mean square of the uncertainty (± 1σ) to the mean annual P, E and Q at each grid-box following the procedure used by Milly and Dunne (2002a). Note that the long term mean ΔS is zero by construction in the CDR database, and for that reason we did not use ΔS to calculate the relative uncertainty. Grid-boxes with a relative uncertainty (in P, E and Q) of more than 10% are deemed to have high relative uncertainty (Milly and Dunne, 2002a) and were excluded from the study extent. The excluded grid-boxes were mostly in the Himalayan region, the Sahara Desert and in Greenland. The final spatial mask is shown in Fig. S2 and this has been applied throughout this study.

2.4 Further Evaluation of CDR Data for Variability Analysis

In the original work, the CDR database was validated by comparison with independent observations including (i) mean seasonal cycle of Q from 26 large basins (see Fig. 8 in Zhang et al., 2018), (ii) mean seasonal cycle of ΔS

Deleted: On

Deleted: grounds

Deleted: that

Deleted:

Deleted:

Deleted: were the water storage capacity and the presence of ice/snow at the surface from 12 large basins (Fig. 10 in Zhang et al., 2018), (iii) monthly runoff from 165 medium size basins and a further 862 small basins (Fig. 14 in Zhang et al., 2018), (iv) summer *E* from 47 flux towers (Fig. 16 in Zhang et al., 2018). Those evaluations did not directly address variability in various water cycle elements. With our focus on the variability we decided to conduct further validations of the CDR database beyond those described in the original work. In particular, we focussed on further independent assessments of *E* and we use monthly (as opposed to summer) observations of *E* from FLUXNET to evaluate the variability in *E*. We also compare the evapotranspiration *E* in the CDR with two other gridded global *E* products that were not used to develop the CDR including the LandFluxEval database (1° × 1°, monthly, 1989-2005) (Mueller et al., 2013) and the Max Planck Institute database (MPI, 0.5° × 0.5°, monthly, 1982-2011) (Jung et al., 2010). The runoff *Q* in the CDR is further compared with the gridded European *Q* product E-RUN (0.5° × 0.5°, monthly, 1951-2015) (Gudmundsson and Seneviratne, 2016).

For the comparison to FLUXNET observations (Baldocchi et al., 2001; Agarwal et al., 2010) we identified 32 flux tower sites (site locations are shown in Fig. S3 and details are shown in Table S1) having at least three years of continuous (monthly) measurements using the FluxnetLSM R package (v1.0) (Ukkola et al. 2017). The monthly totals and annual climatology of *P* and *E* from CDR generally follow FLUXNET observations, with high correlations and reasonable Root Mean Square Error (Figs. S4-S5, Table S1). Comparison of the point-based FLUXNET (~ 100 m – 1 km scale) with the grid-based CDR (~ 50 km scale) is problematic since the CDR represents an area that is at least 2500 times larger than the area represented by the individual FLUXNET towers and we anticipate that the CDR record would be "smoothed" relative to the FLUXNET record. With that in mind, we chose to compare the ratio of the standard deviation of *E* to *P* between the CDR and FLUXNET databases and this normalised comparison of the hydrologic variability proved encouraging (Fig. S6).

The comparison of *E* between the CDR and the LandFluxEval and MPI databases also proved encouraging. We found that the monthly mean *E* from the CDR database is slightly underestimated compared with LandFluxEVAL database (Fig. S7a), but agrees closely with the MPI database (Fig. S8a). In terms of variability, the standard deviations of monthly *E* from the CDR are in very close agreement with the LandFluxEVAL database (Fig. S7c), but there is a bias and scaling offset for the comparison with the MPI database particularly for the grid-cells with low standard deviation of *E* (Fig. S8c). The comparison of runoff *Q* between the E-RUN and CDR databases show that the two databases have very similar spatial patterns of both the long-term mean ($\bar{Q}$) and standard deviation

Deleted: was

(σ_Q) of the monthly Q (Fig. S10). The grid-by-grid comparison results are also encouraging, showing slight bias of both the long-term mean and standard deviation of monthly Q in the CDR database compared with the E-RUN database (Fig. S11).

Deleted:

We concluded that while the CDR database was unlikely to be perfect, it was nevertheless suitable for an initial exploratory survey of inter-annual variability in the terrestrial branch of the global water cycle.

3. Mean and Variability of Water Cycle Components

3.1 Mean Annual P, E, Q and the Budyko Curve

The global pattern of mean annual P, E, Q using the CDR data (1984-2007) is shown in Fig. 1. The mean annual P ($\bar{P}$) is prominent in tropical regions, southern China, eastern and western North America (Fig. 1a). The magnitude of mean annual E ($\bar{E}$) more or less follows the pattern of $\bar{P}$ in the tropics (Fig. 1b) while the mean annual Q ($\bar{Q}$) is particularly prominent in the Amazon, South and Southeast Asia, tropical parts of west Africa and in some other coastal regions at higher latitudes (Fig. 1c).

We relate the grid-box level ratio of $\bar{E}$ to $\bar{P}$ in the CDR database to the classical Budyko (1974) curve using the aridity index ($\overline{E_o}/\bar{P}$) (Fig. 2a). As noted previously, in the CDR database, $\overline{\Delta S}$ is forced to be zero and this enforced steady state (i.e., $\bar{P} = \bar{E} + \bar{Q}$) allowed us to also predict the ratio of $\bar{Q}$ to $\bar{P}$ using the same Budyko curve (Fig. 2b). The Budyko curves follow the overall pattern in the CDR data, which agrees with previous studies showing that the aridity index can be used to predict water availability (e.g., Gudmundsson et al., 2016). However, there is substantial scatter due to, for example, regional variations related to seasonality, water storage change and the landscape characteristics (Milly, 1994a, b, Padrón et al., 2017). With that caveat in mind, the overall patterns are as expected with $\bar{E}$ following $\bar{P}$ in dry environments ($\overline{E_o}/\bar{P}$ > 1.0) while $\bar{E}$ follows $\overline{E_o}$ in wet environments ($\overline{E_o}/\bar{P}$ ≤ 1.0) (Fig. 2).

Deleted: trend

3.2 Inter-annual Variability in P, E, Q and ΔS

We use the variance balance equation (Eq. 2) to partition the inter-annual σ_P^2 into separate components due to σ_E^2, σ_Q^2, $\sigma_{\Delta S}^2$ along with the three covariance components ($2cov(E,Q)$, $2cov(E,\Delta S)$, $2cov(Q,\Delta S)$) (Fig. 3). The spatial pattern of σ_P^2 (Fig. 3a) is very similar to that of $\bar{P}$ (Fig. 1a), which implies that the σ_P^2 is positively correlated with $\bar{P}$. In contrast the partitioning of σ_P^2 to the various components is very different from the partitioning of $\bar{P}$ (cf. Fig. 1 and 3). First we note that while the overall spatial pattern of σ_E^2 more or less follows σ_P^2, the overall magnitude of σ_E^2 is much smaller than σ_P^2 and σ_Q^2 in most regions, and in fact σ_E^2 is also generally smaller than $\sigma_{\Delta S}^2$. The prominence of $\sigma_{\Delta S}^2$ (compared to σ_E^2) surprised us. The three covariance components ($cov(E,Q)$, $cov(E,\Delta S)$, $cov(Q,\Delta S)$) are also important in some regions. In more detail, the $cov(E,Q)$ term is prominent in regions where σ_Q^2 is large and is mostly negative in those regions (Fig. 3e), indicating that years with lower E are associated with higher Q and vice-versa. There are also a few regions with prominent positive values for $cov(E,Q)$ (e.g., the seasonal hydroclimates of northern Australia) indicating that in those regions, years with a higher E are associated with higher Q. The $cov(E,\Delta S)$ term (Fig. 3f) has a similar spatial pattern to the $cov(E,Q)$ term (Fig. 3e) but with a smaller overall magnitude. Finally, the $cov(Q,\Delta S)$ term shows a more complex spatial pattern, with both prominent positive and negative values (Fig. 3g) in regions where σ_Q^2 (Fig. 3c) and $\sigma_{\Delta S}^2$ (Fig. 3d) are both large.

These results show that the spatial patterns in variability are not simply a reflection of patterns in the long-term mean state. On the contrary, we find that of the three primary variance terms, the overall magnitude of (inter-annual) σ_E^2 is the smallest implying the least (inter-annual) variability in E. This is very different from the conclusions based on spatial patterns in the mean P, E and Q (see section 3.1). Further, while σ_Q^2 more or less follows σ_P^2 as expected, we were surprised by the magnitude of $\sigma_{\Delta S}^2$ which, in general, substantially exceeds the magnitude of σ_E^2. Further, the magnitude of the covariance terms can be important, especially in regions with high σ_Q^2. However, unlike the variances, the covariance can be both positive and negative and this introduces additional complexity. For example, with a negative covariance it is possible for the variance in Q (σ_Q^2) to exceed the variance in P (σ_P^2). To examine that in more detail we calculated the equivalent frequency distribution for each of the plots in Fig. 3. The results (Fig. S9) further emphasise that in general, σ_E^2 is the smallest of the variances (Fig. S9b). We also note that the frequency distributions for the covariances (Fig. S9efg) are not symmetrical. In summary, it is clear that spatial patterns in the inter-annual variability of the water cycle (Fig. 3) do not simply follow the spatial patterns for the inter-annual mean (Fig. 1).

3.3 Relation Between Variability and the Mean State for P, E, Q

Differences in the spatial patterns of the mean (Fig. 1) and inter-annual variability (Fig. 3) in the global water cycle led us to further investigate the relation between the mean and the variability for each separate component. Here we relate the standard deviation (σ_P, σ_E, σ_Q) instead of the variance to the mean of each water balance flux (Fig. 4) since the standard deviation has the same physical units as the mean making the results more comparable. As inferred previously, we find σ_P to be positively correlated with $\bar{P}$ but with substantial scatter (Fig. 4a). The same result more or less holds for the relation between σ_Q and $\bar{Q}$ (Fig. 4c). In contrast the relation between σ_E and $\bar{E}$ is very different (Fig. 4b). In particular, σ_E is a small fraction of $\bar{E}$ and this complements the earlier finding (Fig. 4b) that the inter-annual variability for E is generally smaller than for the other physical variables (P, Q and ΔS). (The same result was also found using both LandFluxEVAL and MPI databases, see Fig. S12 in the Supplementary Material.) Importantly, unlike P and Q, E is constrained by both water and energy availability (Budyko, 1974) and the limited inter-annual variability in E presumably reflects limited inter-annual variability in the available (radiant) energy (E_o). This is something that could be investigated in a future study.

Deleted: S10

4. Relating the Variability of Water Cycle Components to Aridity

In the previous section, we investigated spatial patterns of the mean and the variability in the global water cycle. In this section, we extend that by investigating the partitioning of σ_P^2 to the three primary physical terms (σ_E^2, σ_Q^2, $\sigma_{\Delta S}^2$) along with the three relevant covariances. For that, we begin by comparing the Koster and Suarez (1999) theory against the CDR data and then investigate how the partitioning of the variance is related to the aridity index $\overline{E_o}/\bar{P}$ (see Fig. S1a in the Supplementary Material). Following that, we investigate variance partitioning in relation to both our estimate of the storage capacity S_{max} (see Fig. S1b in the Supplementary Material) as well as the mean annual air temperature $\overline{T_a}$ (see Fig. S1c in the Supplementary Material) that we use as a surrogate for snow/ice cover. We finalise this section by examining the partitioning of variance at three selected study sites that represent extremely dry/wet, high/low water storage capacity and the hot/cold spectrums.

4.1 Comparison with the Koster and Suarez (1999) Theory

We first evaluate the classical empirical curve of Koster and Suarez (1999) by relating ratios σ_E/σ_P and σ_E/σ_P to the aridity index (Fig. 5). The ratio σ_E/σ_P in the CDR database is generally overestimated by the empirical Koster and Suarez curve, especially in dry environments (e.g., $\overline{E_o}/\overline{P}$ > 3) (Fig. 5a). The inference here is that the Koster and Suarez theory predicts σ_E/σ_P to approach unity in dry environments while the equivalent value in the CDR data is occasionally unity but is generally smaller. With σ_E/σ_P generally overestimated by the Koster and Suarez theory we expect, and find, that σ_Q/σ_P is generally underestimated by the same theory (Fig. 5b). The same overestimation was found based on the other two independent databases for E (LandFluxEVAL and MPI) (Fig. S13). This overestimation is discussed further in section 5.

Deleted: S11

4.2 Relating Inter-annual Variability to Aridity

Here we examine how the fraction of the total variance in precipitation accounted for by the three primary variance terms along with the three covariance terms varies with the aridity index ($\overline{E_o}/\overline{P}$) (Fig. 6). (Also see Fig. S14 for the spatial maps.) The ratio σ_E^2/σ_P^2 is close to zero in extremely wet regions and has an upper limit noted previously (Fig. 5a) that approaches unity in extremely dry regions (Fig. 6a). The ratio σ_Q^2/σ_P^2 is close to zero in extremely dry regions but approaches unity in extremely wet regions but with substantial scatter (Fig. 6b). The ratio $\sigma_{\Delta S}^2/\sigma_P^2$ is close to zero in both extremely dry/wet regions (Fig. 6c) and shows the largest range at an intermediate aridity index ($\overline{E_o}/\overline{P}$ ~ 1.0).

Deleted: S12

The covariance ratios are all small in extremely dry (e.g., $\overline{E_o}/\overline{P}$ ≥6.0) environments and generally show the largest range in semi-arid and semi-humid environments. The peak magnitudes for the three covariance components consistently occur when $\overline{E_o}/\overline{P}$ is close to 1.0 which is the threshold often used to separate wet and dry environments.

4.3 Further Investigations on the Factors Controlling Partitioning of the Variance

Results in the previous section demonstrated that spatial variation in the partitioning of σ_P^2 into σ_E^2, σ_Q^2, $\sigma_{\Delta S}^2$ and the three covariance components is complex (Fig. 6). To help further understand inter-annual variability of the terrestrial water cycle, we conduct further investigations in this section using two factors likely to have a major influence on the variance partitioning of σ_P^2. The first is the storage capacity $S_{\max}$ (see Fig. S1b in the Supplementary Material). The second is the mean annual air temperature $\overline{T_a}$ (see Fig. S1c in the Supplementary Material) which is used here as a surrogate for snow/ice presence.

4.3.1 Relating Inter-annual Variability to Storage Capacity

We first relate the partitioning of σ_P^2 to water storage capacity ($S_{\max}$) by repeating Fig. 6 but instead we use a logarithmic scale for the x-axis and we distinguish $S_{\max}$ via the background colour (Fig. 7). To eliminate the possible overlap of grid-cells in the colouring process, all the grid-cells over land are further separated using different latitude ranges (as shown in the four columns of Fig. 7), i.e., 90N-60N, 60N-30N, 30N-0 and 0-90S. We find that $S_{\max}$ is relatively high in wet environments ($\overline{E_o}/\overline{P} \leq 1.0$, Fig. 7a) but shows no obvious relation to the partitioning of σ_P^2. However, in dry environments ($\overline{E_o}/\overline{P} > 1.0$) the ratio σ_E^2/σ_P^2 apparently decreases with the increase of $S_{\max}$ (Fig. 7a-d). That relation is particularly obvious in extremely dry environments ($\overline{E_o}/\overline{P} \geq 6.0$) at equatorial latitudes where there is an upper limit of σ_E^2/σ_P^2 close to 1.0 when $S_{\max}$ is small (blue grid-cells in Fig. 7c). The interpretation for those extremely dry environments is that when $S_{\max}$ is small, σ_P^2 is almost completely partitioned into σ_E^2 (Fig. 7bc) with the other variance and covariance components close to zero. While for those same extremely dry environments, as $S_{\max}$ increases, the partitioning of σ_P^2 is shared between σ_E^2 and $\sigma_{\Delta S}^2$ and their covariance (Fig. 7cks) while σ_Q^2 and its covariance components remain close to zero (Fig. 7gow). However, at polar latitudes in the northern hemisphere (panels in the first and second columns of Fig. 7) there are variations that could not be easily associated with variations in $S_{\max}$ which led us to further investigate the role of snow/ice on the variance partitioning in the following section.

4.3.2 Relating Inter-annual Variability to Mean Air Temperature

To understand the potential role of snow/ice in modifying the variance partitioning, we repeat the previous analysis (Fig. 7) but here we use the mean annual air temperature ($\overline{T_a}$) to colour the grid-cells to (crudely) indicate the presence of snow/ice (Fig. 8). The results are complex and not easy to simply understand. The most important difference revealed by this analysis is in the hydrologic partitioning between cold (first column) and hot (third column) conditions in wet environments ($\overline{E_o}/\overline{P} \leq 0.5$). In particular, when $\overline{T_a}$ is high, σ_P^2 is almost completely partitioned into σ_Q^2 in wet environments (e.g., $\overline{E_o}/\overline{P} \leq 0.5$, Fig. 8g). In contrast, when $\overline{T_a}$ is low in a wet environment ($\overline{E_o}/\overline{P} \leq 0.5$ in first column of Fig. 8), there are substantial variations in the hydrologic partitioning. That result reinforces the complexity of variance partitioning in the presence of snow/ice.

4.4 Case Studies

The previous results (Section 4.3) have demonstrated that the partitioning of σ_P^2 is influenced by the water storage capacity ($S_{\max}$) in extremely dry environments ($\overline{E_o}/\overline{P}$ ≥6.0) and that the presence of snow/ice is important (as indicated by mean air temperature ($\overline{T_a}$)) in extremely wet environments ($\overline{E_o}/\overline{P}$ ≤0.5). In this section, we examine, in greater detail, several sites to gain deeper understanding of the partitioning of σ_P^2. For that purpose, we selected three sites based on extreme values for the three explanatory parameters, i.e., $\overline{E_o}/\overline{P}$ (Fig. S1a), $S_{\max}$ (Fig. S1b) and $\overline{T_a}$ (Fig. S1c). The criteria to select three climate sites are as follows, Site 1: dry ($\overline{E_o}/\overline{P} \geq 6.0$) and small $S_{\max}$ ($S_{\max}$ ≈ 0), Site 2: dry ($\overline{E_o}/\overline{P} \geq 6.0$) and relatively large $S_{\max}$ ($S_{\max} \gg 0$) and Site 3: wet ($\overline{E_o}/\overline{P} \leq 0.5$) and hot ($\overline{T_a}$ > 25 ˚C). For each of the three classes, we use a representative grid-cell (Fig. 9) to show the original time series (Fig. 10) and the partitioning of the variability (Fig. 11).

We show the P, E, Q and ΔS time series along with the relevant variances and covariances in Fig. 10. Starting with the two dry sites, at the site with low storage capacity (Site 1), the time series shows that E closely follows P leaving annual Q and ΔS close to zero (Fig. 10a). The variance of P (σ_P^2 = 206.9 mm^2) is small and almost completely partitioned into the variance of E (σ_E^2 = 196.9 mm^2), leaving very limited variance for Q, ΔS and all three covariance components (Fig. 10b). At the dry site with larger storage capacity (Site 2), E, Q and ΔS do not simply follow P (Fig. 10c). As a consequence, the variance of P (σ_P^2 = 2798.0 mm^2) is shared between E (σ_E^2 = 1150.2 mm^2), ΔS ($\sigma_{\Delta S}^2$ = 800.5 mm^2) and their covariance component ($2cov(E, \Delta S)$ = 538.4 mm^2, Fig. 10d). Switching now to the remaining wet and hot site (Site 3), we note that Q closely follows P, with ΔS close to zero and E showing little inter-annual variation (Fig. 10e). The variance of P (σ_P^2 = 57374.4 mm^2) is relatively large and almost completely partitioned into the variance of Q (σ_Q^2 = 57296.4 mm^2), leaving very limited variance for E and ΔS and the three covariance components (Fig. 10f). We also examined numerous other sites with similar extreme conditions as the three case study sites and found the same basic patterns as reported above.

To put the data from the three case study sites into a broader variability context we position the site data onto a backdrop of original Fig. 6. As noted previously, at Site 1, the ratio σ_E^2/σ_P^2 is very close to unity (Fig. 11a), and under this extreme condition, we have the following approximation,

$$\sigma_P^2 \approx \sigma_E^2 \quad \text{(Site 1, dry and } S_{\max} \approx 0) \qquad (3)$$

In contrast, for Site 2 with the same aridity index but higher $S_{\max}$, we have,

$$\sigma_P^2 \approx \sigma_E^2 + \sigma_{\Delta S}^2 + 2cov(E, \Delta S) \quad \text{(Site 2, dry and } S_{\max} \gg 0) \tag{4}$$

Finally, at Site 3, we have,

$$\sigma_P^2 \approx \sigma_Q^2 \quad \text{(Site 3, wet and hot)} \tag{5}$$

4.5 Synthesis

The above simple examples demonstrate that aridity $\overline{E_o}/\overline{P}$, storage capacity $S_{\max}$ and to a lesser extent, air temperature $\overline{T_a}$, all play some role in the partitioning of σ_P^2 to the various components. Our synthesis of the results for the partitioning of σ_P^2 is summarised in Fig. 12. In dry environments with low storage capacity ($S_{\max} \approx 0$) we have minimal runoff and expect that σ_P^2 is more or less completely partitioned into σ_E^2 (Fig. 12a). In those environments, (inter-annual) variations in storage $\sigma_{\Delta S}^2$ play a limited role in setting the overall variability. However, in dry environments with larger storage capacity ($S_{\max} \gg 0$), σ_E^2 is only a small fraction of σ_P^2 (Fig. 12a) leaving most of the overall variance in σ_P^2 to be partitioned to $\sigma_{\Delta S}^2$ and the covariance between E and ΔS (Fig. 12c and Fig. 12e). This emphasises the hydrological importance of water storage capacity in buffering variations of the water cycle under dry conditions.

Under extremely wet conditions, the largest difference in variance partitioning is not due to differences in storage capacity but is instead related to differences in mean air temperature. In wet and hot environments, we have maximum runoff and find that σ_P^2 is more or less completely partitioned into σ_Q^2 (Fig. 12b) while the partitioning to σ_E^2 and $\sigma_{\Delta S}^2$ is small. However, in wet and cold environments, the variance partitioning shows great complexity with σ_P^2 being partitioned into all possible components. We suggest that this emphasises the hydrological importance of thermal processes (melting/freezing) under extremely cold conditions.

However, the most complex patterns to interpret are those for semi-arid to semi-humid environments (i.e., $\overline{E_o}/\overline{P}$ ~1.0). Despite a multitude of attempts over an extended period we were unable to develop a simple useful synthesis to summarise the partitioning of variability in those environments. We found that the three covariance terms all play important roles and we also found that simple environmental gradients (e.g., dry/wet, high/low storage capacity, hot/cold) could not easily explain the observed patterns. We anticipate that vegetation related processes (e.g., phenology, rooting depth, gas exchange characteristics, disturbance, etc.) may prove to be important in explaining hydrologic variability in these biologically productive regions that support most of human population. This result implies that a major scientific effort will be needed to develop a synthesis of the controlling factors for variability of the water cycle in these environments.

5. Discussion and Conclusions

Importantly, hydrologists have long been interested in hydrologic variability, but without readily available databases it has been difficult to quantify water cycle variability. For example, we are not aware of maps showing global spatial patterns in variance for any terms of the water balance (except for *P*). In this study, we describe an initial investigation of the inter-annual variability of the terrestrial branch in the global water cycle that uses the recently released global monthly Climate Data Record (CDR) database for *P*, *E*, *Q* and Δ*S*. The CDR is one of the first dedicated hydrologic reanalysis databases and includes data for a 27-year period. Accordingly, we could only examine hydrologic variability over this relatively short period. Further, we expect future improvements and modifications as the hydrologic community seeks to further develop and refine these new reanalysis databases. With those caveats in mind, we started this analysis by first investigating the partitioning of *P* in the water cycle in terms of long-term mean and then extended that to the inter-annual variability using a theoretical variance balance equation (Eq. 2). Despite the initial nature of this investigation we have been able to establish some useful general principles.

The mean annual *P* is mostly partitioned into mean annual *E* and *Q*, as is well known, and the results using the CDR were generally consistent with the earlier Budyko framework (Fig. 2). Having established that, the first general finding is that the spatial pattern in the partitioning of inter-annual variability in the water cycle is not simply a reflection of the spatial pattern in the partitioning of the long-term mean. In particular, with the variance calculations, the annual anomalies are squared and hence the storage anomalies do not cancel out like they do when calculating the mean. With that in mind, we were surprised that the inter-annual variability of water storage change ($\sigma_{\Delta S}^2$) is typically larger than the inter-annual variability of evapotranspiration (σ_E^2) (cf. Fig. 3b and 3d). The consequence is that $\sigma_{\Delta S}^2$ is more important than σ_E^2 for understanding inter-annual variability of global water cycle. A second important generalisation is that unlike the variance components which are all positive, the three covariance components in the theory (Eq. 2) can be both positive and negative. We report results here showing both large positive and negative values for the three covariance terms (Fig. 3efg). This was especially prevalent in biologically productive regions ($0.5<\overline{E_o}/\overline{P}<1.5$, Fig. 3eg). When examining the mean state, we are accustomed to think that P sets a limit to E, Q and ΔS, as per the mass balance (Eq. 1). But the same thinking does not extend to the variance balance since the covariance terms on the right hand side of Eq. 2 can be both large and negative leading to circumstances where the variability in the sinks (σ_E^2, σ_Q^2, $\sigma_{\Delta S}^2$) could actually exceed variability in the source (σ_P^2). These general principles of variance partitioning in the water cycle above may vary at different time scales (e.g., monthly, daily), and we expect more details of the variability partitioning across various temporal scales to be investigated in future studies.

Deleted: propagation

Deleted: the

Our initial attempt to develop deeper understanding of variance partitioning was based on a series of case studies located in extreme environments (wet/dry vs hot/cold vs high/low water storage capacity). The results offered some further insights about hydrologic variability. For example, under extremely dry (water-limited) environments, with limited storage capacity (S_{max}) we found that E follows P and σ_E^2 follows σ_P^2, with σ_Q^2 and $\sigma_{\Delta S}^2$ both approaching zero. However, as S_{max} increases, the partitioning of σ_P^2 progressively shifts to a balance between σ_E^2, $\sigma_{\Delta S}^2$ and cov(E, ΔS) (Figs. 10-12). This result explains the overestimation of σ_E/σ_P by the empirical theory of Koster and Suarez (1999) which implicitly assumed no inter-annual change in storage. The Koster and Suarez empirical theory is perhaps better described as an upper limit that is based on minimal storage capacity, and that any increase in storage capacity would promote the partitioning of σ_P^2 to $\sigma_{\Delta S}^2$ particularly under dry conditions (Figs. 10-12).

In extremely wet/hot environments (i.e., no snow/ice presence) we found σ_P^2 to be mostly partitioned to σ_Q^2 (with both σ_E^2 and $\sigma_{\Delta S}^2$ approaching zero, Fig. 10). In contrast, in extremely wet/cold environments, the partitioning of σ_P^2 was highly (spatially) variable presumably because of spatial variability in the all-important thermal processes (freeze/melt).

The most complex results were found in mesic biologically productive environments ($0.5<\overline{E_o}/\overline{P}<1.5$), where all three covariance terms (Eq. 2) were found to be relatively large and therefore they all played critical roles in the overall partitioning of variability (Fig. 6). As noted above, in many of these regions, the (absolute) magnitudes of the covariances were actually larger than the variances of the water balance components E, Q and ΔS (e.g., Fig. 3). That result demonstrates that deeper understanding of the process-level interactions that are embedded within each of the three covariance terms (e.g., the role of seasonal vegetation variation) will be needed to develop process-based understanding of variability in the water cycle in these biologically productive regions (0.5<$\overline{E_o}/\overline{P}$ <1.5).

The syntheses of the long-term mean water cycle originated in 1970s (Budyko, 1974), and it took several decades for those general principles to become widely adopted in the hydrologic community. The hydrologic data needed to understand hydrologic variability are only now becoming available. With those data we can begin to develop a process-based understanding of hydrologic variability that can be used for a variety of purposes, e.g., deeper understanding of hydro-climatic behaviour, hydrologic risk analysis, climate change assessments and hydrologic sensitivity studies are just a few applications that spring to mind. The initial results presented here show that a major intellectual effort will be needed to develop a general understanding of hydrologic variability.

Acknowledgements

This research was supported by the Australian Research Council (CE11E0098, CE170100023), and D.Y. also acknowledges support by the National Natural Science Foundation of China (51609122). We thank Dr Anna Ukkola for help in accessing the FLUXNET database. We thank the reviewers (including Dr René Orth and two anonymous reviewers) for helpful comments that improved the manuscript. The authors declare that there is no conflict of interests regarding the publication of this paper. All data used in this paper are available online as referenced in the 'Methods and Data' section.

References

Agarwal, D. A., Humphrey, M., Beekwilder, N. F., Jackson, K. R., Goode, M. M., and van Ingen, C.: A data-centered collaboration portal to support global carbon-flux analysis, Concurr. Comp-Pract. E., 22, 2323-2334, https://doi.org/10.1002/cpe.1600, 2010.

Baldocchi, D., Falge, E., Gu, L., Olson, R., Hollinger, D., Running, S., Anthoni, P., Bernhofer, C., Davis, K., Evans, R., Fuentes, J., Goldstein, A., Katul, G., Law, B., Lee, X., Malhi, Y., Meyers, T., Munger, W., Oechel, W., Paw U, K. T., Pilegaard, K., Schmid, H. P., Valentini, R., Verma, S., Vesala, T., Wilson, K., and Wofsy, S.: FLUXNET: A New Tool to Study the Temporal and Spatial Variability of Ecosystem-Scale Carbon Dioxide, Water Vapor, and Energy Flux

Densities, B. Am. Meteorol. Soc., 82, 2415-2434, https://doi.org/10.1175/1520-0477(2001)082<2415:FANTTS>2.3.CO;2, 2001.

Balsamo, G., Albergel, C., Beljaars, A., Boussetta, S., Brun, E., Cloke, H., Dee, D., Dutra, E., Muñoz-Sabater, J., Pappenberger, F., de Rosnay, P., Stockdale, T., and Vitart, F.: ERA-Interim/Land: a global land surface reanalysis data set, Hydrol. Earth Syst. Sci., 19, 389-407, 10.5194/hess-19-389-2015, 2015.

Budyko, M. I.: Climate and Life. Academic Press, London, 1974.

Choudhury, B. J.: Evaluation of an empirical equation for annual evaporation using field observations and results from a biophysical model, J. Hydrol., 216, 99-110, https://doi.org/10.1016/S0022-1694(98)00293-5, 1999.

Dee, D. P., Uppala, S. M., Simmons, A. J., Berrisford, P., Poli, P., Kobayashi, S., Andrae, U., Balmaseda, M. A., Balsamo, G., Bauer, P., Bechtold, P., Beljaars, A. C. M., van de Berg, L., Bidlot, J., Bormann, N., Delsol, C., Dragani, R., Fuentes, M., Geer, A. J., Haimberger, L., Healy, S. B., Hersbach, H., Hólm, E. V., Isaksen, L., Kållberg, P., Köhler, M., Matricardi, M., McNally, A. P., Monge‐Sanz, B. M., Morcrette, J. J., Park, B. K., Peubey, C., de Rosnay, P., Tavolato, C., Thépaut, J. N., and Vitart, F.: The ERA‐Interim reanalysis: configuration and performance of the data assimilation system, Q. J. R. Meteorol. Soc., 137, 553-597, https://doi.org/10.1002/qj.828, 2011.

Donohue, R. J., Roderick, M. L., and McVicar, T. R.: Can dynamic vegetation information improve the accuracy of Budyko's hydrological model?, J. Hydrol., 390, 23-34, https://doi.org/10.1016/j.jhydrol.2010.06.025, 2010.

Fu, B. P.: On the Calculation of the Evaporation from Land Surface, Sci. Atmos. Sin., 5, 23-31, 1981.

Gudmundsson, L., Greve, P., and Seneviratne, S. I.: The sensitivity of water availability to changes in the aridity index and other factors—A probabilistic analysis in the Budyko space, Geophys. Res. Lett., 43, 6985-6994, https://doi.org/10.1002/2016GL069763, 2016.

Gudmundsson, L., and Seneviratne, S. I.: Observation-based gridded runoff estimates for Europe (E-RUN version 1.1), Earth Syst. Sci. Data, 8, 279-295, 10.5194/essd-8-279-2016, 2016.

Harris, I., Jones, P. D., Osborn, T. J., and Lister, D. H.: Updated high‐resolution grids of monthly climatic observations–the CRU TS3. 10 Dataset, Int. J. Climatol., 34, 623-642, https://doi.org/10.1002/joc.3711, 2014.

Huning, L. S., and AghaKouchak, A.: Mountain snowpack response to different levels of warming, Proc. Natl. Acad. Sci. U. S. A., 115, 10932, https://doi.org/10.1073/pnas.1805953115, 2018.

Jackson, R. B., Canadell, J., Ehleringer, J. R., Mooney, H. A., Sala, O. E., and Schulze, E. D.: A Global Analysis of Root Distributions for Terrestrial Biomes, Oecologia, 108, 389-411, https://doi.org/10.1007/BF00333714, 1996.

Jung, M., Reichstein, M., Ciais, P., Seneviratne, S. I., Sheffield, J., Goulden, M. L., Bonan, G., Cescatti, A., Chen, J., de Jeu, R., Dolman, A. J., Eugster, W., Gerten, D., Gianelle, D., Gobron, N., Heinke, J., Kimball, J., Law, B. E., Montagnani, L., Mu, Q., Mueller, B., Oleson, K., Papale, D., Richardson, A. D., Roupsard, O., Running, S., Tomelleri, E., Viovy, N., Weber, U., Williams, C., Wood, E., Zaehle, S., and Zhang, K.: Recent decline in the global land evapotranspiration trend due to limited moisture supply, Nature, 467, 951, https://doi.org/10.1038/nature09396, 2010.

Koster, R. D., and Suarez, M. J.: A Simple Framework for Examining the Interannual Variability of Land Surface Moisture Fluxes, J. Clim., 12, 1911-1917, https://doi.org/10.1175/1520-0442(1999)012<1911:ASFFET>2.0.CO;2, 1999.

McMahon, T. A., Peel, M. C., Pegram, G. G. S., and Smith, I. N.: A Simple Methodology for Estimating Mean and Variability of Annual Runoff and Reservoir Yield under Present and Future Climates, J. Hydrometeorol., 12, 135-146, https://doi.org/10.1175/2010jhm1288.1, 2011.

Milly, P. C. D.: Climate, soil water storage, and the average annual water balance, Water Resour. Res., 30, 2143-2156, https://doi.org/10.1029/94WR00586, 1994a.

Milly, P. C. D.: Climate, interseasonal storage of soil water, and the annual water balance, Adv. Water Resour., 17, 19-24, https://doi.org/10.1016/0309-1708(94)90020-5, 1994b.

Milly, P. C. D., and Dunne, K. A.: Macroscale water fluxes 1. Quantifying errors in the estimation of basin mean precipitation, Water Resour. Res., 38, 23-21-23-14, https://doi.org/10.1029/2001WR000759, 2002a.

Milly, P. C. D., and Dunne, K. A.: Macroscale water fluxes 2. Water and energy supply control of their interannual variability, Water Resour. Res., 38, 24-21-24-29, https://doi.org/10.1029/2001WR000760, 2002b.

Mueller, B., Hirschi, M., Jimenez, C., Ciais, P., Dirmeyer, P. A., Dolman, A. J., Fisher, J. B., Jung, M., Ludwig, F., Maignan, F., Miralles, D. G., McCabe, M. F., Reichstein, M., Sheffield, J., Wang, K., Wood, E. F., Zhang, Y., and Seneviratne, S. I.: Benchmark products for land evapotranspiration: LandFlux-EVAL multi-data set synthesis, Hydrol. Earth. Syst. Sci., 17, 3707-3720, https://doi.org/10.5194/hess-17-3707-2013, 2013.

Norby, R. J., Ledford, J., Reilly, C. D., Miller, N. E., and O'Neill, E. G.: Fine-root production dominates response of a deciduous forest to atmospheric CO2 enrichment, Proc. Natl. Acad. Sci. U. S. A., 101, 9689-9693, https://doi.org/10.1073/pnas.0403491101, 2004.

Orth, R., and Destouni, G.: Drought reduces blue-water fluxes more strongly than green-water fluxes in Europe, Nat. Commun., 9, 3602, https://doi.org/10.1038/s41467-018-06013-7, 2018.

Padrón, R. S., Gudmundsson, L., Greve, P., and Seneviratne, S. I.: Large-Scale Controls of the Surface Water Balance Over Land: Insights From a Systematic Review and Meta-Analysis, Water Resources Research, 53, 9659-9678, 10.1002/2017WR021215, 2017.

Reichle, R. H., Koster, R. D., De Lannoy, G. J. M., Forman, B. A., Liu, Q., Mahanama, S. P. P., and Touré, A.: Assessment and Enhancement of MERRA Land Surface Hydrology Estimates, Journal of Climate, 24, 6322-6338, 10.1175/JCLI-D-10-05033.1, 2011.

Rodell, M., Beaudoing, H. K., L'Ecuyer, T. S., Olson, W. S., Famiglietti, J. S., Houser, P. R., Adler, R., Bosilovich, M. G., Clayson, C. A., Chambers, D., Clark, E., Fetzer, E. J., Gao, X., Gu, G., Hilburn, K., Huffman, G. J., Lettenmaier, D. P., Liu, W. T., Robertson, F. R., Schlosser, C. A., Sheffield, J., and Wood, E. F.: The Observed State of the Water Cycle in the Early Twenty-First Century, J. Clim., 28, 8289-8318, https://doi.org/10.1175/JCLI-D-14-00555.1, 2015.

Roderick, M. L., and Farquhar, G. D.: A simple framework for relating variations in runoff to variations in climatic conditions and catchment properties, Water Resour. Res., 47, https://doi.org/10.1029/2010WR009826, 2011.

Sankarasubramanian, A., and Vogel, R. M.: Annual hydroclimatology of the United States, Water Resour. Res., 38, 19-11-19-12, https://doi.org/10.1029/2001WR000619, 2002.

Scanlon, B. R., Zhang, Z., Save, H., Sun, A. Y., Müller Schmied, H., van Beek, L. P. H., Wiese, D. N., Wada, Y., Long, D., Reedy, R. C., Longuevergne, L., Döll, P., and Bierkens, M. F. P.: Global models underestimate large decadal declining and rising water storage trends relative to GRACE satellite data, Proc. Natl. Acad. Sci. U. S. A., https://doi.org/10.1073/pnas.1704665115, 2018.

Sposito, G.: Understanding the Budyko Equation, Water, 9, https://doi.org/10.3390/w9040236, 2017.

Stackhouse, P. W., Gupta, S. K., Cox, S. J., Mikovitz, J. C., Zhang, T., and Hinkelman, L. M.: The NASA/GEWEX Surface Radiation Budget Release 3.0: 24.5-Year Dataset. In: GEWEX News, No. 1, 2011.

Ukkola, A. M., Haughton, N., De Kauwe, M. G., Abramowitz, G., and Pitman, A. J.: FluxnetLSM R package (v1.0): a community tool for processing FLUXNET data for use in land surface modelling, Geosci. Model. Dev., 10, 3379-3390, https://doi.org/10.5194/gmd-10-3379-2017, 2017.

Wang, D., and Alimohammadi, N.: Responses of annual runoff, evaporation, and storage change to climate variability at the watershed scale, Water Resour. Res., 48, https://doi.org/10.1029/2011WR011444, 2012.

Wang-Erlandsson, L., Bastiaanssen, W. G. M., Gao, H., Jägermeyr, J., Senay, G. B., van Dijk, A. I. J. M., Guerschman, J. P., Keys, P. W., Gordon, L. J., and Savenije, H. H. G.: Global root zone storage capacity from satellite-based evaporation, Hydrol. Earth Syst. Sci., 20, 1459-1481, https://doi.org/10.5194/hess-2015-533, 2016.

Yang, H., Yang, D., Lei, Z., and Sun, F.: New analytical derivation of the mean annual water-energy balance equation, Water Resour. Res., 44, https://doi.org/10.1029/2007WR006135, 2008.

Yang, Y., Donohue, R. J., and McVicar, T. R.: Global estimation of effective plant rooting depth: Implications for hydrological modeling, Water Resour. Res., 52, 8260-8276, https://doi.org/10.1002/2016WR019392, 2016.

Zeng, R., and Cai, X.: Assessing the temporal variance of evapotranspiration considering climate and catchment storage factors, Adv. Water Resour., 79, 51-60, https://doi.org/10.1016/j.advwatres.2015.02.008, 2015.

Zhang, L., Potter, N., Hickel, K., Zhang, Y., and Shao, Q.: Water balance modeling over variable time scales based on the Budyko framework – Model development and testing, J. Hydrol., 360, 117-131, https://doi.org/10.1016/j.jhydrol.2008.07.021, 2008.

Zhang, Y., Pan, M., Sheffield, J., Siemann, A. L., Fisher, C. K., Liang, M. L., Beck, H. E., Wanders, N., MacCracken, R. F., Houser, P. R., Zhou, T., Lettenmaier, D. P., Ma, Y., Pinker, R. T., Bytheway, J., Kummerow, C. D., and Wood, E. F.: A Climate Data Record (CDR) for the global terrestrial water budget: 1984-2010, Hydrol. Earth Syst. Sci., 22, 241-263, https://doi.org/10.5194/hess-22-241-2018, 2018.

List of Figures:

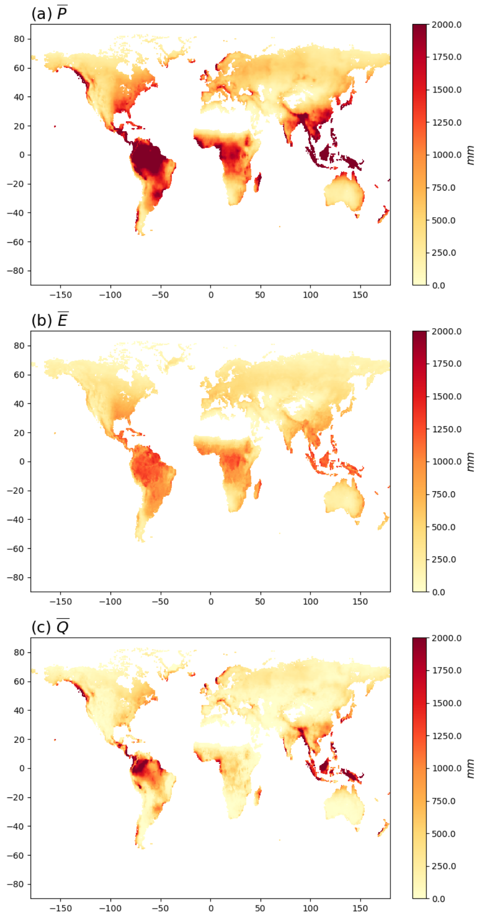

Figure 1. Mean annual (1984-2010) (a) *P*, (b) *E* and (c) *Q*. Note that the mean annual Δ*S* in the CDR database is zero by construction and is not shown.

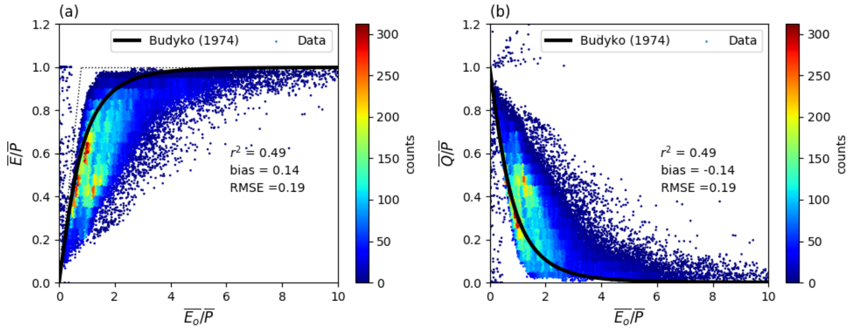

Figure 2. Relationship of mean annual (a) evapotranspiration ($\overline{E}/\overline{P}$) and (b) runoff ($\overline{Q}/\overline{P}$) ratios to the aridity index ($\overline{E_o}/\overline{P}$) from the CDR and SRB databases. For comparison, the Budyko (1974) curve is shown on the left panel (Fig. 2a). The curve on the right panel (Fig. 2b) is calculated assuming a steady state ($\overline{Q}/\overline{P} = 1 - \overline{E}/\overline{P}$).

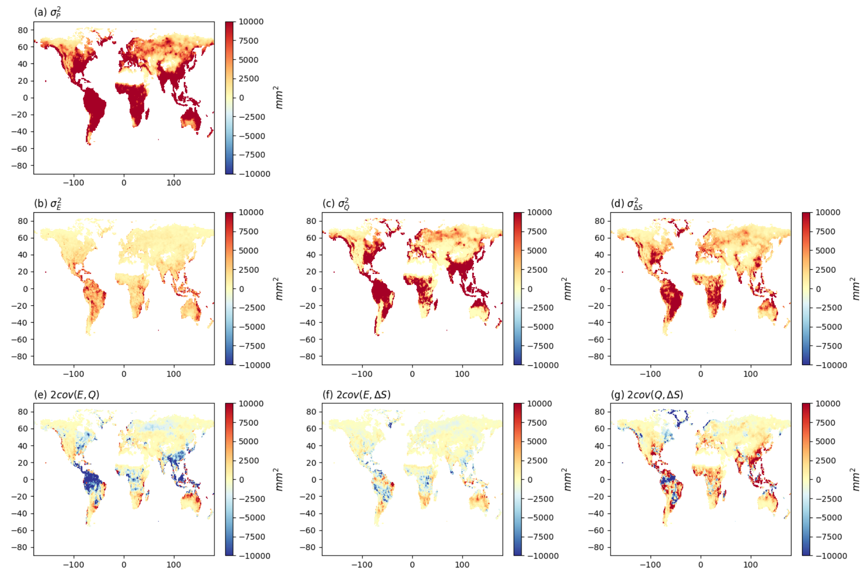

Figure 3. Water cycle variances (σ_P^2, σ_E^2, σ_Q^2, $\sigma_{\Delta S}^2$) and covariances ($cov(E, Q)$, $cov(E, \Delta S)$, $cov(Q, \Delta S)$). Note that we have multiplied the covariances by two (see Eq. 2).

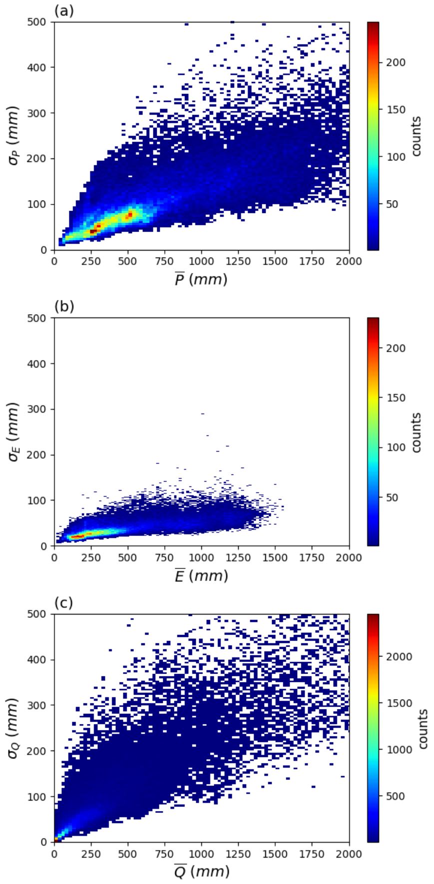

Figure 4. Relation between inter-annual mean and standard deviation for (a) *P*, (b) *E* and (c) *Q* from the CDR database. Note that the mean annual ∆*S* is zero by construction and is not shown.

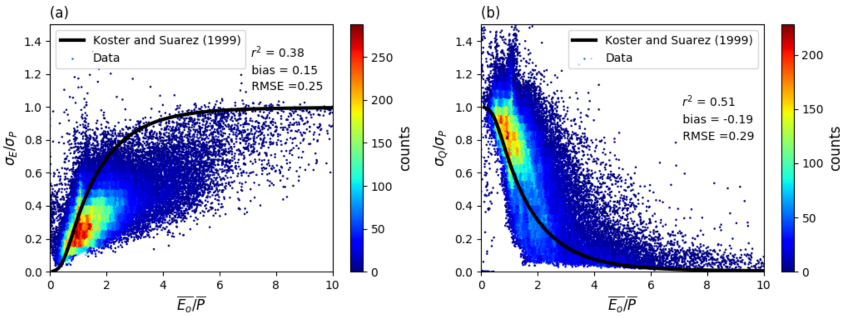

Figure 5. Relationship of inter-annual standard deviation of (a) evapotranspiration (σ_E/σ_P) and (b) runoff (σ_Q/σ_P) ratios to aridity ($\overline{E_o}/\overline{P}$). The curves represent the semi-empirical relations from Koster and Suarez (1999).

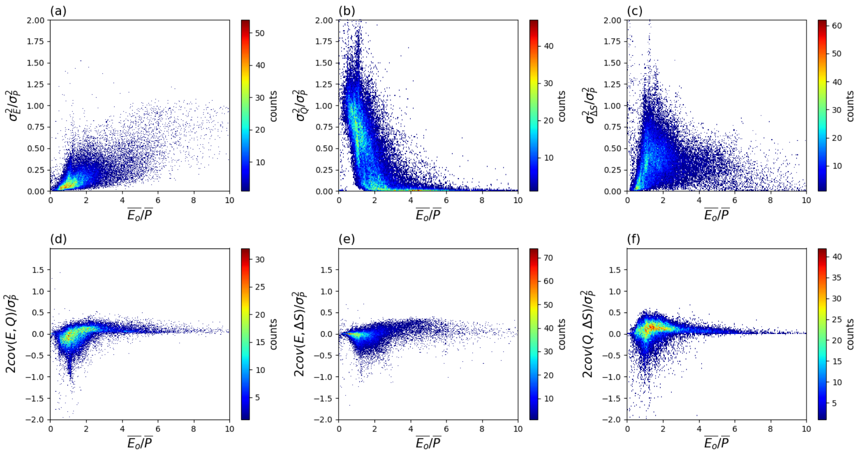

Figure 6. Relation between water cycle variances-covariances (see Fig. 3b-g) as a fraction of the variance of P (σ_P^2) and the aridity index ($\overline{E_o}/\overline{P}$) coloured by density. Note that we have multiplied the covariance components by two (see Eq. 2).

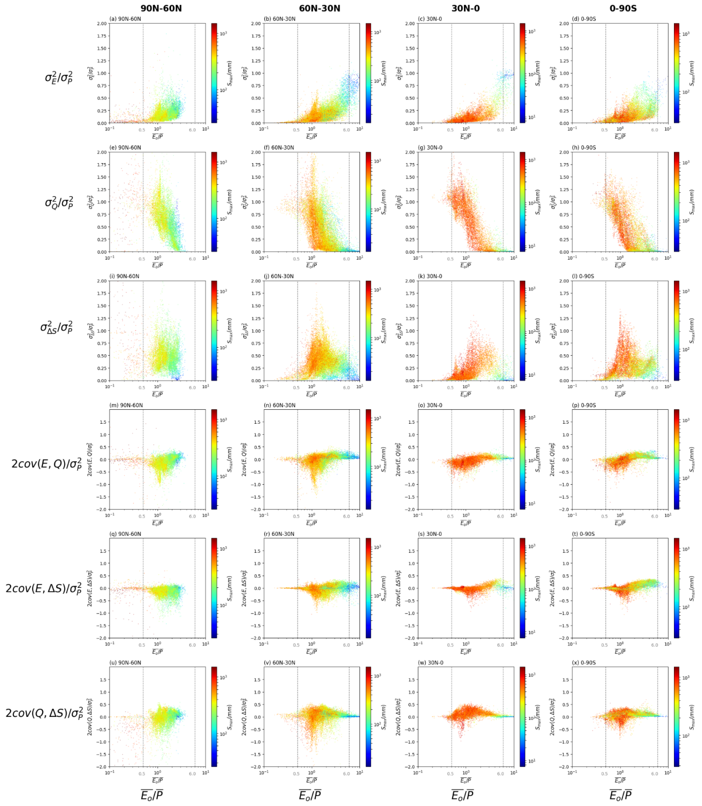

Figure 7. Relation between water cycle variances-covariances (see Fig. 3b-g) as a fraction of the variance for P (σ_P^2) and the aridity index ($\overline{E_o}/\overline{P}$) for grid-cells over different latitude ranges (i.e., 90N-60N, 60N-30N, 30N-0 and 0-90S). The colours relate to the water storage capacity $S_{\max}$. Note that we have multiplied the covariances by two (see Eq. 2). The vertical grey dashed lines represent thresholds used to separate extremely dry ($\overline{E_o}/\overline{P} \geq 6.0$) and wet ($\overline{E_o}/\overline{P} \leq 0.5$) environments. Note the use of a logarithmic x-axis and scale bar for $S_{\max}$.

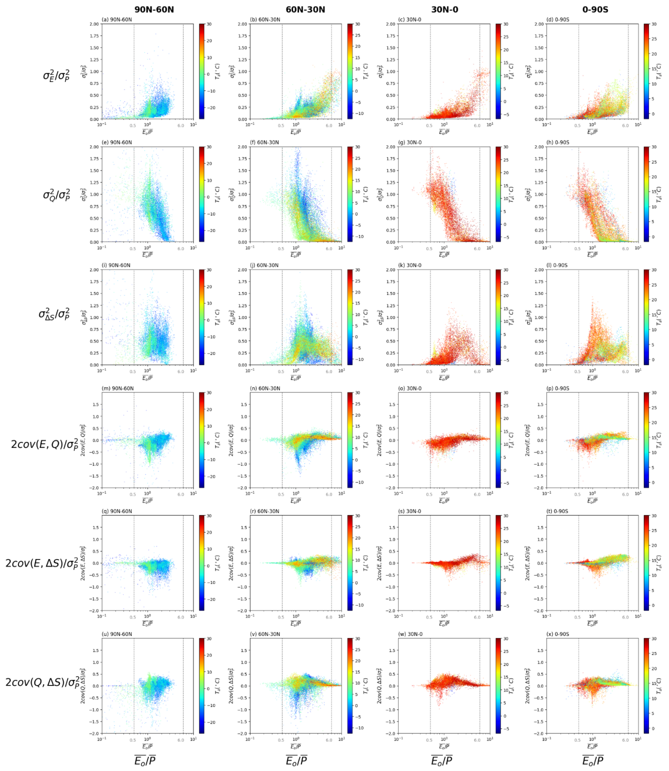

Figure 8. Relation between water cycle variances-covariances (see Fig. 3b-g) as a fraction of the variance for P (σ_P^2) and the aridity index ($\overline{E_o}/\overline{P}$) for grid-cells over different latitude ranges (i.e., 90N-60N, 60N-30N, 30N-0 and 0-90S). The colours relate to the mean air temperature ($\overline{T_a}$). Note that we have multiplied the covariances by two (see Eq. 2). The vertical grey dashed lines represent thresholds used to separate extremely dry ($\overline{E_o}/\overline{P} \geq 6.0$) and wet ($\overline{E_o}/\overline{P} \leq 0.5$) environments.

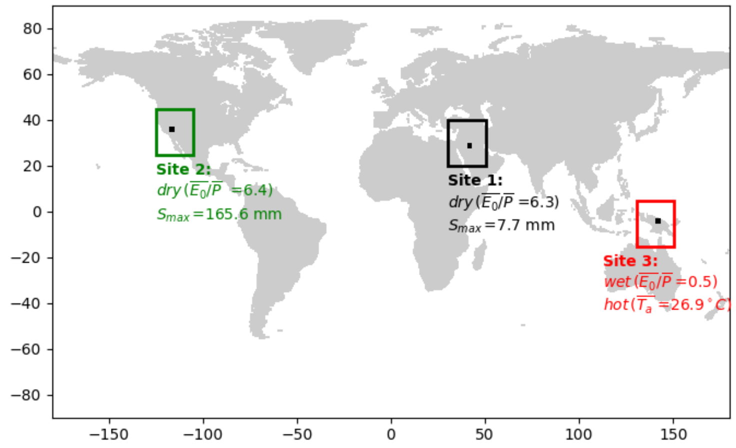

Figure 9. Locations of three representative grid-cells used as case study sites.

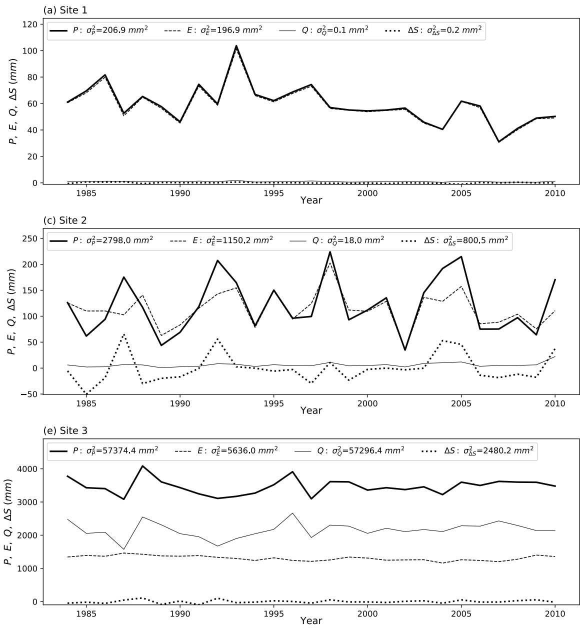

(b) Variance-covariance matrix (Site 1, unit: mm^2)

	E	Q	ΔS
E	196.9	3.4	1.5
Q	3.4	0.1	0.0
ΔS	1.5	0.0	0.2
Inter-annual variance of P : 206.9			

*Note: The values along the diagonal of each line are variance values for E, Q, and ΔS, and other values are covariance values between the two crossed components.

(d) Variance-covariance matrix (Site 2, unit: mm^2)

	E	Q	ΔS
E	1150.2	71.2	269.2
Q	71.2	18.0	74.3
ΔS	269.2	74.3	800.5
Inter-annual variance of P : 2798.0			

(f) Variance-covariance matrix (Site 3, unit: mm^2)

	E	Q	ΔS
E	5636.0	-4548.6	651.7
Q	-4548.6	57296.4	-122.2
ΔS	651.7	-122.2	2480.2
Inter-annual variance of P : 57374.4			

Figure 10. Inter-annual time series (*P*, *E*, *Q* and Δ*S*) and the associated variance-covariance matrix (*E*, *Q* and Δ*S*) for case study Sites 1-3. Left column shows time series for (a) Site 1, (c) Site 2 and (e) Site 3, with right column i.e., (b), (d) and (f), the associated variance-covariance matrix for three sites. Note that the covariance values in the tables should be multiplied by two to agree with the variance-covariance balance in Eq. (2).

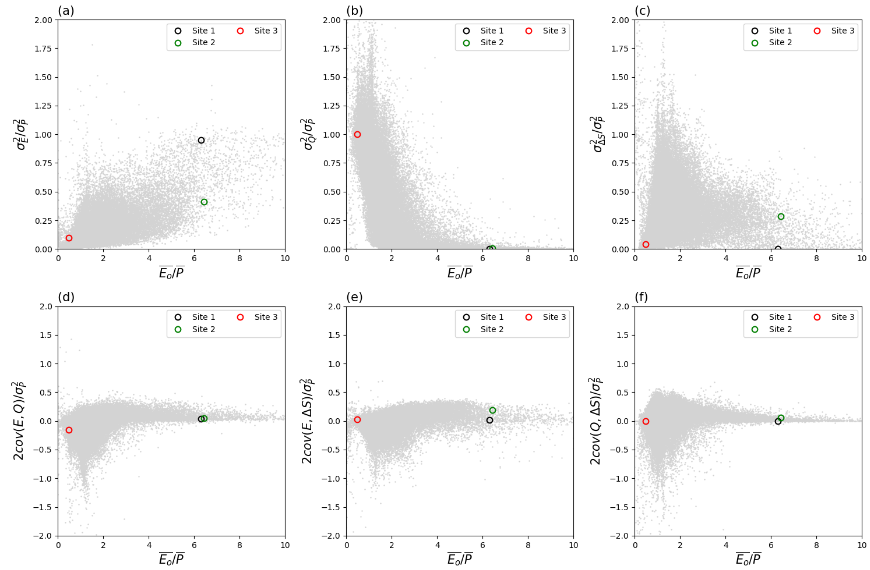

Figure 11. Location of three case study sites in the water cycle variability space. The grey background dots are from Fig. 6.

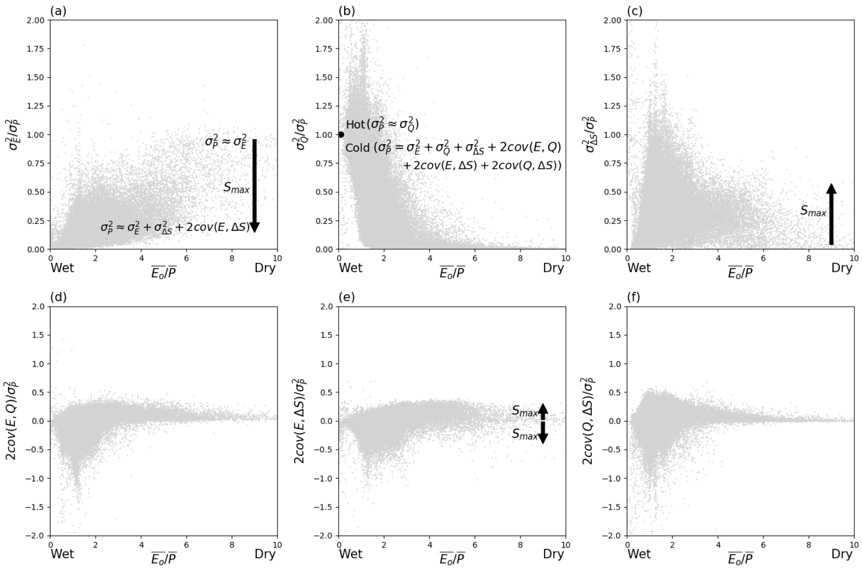

Figure 12. Synthesis of factors controlling variance partitioning. The arrows denote trends with increasing S_{max}. The grey background dots are from Fig. 6.

In this study, we have used a recently released global gridded hydrologic re-analysis product, i.e., the Climate Data Record (CDR) to conduct an initial investigation of inter-annual variability in the terrestrial branch of the global water cycle. To the best of our knowledge, the results in our manuscript present the first attempt to gain a global overview of the magnitude for various terms (Eq. 2) that document variability in the water cycle. Our results demonstrate that the global patterns of inter-annual variability in the water cycle do not simply follow those of the long-term mean. In particular, with the variance calculations, the annual anomalies are squared and hence do not cancel out (like they do when calculating the mean). Hence we were initially surprised that the inter-annual variability of water storage change ($\sigma_{\Delta S}^2$) is typically larger than the inter-annual variability of evapotranspiration (σ_E^2). Moreover, the covariance components are also prominent and can be negative, which means that it is possible for the variability in the sinks (e.g., σ_Q^2, $\sigma_{\Delta S}^2$) can actually exceed the variability in the source (σ_P^2) (Eq. 2).

Our further analysis based on six climate end members, dry/wet, high/low water storage capacity and hot/cold offered some further general insights about hydrologic variability. For example, under extremely dry (water-limited) conditions, with limited storage capacity ($S_{\max}$) we found that E follows P and σ_E^2 follows σ_P^2, with σ_Q^2 and $\sigma_{\Delta S}^2$ approaching zero. However, as $S_{\max}$ increases, the partitioning of σ_P^2 progressively shifts to a balance between σ_E^2 , $\sigma_{\Delta S}^2$ and cov (E, ΔS) (Fig. 12Figs. 10-12-14). Under extremely wet (energy-limited) and hot environments (i.e., no snow/ice impact) we found the inter-annual variations in P mostly be partitioned to inter-annual variations in Q (with both σ_E^2 and $\sigma_{\Delta S}^2$ approaching zero). However, in wet environments that were cold, we expected thermal processes (freeze/melt) to play a critical role in the hydrologic variability. Our results confirm that, with the finding that hydrologic partitioning of variability was highly (spatially) variable under extremely cold conditions (Figs. 10-1212-14) and we were unable to provide any useful simplifications to summarise the data. These results highlight a key point that while the long-term mean state is not especially sensitive to variations in hydrologic water storage or phase, the long-term variability is very sensitive to those same variations.

The most complex results were found in semi-arid/semi-humid (0.5<$\overline{E_o}/\overline{P}$ <1.5) environments, where all three covariances (Eq. 2) were found to play critical roles in the overall partitioning of variability (Figs. 3 and Fig. S94-5). In many regions, the (absolute) magnitudes of the covariances were actually larger than the variances of the water balance components E, Q and ΔS (e.g., Fig. 8Fig. 6). That result demonstrates that deeper understanding of the process-level interactions that are embedded within each of the three covariance terms is still needed to help understand variability in the water cycle in these biologically productive regions (0.5<$\overline{E_o}/\overline{P}$ <1.5).

This study should be viewed as an initial investigation of the inter-annual variability in the global land water cycle. We managed to obtain some syntheses based on the availability of current data, and we expect that with the improvement of hydrologic databases over the coming years some of the detailed spatial patterns may change. However, even from this initial investigation, some general principles do already appear clear. One general finding is that the global pattern in the partitioning of inter-annual variability in the water cycle is not simply a reflection of patterns in the partitioning of the long-term mean. For example, while the inter-annual water storage change is often (safely) assumed to be negligible in terms of the long-term mean state, it is clear that storage variations are central to understanding inter-annual variability of global water cycle. A second generalisation is that the covariance components (Eq. 2) can be relatively large and are negative in some regions. The consequence is that variability in the sinks (e.g., σ_Q^2, $\sigma_{\Delta S}^2$) can, and do, exceed the variability in the source (σ_P^2), especially in biologically productive regions (Fig. 4Fig. 3).

The syntheses of the long-term mean water cycle originated in 1970s (Budyko, 1974), and it took several decades for those general principles to become widely adopted in the hydrologic community. It remains a challenge to develop a synthesis of hydro-climatic variability in the terrestrial branch of the water cycle, and major intellectual efforts will be needed to develop generally applicable principles.

6. Conclusions

Page 37: [2] Deleted	**yindcq7@gmail.com**	**9/8/19 9:01:00 PM**

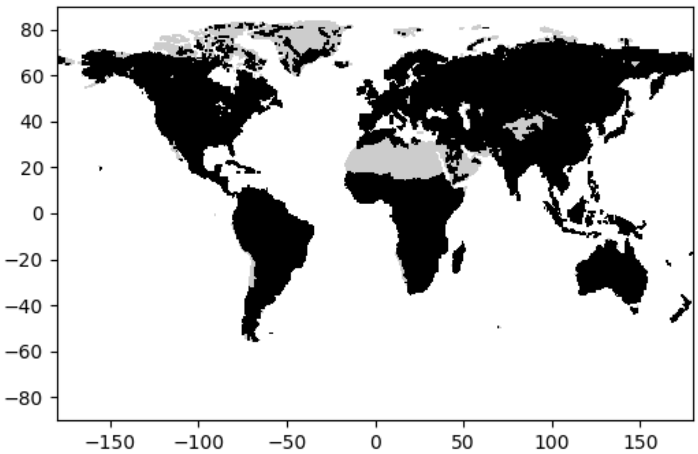

Figure 1. Spatial mask used in this study. Grey areas (Himalayan region, Sahara Desert, Greenland) have been masked out of the CDR database.

Page 40: [3] Deleted	yindcq7@gmail.com	9/8/19 9:03:00 PM

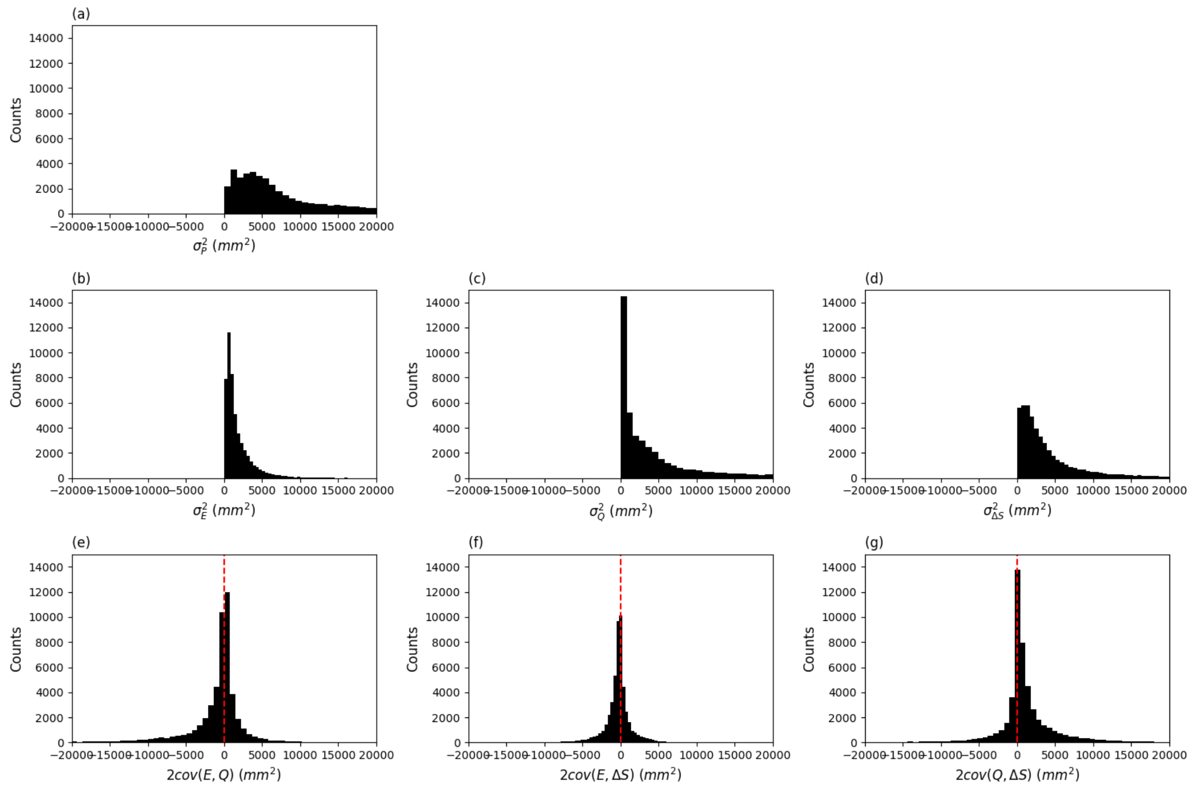

Figure 5. Distribution of water cycle variances (σ_P^2, σ_E^2, σ_Q^2, $\sigma_{\Delta S}^2$) and covariances ($cov(E,Q)$, $cov(E,\Delta S)$, $cov(Q,\Delta S)$). Note that we have multiplied the covariances by two (see Eq. 2).